AMER SAAD ANALYSIS AND SIMULATION OF SINGLE PHASE BUCK- BOOST AC-AC Z-SOURCE CONVERTER MASTER THESIS 2024

NEAR EAST UNIVERSITY

INSTITUTE OF GRADUATE STUDIES

DEPARTMENT OF ELECTRICAL AND ELECTRONIC ENGINEERING

ANALYSIS AND SIMULATION OF SINGLE PHASE BUCK-BOOST AC-AC Z-SOURCE CONVERTER

M.Sc. THESIS

Amer SAAD

Nicosia

May, 2024

NEAR EAST UNIVERSITY

INSTITUTE OF GRADUATE STUDIES

DEPARTMENT OF ELECTRICAL AND ELECTRONIC ENGINEERING

ANALYSIS AND SIMULATION OF SINGLE PHASE BUCK-BOOST AC-AC Z-SOURCE CONVERTER

M.Sc. THESIS

Amer SAAD

Supervisor
Prof. Dr. Ebrahim BABAEI

Nicosia
May, 2024

Approval

We certify that we have read the thesis submitted by AMER SAAD titled "**ANALYSIS AND SIMULATION OF SINGLE PHASE BUCK-BOOST AC-AC Z-SOURCE CONVERTER**" and that in our combined opinion it is fully adequate, in scope and in quality, as a thesis for the degree of Master of Educational Sciences.

Examining Committee	Name-Surname	Signature
Head of the Committee:	Prof. Dr. Kamil Dimililer	....
Committee Member*:	Assist. Prof. Dr. Samuel N. Tackie	....
Supervisor:	PROF. DR. EBRAHIM BABAEI	....

Approved by the Head of the Department

30./10./2024

....Prof.Dr.Bülent BİLGEHAN

Title, Name-Surname

Head of Department

Approved by the Institute of Graduate Studies

..../..../20....

Prof. Dr. Kemal Hüsnü Can Başer

Head of the Institute

Declaration

I hereby declare that all information, documents, analysis and results in this thesis have been collected and presented according to the academic rules and ethical guidelines of Institute of Graduate Studies, Near East University. I also declare that as required by these rules and conduct, I have fully cited and referenced information and data that are not original to this study.

AMER SAAD

…../…../…..

Day/Month/Year

Acknowledgments

I want to take this opportunity to applaud my professor and thesis supervisor Prof. Dr. EBRAHIM BABAEI for the mentorship, support and valuable insight that I have been privileged to receive in the process of developing this thesis. With his guidance, support, respect and patience, the result of my work changed significantly; thus, I am deeply thankful for his mentorship.

I cannot also end without thanking my parents for their love, hope and belief in me which never changed. The continuous support and sacrifices that they have made, through these academic years, have been the main pillar of my academic journey; I will never be able to express through poor words the debt that I owe to them.

Furthermore, I would like to thank all my friends and colleagues whose love and enthusiasm accompanied me through this period. They have believed in me so much and it has been the power that kept me going.

Ultimately, I would like to extend my deepest gratitude to Near East University for its tremendous contribution to creating a suitable environment for learning and academic exploration. The wider research environment with a variety of resources, facilities, and opportunities of the university has had a great impact for the successful completion of the thesis.

This thesis is as a result of the collective aspirations, approval and wishes of many individuals and institutions, and I deeply and sincerely appreciate them.

AMER SAAD

Abstract

ANALYSIS AND SIMULATION OF SINGLE PHASE BUCK-BOOST AC-AC Z-SOURCE CONVERTER

AMER SAAD

M.Sc, Department of Electrical and Electronic Engineering

May, 2024, 110 pages

This thesis proposes analysis and simulation of a single-phase AC-AC converter with impedance source buck-boost inbuilt function, which is designed for load voltage bucking and boosting applications. The converter employs an impedance source network as an input impedance to help regulate the output frequency and voltage levels; it operates in bucking mode for duty cycles between 0 and 0.33 and then moves to a boosting mode for duty cycles varying from 0.33 to 1. The switching control is implemented to achieve voltage regulation. Moreover, it is possible to independently control the magnitude and frequency of the outbound voltage. Integration of capacitance across the outer closed loop yields fully compatible performance, the feature being such that it mitigates soft commutation and short-circuiting and actually improves the input current's waveform quality. Versatility is the main characteristic of the converter that is necessary to implement it on shunt and traction systems. Simulation is carried out by PSCAD software. These simulation results were found to be in agreement with the theoretical analyses.

Keywords: Z-source converter; AC-AC converter; Buck-Boost; PSCAD software.

Özet

ANALYSIS AND SIMULATION OF SINGLE PHASE BUCK-BOOST AC-AC Z-SOURCE CONVERTER

AMER SAAD
M.Sc, Department of Electrical and Electronic Engineering
May, 2024, 110 pages

Bu makale, tek fazlı AC-AC dönüştürücünün analizi ve uyarlaması için gerilim artırma ve yük azaltma uygulamaları üzerine tasarlanmıştır.Giriş empadans ağı çıkış frekansını ve gerilim seviyelerini düzenlemeye yardımcı olmak için kullanılır; 0 ile 0,33 arasındaki iş kısımları için azaltma modunda çalışırken, ardından 0,33 ila 1 arasında değiSet noktası tabanlı anahtar değiştirme kontrolü uygulanmıştır, bu durum gerilim regülasyonunu sağlamak için yapılmıştır.Ayrıca, çıkış gerilimi ve frekansı bağımsız olarak kontrol edilebilir.Dış kapalı döngüye kondansatör entegrasyonu tamamen uyumlu bir performans sağlar, bu özellik yumuşak komütasyonu ve kısa devreyi azaltır ve aynı zamanda giriş akımının dalga formu kalitesini artırır.Dönüştürücünün, akım şebekesi ve traksiyon sistemlerine uygulanmasının gerekli olduğu ana özellik çok yönlülüktür.Uyarım, PSCAD yazılımı ile yapılır.Simülasyon sonuçları teorik analizlerle uyumlu bulunmuştur.Bu yeni dönüştürücü, sadece güç sistemleri uygulamaları için değil, aynı zamanda diğer sistem uygulamaları için de mevcut olan bir gerilim sorunudur.

Anahtar kelimeler: Z-kaynak dönüştürücü; AC-AC dönüştürücü; Buck-Boost; PSCAD yazılımı.

Table of contents

Approval……………………………………………………………………………….1
Declaration……………………………………………………………………………2
Acknowledgements…………………………………………………………………3
Abstract……………………………………………………………………………...4
Özet……………………………………………………………………………………5
Table of Contents…………………………………………………………………...6
List of Tables…………………………………………………………......................8
List of Figures…………………………………………………………..………..9
List of Abbreviations…………………………………………………………………12

CHAPTER I

Introduction…………………………………………………………………………..13
Overview……………………………………………………………………..13
Statement of The Problem ………………………………………………………22
Significance of The Study...……………………………………………………..23
Limitations of The Study……………………………………………...……24
Overview of The Thesis………..……………………………………………..24

CHAPTER II

Literature Review………………………………….……………………………26
Introduction…………………………………………………………………..26
AC-AC Direct Buck Converter With Two Inductances. ………………………...26
AC Boost Voltage Regulator Transformer Less Based on Z-Source Network…..33
AC–AC Converter Without Commutation Problem……………………………40
Z-Source PWM AC-AC Converters…………………………….……………46

CHAPTER III

Proposed Topology and Simulation Results……………………………………………….53
Introduction……………………………………………………………………..53
Power Circuit……………………………………………………………………54
Switching Logic and Operational Principle……………………………………55
Generation of Positive Cycle……………………………………….....56
Generation of Negative Cycle…………………………………………58
Design Losses and Analysis……………………………………………………63
Selecting The Maximum Voltage For Semiconductor Elements……....64
Selecting The Currents of The Switches………………………………..66
Simulation and Results…………………………………………………………68
Boost Mode With a Frequency of 50Hz………………..……………69
Buck Mode With a Frequency of 50Hz…………………..…………..80
Boost Mode With a Frequency of 25HZ……………..…………..……...83
Buck Mode With a Frequency of 25Hz……………………….……..85
Boost Mode with a Frequency of 100HZ……………………..……..87
Buck Mode With a Frequency of 100HZ……………………..……...90
Summary of The Obtained Results……………………………………..……92

CHAPTER IV

Conclusion……………………………………………………………………………93
Recommendations and Future Work……………………………………………..94
References……………………………………………………………………………95
Appendices…………………………………………………………………………100

List of Tables

Page

Table 3.1 Numerical values of the parameters used in the simulation…………………68

Table 3.2 Total Harmonic Distortion (THD) of Input and Output Components of the Converter……………………………………………………………...…………...92

List of Figures

Page

Figure 1.1 Circuit diagram of AC-DC converter……………………………………..14

Figure 1.2 Circuit diagram of DC-AC converter………………………………………15

Figure 1.3 Circuit diagram of three phase to single phase AC-AC converter……………20

Figure 1.4 Circuit diagram of four type DC-DC converters……………………………..21

Figure 2.1 Equivalent circuit of AC-AC single phase buck converter…………………..28

Figure 2.2 Detailed circuit of the suggested AC-AC single phase buck converter………29

Figure 2.3 Waveforms of the voltage V_1, V_{11}, V_{12}, i_{L1}, i_{L2}……………………………...30

Figure 2.4 Control circuit of the suggested AC-AC single-phase buck converter………31

Figure 2.5 Waveform of the V_{ac} voltage, V_0 voltage current and i_0 current, for D = 0.3…………………………………………………………………………….32

Figure 2.6 Waveforms of the V_{ac} voltage, V_0 voltage, i_{ac} current and i_0 current, for D = 0.5……………………………………………………………………………32

Figure 2.7 Waveforms of the V_{ac} voltage, V_0 voltage, i_{ac} current and i_0 current, for D = 0.7…………………………………………………………………………….33

Figure 2.8 Block diagram of the system is shown in **(a)**. S_1 or S_2 switches as a bi-polar combination of two IGBTs are shown in **(b)**……………………...…………34

Figure 2.9 Equivalent circuit when S_1 is on and S_2 is off during state 1 **(a)**, and when S_1 is off and S_2 is on during state 2 **(b)**…………………...…………………36

Figure 2.10 Generated Pulse width modulated signal…………………………………...37

Figure 2.11 Traditional DC-DC converter in **(a),** traditional AC–AC converter in **(b)** and Switching Cell (SC) AC–AC converter in **(c)**……………………………………41

Figure 2.12 **(a)** commutation problem in overlap time. **(b)** commutation problem in dead time…………………………………………………………………………..42

Figure 2.13 **(a)** reverse recovery problem of the body diode using a buck-type AC–AC converter. **(b)** reverse recovery problem of body diode when switch S_1 is on……….43

Figure 2.14 Two types of SCs……………………………………………………………..44

Figure 2.15 **(a)** voltage-fed single-phase Z-source AC–AC converter, **(b)** current-fed single-phase Z-source AC–AC converter………………………………47

Figure 2.16 Duty-ratio control of Z-source AC–AC converters…………………………...48
Figure 2.17 (a) state 1 when S_1 is off and S_2 is on. **(b)** state 2: S_1 is on and S_2 is off……..48
Figure 3.1 Power circuit of impedance-source AC-AC converter……………………………...54
Figure 3.2 Logic diagram for the switching of the converter presented…………………55
Figure 3.3 Equivalent circuit of the impedance-source converter for positive cycle operation; **(a)** Mode 1, **(b)** Mode 2…………………………………………………...58
Figure 3.4 Equivalent circuit of the impedance source converter for negative cycle operation; **(a)** Mode 3, **(b)** Mode 4…………………………………………………...61
Figure 3.5 A graph showing the voltage conversion ratio versus duty cycle plot. **A:** Presented impedance source converter AC-AC. **B:** Buck-Boost AC-AC converter…63
Figure 3.6 Waveforms of the input and output voltages of the converter in boost mode; **(a)** Input voltage; **(b)** Output voltage………………………………………69
Figure 3.7 Waveforms of the input and output currents of converter in boost mode; **(a)** Input current; **(b)** Output current………………………………………70
Figure 3.8 Voltage waveforms across the terminals of the switches of the presented converter in the boost mode; **(a)** Voltage across the terminals of switches S_{1P} and S_{1N}; **(b)** Voltage across the terminals of switches S_1, S_2, S_3, and S_4……………………………71
Figure 3.9 Current waveforms of the switches in the boost mode; **(a)** Current waveform of switch S_{1P}, **(b)** Current waveform of switch S_{1N}, **(c)** Current waveform of switches S_1 and S_2, **(d)** Current waveform of switches S_3 and S_4………...72
Figure 3.10 Voltage waveforms across the capacitors in the boost mode; **(a)** Voltage waveform across capacitor C_N; **(b)** Voltage waveform across capacitor C_P……..……..75
Figure 3.11 Current waveform across capacitor C_L in the boost mode………………...76
Figure 3.12 Waveforms of the current across the coils in the boost state; **(a)** Waveform of the current across coils L_{1P} and L_{2P}; **(b)** Waveform of the current across coils L_{1N} and L_{2N}…………………………………………………...............………76
Figure 3.13 Voltage waveforms across the coils in the boost state; **(a)** Voltage waveform across coils L_{1P} and L_{2P}, **(b)** Voltage waveform across coils L_{1N} and L_{2N}……77
Figure 3.14 Voltage waveforms across the diodes in boost mode; **(a)** Voltage waveform of diodes D_{1P} and D_{3P}; **(b)** Voltage waveform of diodes D_{1N} and D_{3N}; **(c)** Voltage

waveform of diodes D_{2P} and D_{4P}; **(d)** Voltage waveform of diodes D_{2N} and D_{4N}; **(e)** Voltage waveform of diode D_{5P}; **(f)** Voltage waveform of diode D_{5N}……………………...**78**

Figure 3.15 Voltage waveforms of the input and output of converter in Buck mode; **(a)** Input voltage; **(b)** Output voltage…....…………………………………………..…...**81**

Figure 3.16 Waveforms of input and output currents of the converter in Buck mode; **(a)** Input current waveform, (**b)** Output current waveform…………………………......**82**

Figure 3.17 Waveforms of the input and output voltages of the converter in the Boost mode; **(a)** Input voltage; **(b)** Output voltage…………………………………………**83**

Figure 3.18 Waveforms of the input and output currents of the converter in the Boost mode; **(a)** Input current; **(b)** Output current………………………………..………..**84**

Figure 3.19 Waveforms of the input and output voltages of the converter in the Buck mode; **(a)** Input voltage; **(b)** Output voltage…………………...………………………**85**

Figure 3.20 Waveforms of the input and output currents of the converter in the Buck mode; **(a)** Input current waveform; **(b)** Output current waveform……………..……….**86**

Figure 3.21 Voltage waveforms of the input and output of the converter in boost mode; **(a)** Input voltage; **(b)** Output voltage………………………………………...……**88**

Figure 3.22 Waveforms of the input and output currents of the converter in the boost mode; **(a)** Input current waveform; **(b)** Output current waveform……………………...**89**

Figure 3.23 Waveforms of the input and output voltages of the converter in the Buck mode; **(a)** Input voltage; **(b)** Output voltage……………………..………………..…**90**

Figure 3.24 Waveforms of the input and output currents of the converter in Buck mode; **(a)** Input current waveform; **(b)** Output current waveform……………………………..**91**

List of Abbreviations

AC: Alternating Current

DC: Direct Current

EV: Electrical Vehicle

THD: Total Harmonic Distortion

MOS: Metal-Oxide-Semiconductor

IGBT: Insulated-Gate Bipolar Transistor

MOSFET: Metal-Oxide-Semiconductor Field-Effect Transistor

PWM: Puls Width Modulation

PSCAD: Power System Computer Aided Design

PFC: Power Factor Correction

PLC: Programmable Logic Controller

UPS: Uninterruptible Power Supply

Variac: AC Voltage Regulator

ZSI: Z-Source Inverters

CHAPTER I

Introduction

1. Overview

Electrical power can be efficiently converted, controlled, and managed thanks to the significant area of power electronics. It provides the foundation for a wide range of techniques and programs that support environmental conservation, energy effectiveness, and a general operation of contemporary electrical networks that use electronic equipment to effectively convert and regulate electricity for a huge range of uses, including electrical appliances, clean energy, electric automobiles, motor drives, power transmission and distribution networks. Power electronics is essential to modern electrical networks because it increases power system flexibility, improves energy productivity, precisely controls electrical parameters, improves power quality and dependability, and lowers consumption of energy and environmental effects. Also, it is responsible for a wide range of functions, including voltage conversion, frequency adjustment, power factor correction, and so much more. As power electronics continue to evolve, the creation of sophisticated and adaptable converters is essential to fulfill the growing needs for effective energy distribution and control. Therefore, it is critical to focus on improving the performance of AC-AC converters, especially in situations where smooth transfer from buck to boost operation or the opposite is required due to dynamic voltage conditions. In power electronics, the Key Components and Concepts are**:**

1. **Switching Devices:** Power electronics rely on electronic switches, such as transistors (MOSFETs, IGBTs), diodes, and thyristors (SCRs), to control the flow of electrical current. These switches can be rapidly turned on and off to regulate power.
2. **Pulse-Width Modulation (PWM):** It is a topology used to control the average voltage delivered to loads. By rapidly switching power on and off, power electronics can precisely control the amount of power delivered to devices.

3. **Rectification and Inversion:** Some types of circuits in power electronics can change the properties of the current from (AC) to (DC) through the rectification technique or change (DC) to (AC) through the inversion technique. Rectifiers convert AC to DC, while inverters transform DC to AC.

    3.1. An AC-DC converter is also known as a rectifier device, it changes the current from (AC) into (DC). The rectifier is divided into three categories: full wave, half wave, and bridge rectifier. Many electronic equipment and gadgets that need a steady, unidirectional passage of electrical current depend on this process of conversion. To produce a DC output wave, this process includes rectification of the AC waveform by four diodes between the positive and negative cycles.

Figure 1.1:

*Image Showing The Circuit Diagram of AC-DC Converter (*RayMingPCB., 2023*).*

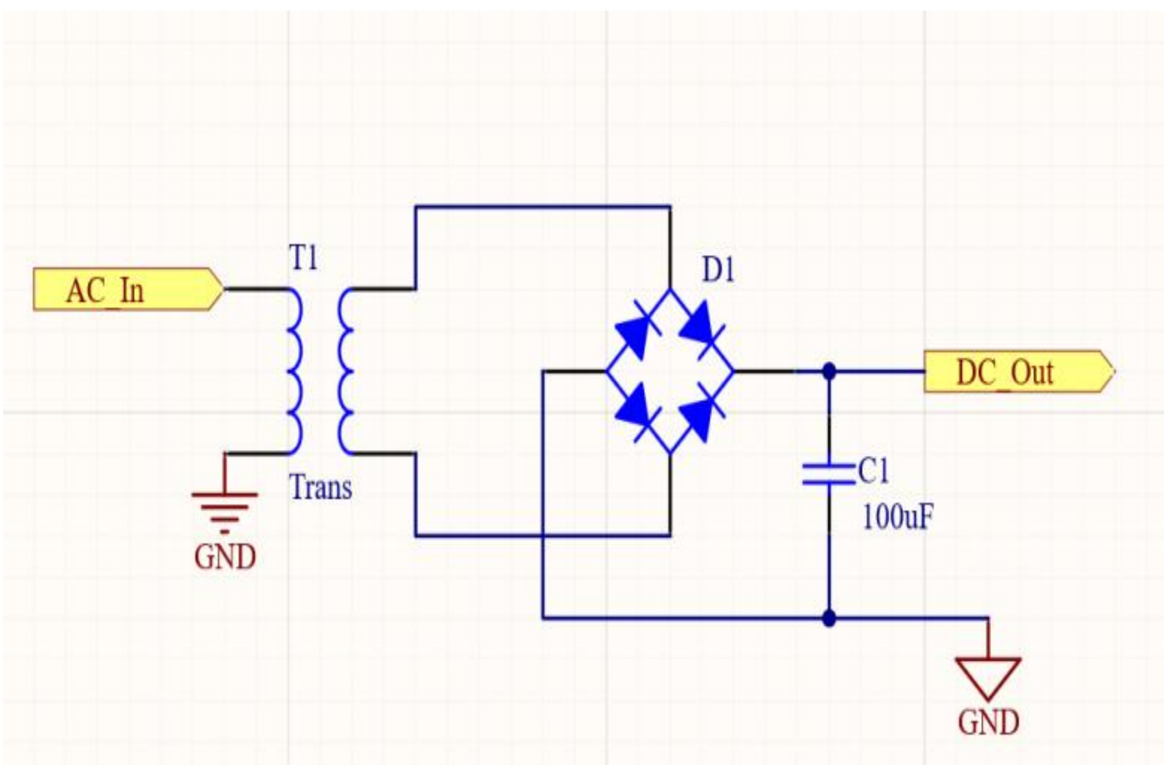

3.2. The device known as an inverter, which is reverse to the above-mentioned AC to DC converter, alternatively converts direct current (DC) to alternating current (AC). Inverter is divided into three categories: The basic categorization of inverters is of three types which are; square wave, modified sine wave, and multilevel inverters. In situations where AC power is needed, but only DC power supply is available then inverter is highly needed. It is very important to a wide range of systems, for instance renewable energy sources systems, and Uninterruptible electrical power supplies (UPS).

Figure 1.2:

*Circuit Diagram of DC-AC Converter (*Martinez., 2020*).*

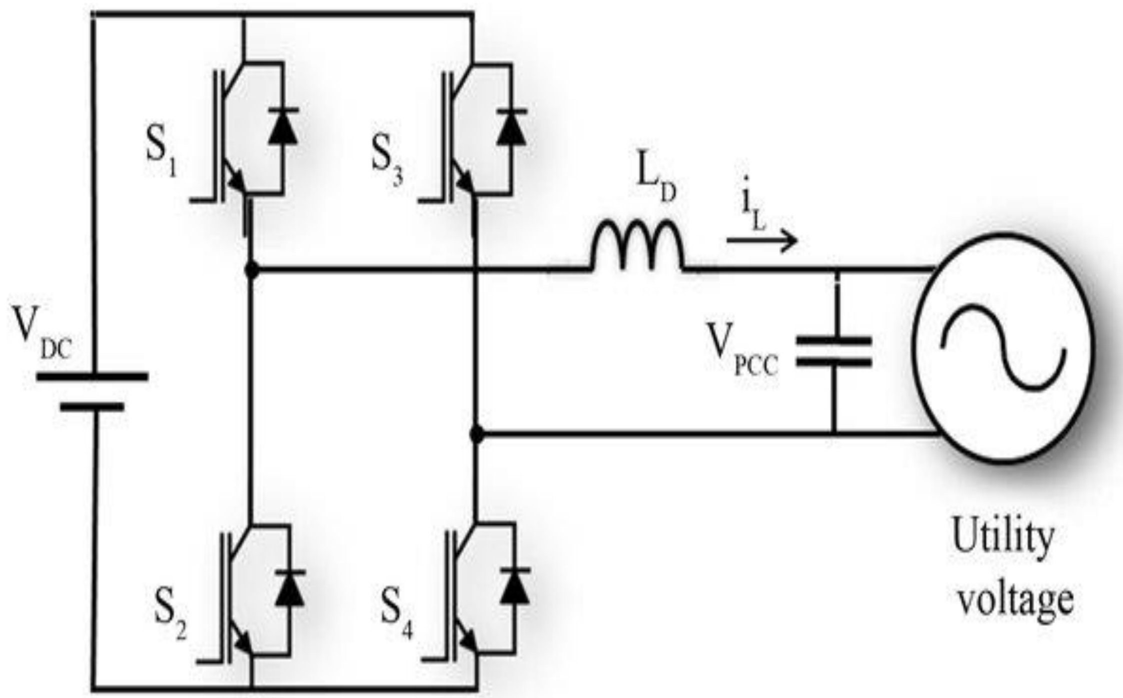

4. **DC-DC Conversion:** The DC-DC converters divide into five groups which are; Buck-Boost converter; buck converter; flyback converter; boost converter and cuck converter. These voltage converter's DC-DC converter control the direct current voltage to the needed level or intended voltage level. This has much significance to battery charging, voltage regulation, and power conservation procedures, for instance.

5. **AC-AC Conversion:** AC-AC converters are required in motor control, voltage control, power control, and enhancement of power quality, they change the features of the AC wave either regarding voltage or frequency or phase sequence.

An AC-AC converters is also known as an AC-to-AC converter; it is electronic circuit that transforms the input source within a particular form to another form required at the output. Since the AC-AC converter requires AC input voltage for it to operate efficiently, an input voltage must be transformed to the targeted output voltage. These may include variations to the voltage level, frequency, or phase or indeed any combination of these may be introduced during the converting cycle (Mathew et al., 2015). There are several types of AC-AC converters, each designed for specific voltage transformation needs like: Various types of converters include Voltage Transformer (Isolation Transformers), Cycloconverters, AC Voltage Regulator (Variac), Phase-Controlled Converters (Phase angle control), Frequency Converters; etc One of the most used inverters is Single-Phase AC-AC Converter where the source is Z-AC and it provides High Buck-Boost Voltage source. Due to the precise control, these converters allow for, it becomes possible to apply them in numerous areas that require the transformation, regulation or modification of the AC power. These are instrumental when it comes to regulating AC power since different loads need different types of powers and there is need to match when the available power sources do not fit the requirement of the networks or devices.

This is a power electronics device used for voltage control and fluctuation in a one-phase ac network (Mathew et al., 2015). This converter is based on addressing many of the problems of power conversion and providing a superior and more reliable solution to a wide range of applications, it also has the advantage of high voltage gain and easier design, more reliable in dealing with wide fluctuations in the input voltage levels (Babaei et al., 2022). A buck converter and a boost converter are two kinds of DC-to-DC voltage converters that are applied in electronics to either step-down (buck) or step-up (boost) the voltage of a direct current (DC) power supply. They are incorporated in many applications including but not limited to power supply, battery management systems, and electric vehicles. For example, let there be the case where you possess renewable energy system such as solar panel, this will give you a DC voltage which the voltage is dependent on the intensity of light. Thus, the ZAC-Source Converter, which is able to convert this (DC) voltage into stable (AC) voltage compatible with grid integration, is appropriate. This makes it possible to regulate the input voltage fluctuations so that the user gets the optimum out of the desired renewable energy source. The key philosophy of Z-AC-Source technology is not to waste energy at the level of conversion as much as possible throughout the process. First, the attempts to eliminate the drawbacks of traditional AC-AC converters were focused on the control and modulation schemes improvement. The chosen ideas of researchers who wanted converters to be more adaptable and efficient served as inspiration to seek new concepts which contributed towards the development of ZAC-Source technologies. The Z-AC-Source concept is similar to the topologies built into an active clamp flying capacitor converter, according to the following main concept of minimizing energy loss during voltage conversion.

This implies that use of Zero Average Crossing in ZAC-Source converters helps improve the switch-over from the buck to the boost mode of operation while minimizing the energy losses that are brought about by switch operations in the conventional converters. This reduces heat losses and in the same preposition, enhances the overall conversion efficiency (Mousavi et al., 2022). Leading several works together with stressing some conceptual change in the progress of the ZAC-Source topology allows critical efforts of specialists, who attempted to change the Semiconductor parts, circuit patterns, and manage the techniques, in order to ensure the applicability of the ZAC-Source principle. Most of the earlier disadvantages linked to conventional AC-AC converters have been solved by these developments and it has been made possible that a converter can easily move from the buck to the boost voltage conversion. The power electronic has now become a broader field with the introduction of ZAC source technology into this power electronics. Its use is not restricted only to the methods that are used for voltage conversion; it provides more flexibility and actually, faster operation as far as the voltage alteration is concerned. Therefore, the ZAC-Source technology is giving evidence of being a viable means of increasing the versatility and efficiency of power electronics systems. As for as it was concerned, the future growth prospect of the ZAC-Source technology has a very large chance for evolution, the researcher’s future endeavors to develop and diversify for ZAC-Source thought will probably alter the converter structure in future besides upholding the existing trend of the flexible and efficient power conversion opportunities. Amongst the several kinds of power electronic converters employing impedance cells is the Z-source AC-AC converter that has undergone advancement in the recent past. Z-source inverters (ZSI) were first proposed three years before the proposed single-phase Z-source AC-AC converter in the year 2005. Compared to the converter's matrix converters and indirect converters, has several features and advantages in its operating characteristics, single-stage power conversion, out-of-phase buck, in-phase boost, and easy control. Z-source AC-AC converters have evolved into two primary categories: Including various types of electrical supplies like the single-phase supplies and the three phase supplies (Subhani et al., 2021). In particular, new solutions that use uncomfortable impedance cells together with the matrix converters were introduced because the latter one had some difficulties. The first one's Adaptors, the Impedance source AC-AC converter comprises a new impedance name plate, containing in particular in-phase boost, out-of-phase buck was first introduced in 2005 and comprises an X shaped impedance network in circuit. After that, various topologies of converters have been reported and are discussed as follows. These topologies can be categorized based on four distinctive features: Here are the possibles proposed solutions to the problem: Here again it is about trust and openness which are fundamental strategic business values no matter the structure of business entities. failure in interchange of magnetic fields; 4. Consequently, knowing the existence of magnetic coupling it can be concluded that: 1. absence of magnetic coupling; 2. presence of magnetic coupling; 3. capability to alter frequency; 4. inherent commutation. It's noteworthy that converters with magnetic-coupling is classified into two groups: first one which employs High-Frequency Transformers (HFT) for isolation, while the second group operates in a non-isolated configuration (Babaei et al., 2022).

1. Capability to Alter Frequency:

Converters can be classified according to the ability of changing the frequency and depending on the need, a device can then be switched to the needed frequency range. It is useful in designs where variable frequency is needed for the best performance of the affair such as in motor drives and types of power supply.

2. Inherent Commutation:

Inherent commutation is the ability of a converter to change from one state to another and this does not require additional control signals. As previously stated, the converters with inherent commutation contain integrated circuits for switching between the modes of operation and thus seems to have easier control strategies.

3. Absence of Magnetic Coupling:

In the topologies which do not use magnetic coupling there is no mutual connection between the input and the output through the magnetic devices such as transformers. In the case of these converters, the voltage transformation is done through other methods that do not incorporate magnetic parts.

4. Presence of Magnetic Coupling:

However, in those topologies which use magnetic coupling, the converter directs the connection between the input and output by means of magnetic components most often the transformer. This magnetic coupling helps in voltage transformation and is widely used in most of the AC-AC converter circuits.

Within the subset of converters with magnetic coupling. When dealing with converters involving magnetic coupling, there are two particular typologies of them:

- First Group (Isolated):

In products within this group of converters a High-Frequency Transformer (HFT) is employed to achieve input/output isolation. For this, isolation becomes critical in areas where electrical separation (SEPs) is expected due to safety, protection, or standardized business motives.

- Second Group (Non-Isolated):

The converters in the non-isolated group operate without the use of High-Frequency Transformers. These converters, do not possess electrical isolation, are suitable in some application where sacrifice of electrical isolation could be made in order to get the other advantages associated with these converters such as simple, cheaper and efficient.

Figure 1.3:

*Circuit Diagram of Three Phase to Single Phase AC-AC Converter (*Aguiar., 2016*).*

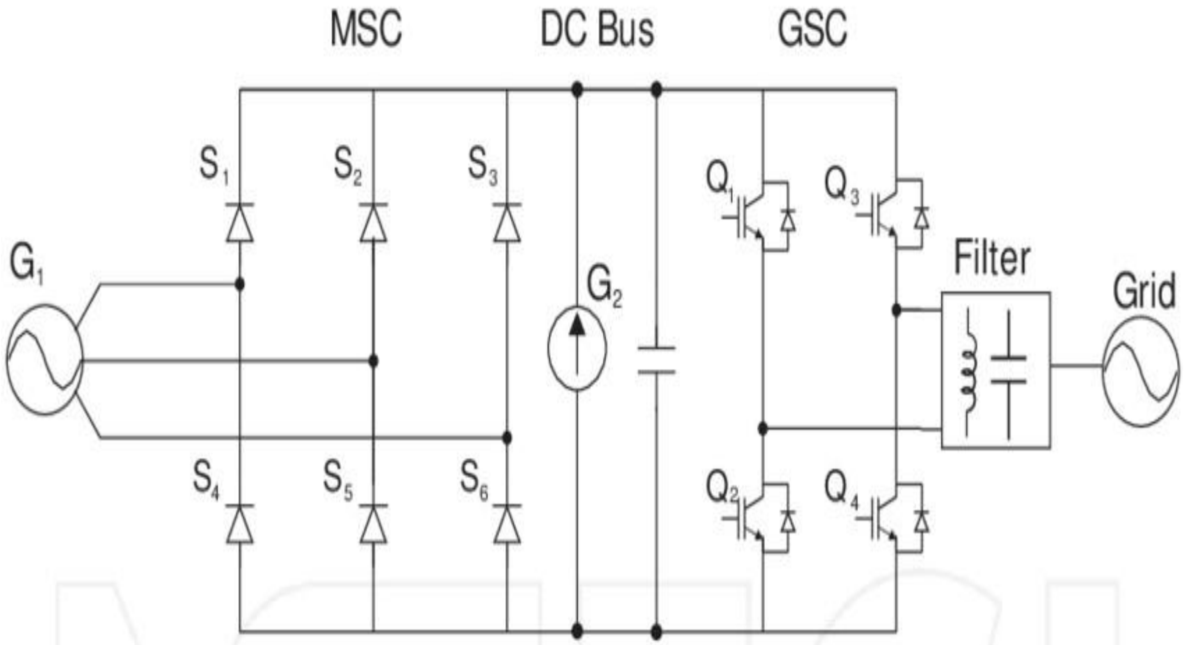

The major characteristics that the converter holds includes:

1. **Z-Source Network:** By far the most crucial portion of the converter in question is the z-source network used at the level of the converter basics. It is formed up of a certain impedance circuit that mainly comprising of passive devices like capacitors and or inductors connected in certain ways. This is to enable it handle the boost and the buck voltage conversion; the boost increases the input voltage oscillations while the buck conversely does the opposite.
2. Wide Input Voltage Range: Another benefit, which can be mentioned in relation to ZAC-Source Converter, is the option of the moderate range of the supplied voltage. It is also equally capable of handling variation of the input voltage as may be realized without integration of any sub parts.
3. High Voltage Gain: The commutation is realized with the increase of the voltage level which is proportional to the topological level of Z-Source. This is particularly useful in different power conversion measured and is very vital when you want to either step up the voltage or step down the voltage in a system.

4. Improved Reliability: It should also be noted that so called Z-Source converters are relatively invulnerable and have rather high immunity to such pathological effects of power quality as harmonics, spikes and voltage sags. Therefore, it is reasonable to argue that participation in employment of ZAC-Source Converter is a right strategy to use in enhancing on the quality and the power purification.
5. Enhanced Robustness: In general, it can be envisaged that the converters, which come under the category of Z-Source, seems to be at a lesser chance of getting affected with defects in comparison with the conventional converters. They can function to the fullest of their capacity even if there are some shortcomings or if the ahead voltage source is substandard.
6. Low Harmonic Distortion: Other studies showed that, the Z-Source converters are capable of reducing or minimizing the harmonic distortion on the output voltage in effect increasing the quality of power supplied.
7. Reduced Component Count: The ZAC-Source Converter is at times constructed with relatively fewer components than some of the typical AC-AC converters, this makes it cheaper since fewer components are usually bought at one time and it is way more reliable because there are fewer things that could go wrong.
8. Efficient Energy Conversion: The Z-Source network is the option of choice in cases where efficiency of energy conversion is an objective since, unlike basic buck/boost converters, it tries to retain a high efficiency of conversion as well as the opportunity for flexibility of observing the voltage level.
9. Buck Mode: The other type of converter is the buck converter also referred to as step down converter since it accepts a higher input voltage and delivers at the output lower voltage; but the output current is almost constant. In the case when the ZAC-Source Converter works in the operation of bucking mode, stepping down of the voltage is done at the output side. This is more advantageous especially for cases where the voltage of the supply has to drop or they have to change or the load they have to power needs less voltage than the supply voltage.
10. Boost Mode: A boost converter also named the step-up converter that receives the low voltage input and gives higher voltage output. This is useful when the voltage has to be supplied in higher levels in order to meet the demand that is offered by the

load for instance in renewable energy systems where output voltage is in DC and needs to be stepped up to AC voltage needed in the grid.

Figure 1.4:

*Circuit Diagram of Four Type DC-DC Converters (*Editorial Team., 2015*).*

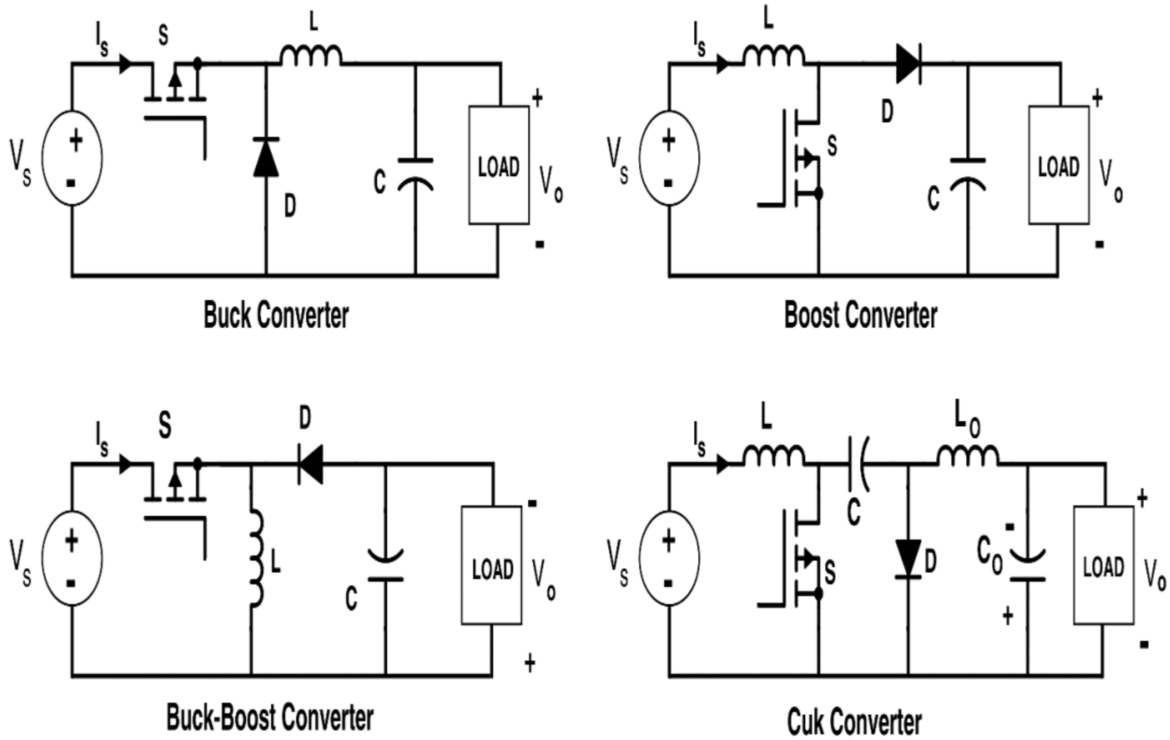

ZAC-Source technology was applied to AC-AC converters mainly due to its special features and possibilities that conform to some requirements and impossibilities of power electronics. The ZAC-Source topology which as the name implies uses a Zero Average Crossing (Z-AC) waveform as its source is a new method of power conversion (Mousavi et al., 2022). This waveform depicts a significant enhancement over conventional sinusoidal waveforms in terms of minimizing power loss and boosting efficiency, and better shifts over voltage conversions are made achievable by ZAC-Source technology due to its capability to exist at Zero Average Crossing, which minimizes switching losses and shifts the efficiency of converters in general. Additionally, the technology is prominently suitable for applications that need voltage look–up since its characteristics offer the foundation for obtaining big buck and boost voltage conversion. The driving force is to use these benefits in order to construct a ZAC-Source Single-Phase AC-AC Converter that will step up or down voltages in high-performance, efficient voltage conversion applications apart from meeting standard AC-AC power conversion applications. The desired effect of choosing ZAC-Source technology is to expand the sphere of power electronics or come up with a different strategy to satisfy new demands of different electrical systems. Thus, the objective of choosing the ZAC-Source technology is to expand the field's areas of power electronics through a new approach to satisfying the new needs of different electrical systems.

2. Statement of Problem

The traditional AC-DC-AC system is capable of producing at the output side a voltage with varying amplitude and frequency. But these conversion systems typically involve more than one stage, where the inclusion of a filter along with capacitor bank increases both the area and expenses of the system. Furthermore, significant power losses occur due to the multiple conversion stages along with low voltage transfer ratio. These converters frequently struggle with controlling the output frequency, which is limited to numerous of the input frequency. They also experience surges in voltage, poor output power quality, as well as the need for the input filter because of the irregular current at the input side. To ensure secure commutations switch operation of the inductive current, a specific period of time or delay within inbound and outbound of switches states is required, that's add to the complexity of the control mechanism. The converter is capable of operating in buck and boost modes with a higher gain factor compared to normal ac-ac converter. The proposed converter offers simple output frequency control without compromising safe operation, and reduced input filter requirements is also possible due to quasi-continuous input current which improve the waveform quality. In addition, it guarantees extremely dependable performance by removing the possibility of shoot-through at the input source, utilizing semiconductors with lower rated properties, enhancing the input current waveform quality, and having an intrinsic self-commutation feature and an easy-to-use switching mechanism. Applications such as induction heaters and medium-frequency transformer isolation for traction converters and wind turbines are possible (Fang et al., 2006). The current generation of single-phase AC-AC converters is not devoid of certain inherent limitations as far as the handling of dynamic voltage situations is concerned – this is especially so where there is also a transition from a high buck to boost voltage conversion or the other way around. Traditional converters face a lot of challenges most of which are as follows especially in areas that allow for a smooth and efficient conversion for systems with different or varying voltages such as utility power quality improvement, Industrial AC drives, and renewable energy. Such modern technologies tend to work more accurately in buck or boost tasks than in the ability to balance both features. Thus, desperately needed is the complex and flexible system to solve these drawbacks and provide the needed requirement ability, which in this case is single-phase AC-AC converter with a high buck and boost voltage conversion ability.

3. Significance of The Study

Applications for the proposed converter include traction systems, induction heating systems, and isolation transformer for wind turbines. Importantly, this suggested converter does not incorporate the snubber circuitry, which looked to be in the previous developed AC-AC regulated converters. Assists in the reduction of circuit complexity and hence cost due to the fact that it has fewer elements. Also, there is the z-source inverter which is different from the three inverters depending on i, source or v, the z-source inverter also possesses buck-boom which makes it has the capability of producing any voltage from the available one. Comparing it to i-source and v-source converters, it operates at a lower duty cycle, has a better waveform quality and it has a larger voltage gain. Due to the compact size and simple structure of the z-source topology, the expenses are low, the area required is low and efficiency is higher. The thesis contributes to the pool of scholarly learning through presenting an extensive analysis of ZAC-Source technology and its possibilities to be implemented in the AC-AC converters. It offers insights that can direct future research in the field of power electronics and lays the groundwork for additional investigation. It has effects on how smart grid systems are developed. The flexibility of the converter complies with the demands of contemporary power distribution networks, enabling the development of smart grids that are more sensitive and secure. Numerous industrial applications may be impacted by the converter's use in uninterrupted power supply (UPS), industrial motor drives, and grid power quality enhancement. Implementation in industrial locations could result in increased operating efficiency, decreased downtime, and better performance (Fang et al., 2006).

4. Limitations of The Study

While the research has been meticulously written and executed thorough consideration and detailed study, it is hard to mention that it is devoid of limitations. Initially, all the simulations are performed utilizing PSCAD software, constraining to the software's scope and limiting control over the outcomes. Although employing computer software for simulations is a customary academic approach, it is undeniable that laboratory experiments would provide a more comprehensive analysis and yield superior results. However, a significant constraint arises from the absence of necessary materials for such experiments. Research reliant on simulations typically exhibits minimal limitations, yet the adept and effective utilization of software tools may pose challenges when users lack sufficient experience. Despite the absence of traditional laboratory inquiries, the selected PSCAD software minimizes discrepancies between laboratory and simulation outcomes. The use of sophisticated control techniques to attain high boost and buck voltage conversion may cause the control circuitry to become more complex. The intricacy of the system could give rise to difficulties concerning its stability, resilience, and instantaneous response. Adopting ZAC-Source technology might necessitate the use of specific parts and control algorithms, which could raise the converter's overall cost. This might have an impact on how economically viable it is to use the technology, especially in situations where costs are a concern, the availability of appropriate testing conditions and equipment may provide obstacles for experimental confirmation of the converter's functionality. External elements that are challenging in controlled conditions may have an impact on testing conducted in real-world scenarios. ZAC-Source converters may not have standard manufacturing procedures and standards because they are a relatively new technology. As a result, there may be obstacles to compatibility and broad adoption because every implementation is different.

5. Overview of The Thesis

The four chapters that make up this thesis are as follows: Chapter one contains the following; Introduction, Problem statement and study significance, limitation of the study and thesis overview. As a part of the previous chapter, the available literature on Z-based AC-AC converters is reviewed. In Chapter 3, the reader will find the Proposed Topology and the obtained Simulation Results. The final chapter is chapter four, which covers the conclusion and suggestions for further research.

CHAPTER II

2. Literature Review

2.1. Introduction

The Z-Source topology takes the leading role among power electronics innovations due to its ability to offer multiple and power-efficient modes of energy conversion in wide areas. Z-source converter is shown as a new alternative to voltage and current source converters, which has some significant advantages, and these mainly use a wide input voltage range and their inherent buck-boost capabilities. This gadget has a special design feature which is the application of an impedance network by the fifth technology that is commonly known as a "Z-network." It has bidirectional power flow and it also has increased flexibility for voltage fluctuations management. The Z-Source Converter is among the key technologies that create strong building blocks for green, smart, and responsive power conversion that sustains diverse industries (Soliero et al., 2011). This introduction attempts to throw light on the theoretical framework, topologies, applications and merits of Z-Source Converter, to extend the understanding of modern power electronics.

2.2. AC-AC Direct Buck Converter With Two Inductances

The direct AC to AC single-phase converter with two inductances currently represents an important development case study in the area of power conversion technology, as the conversion efficiency and performance are substantially enhanced. Designing transformer-less converters involves designing a converter configuration of two inductors which promotes uniform current fashioning and reduces ripple resulting in a competitive efficiency that is better than that of normal AC to AC converters. It utilizes the voltage stepping-down technique of a buck converter without losing significant power. The ultimate prospect that this topology consists of is that it may be used for diverse purposes ranging from renewable energy systems, motor drives, and power supplies for voltage correction and power factor improvement. Through the mastering of the procedure of switching the converter, the voltage is maintained always at the reference level while being subjected to minor losses (Lucanu et al., 2017). The single-phase buck DC-DC converter to direct AC-AC converter with two inductors is an innovation in the field of power electronics because of its ability to maintain high efficiency at continuous operation as well as its precision in superimposing voltage rise at the output. This converter topology is designed to be a solution for the problems existing with a typical AC-AC converter, and thus, it combines two inductances in the circuit configuration, the inductances presented have a major impact on improving the overall behaviour of the converter by giving a ripple current and limiting harmonic distortion. Through two inductors the converter adjusts current ripple and obtains better voltage regulation than that in the case of single-inductor dealings. This results in reduced power losses and a more energy-efficient power system that's the reason why it is best for applications where energy conservation is vital (Alizadeh et al., 2022). This circuit employs two inductances ensures precise power factor correction (PFC); with the active role of PFC the power-transfer efficiency can be improved. Also, the PFC will help the system to meet the grid codes. The converter can adjust the current waveform depending on the input voltage and as this happens, the reactive power can be eliminated and the power distribution system is on normal steady state. The fundamental feature of this converter is its ability to respond to different current and voltage sources of the load (Lucanu et al., 2014). The converter with its wide range of output voltage regulation, can be used efficiently in dynamic load circumstances, e.g. motor drives or those related to renewable energy systems. Furthermore, the outrunner's structure and performance characteristics have been enhanced making it suitable for use in difficult operating environments (Mousavi et al., 2022). Moreover, topology itself possesses upgradability and scalability means by which it may be connected to the present power electronic system or form a component of future power electronic system. Thus, it is suitable, but not limited to many applications such as the grid-tied invertors for the renewable energy source like solar or wind, chargers, adjustable speed motor drive system, UPS, etc, Buck-mode direct AC-AC converter having two inductances not only is more efficient but also provides better result. Because of these additional benefits that allow for the minimizing of the power lost, correction of the power factor, or the flexibility in the changes in the load it is commonly used in most of the industry and commercial applications. Regarding the future work, it is observed from the present study that there is the scope of improvement and enhancement in the power electronics tech with the continued advancements in the current state of research and development (Lucanu et al., 2017).

Figure 2.1:

Image showing the equivalent Circuit of AC-AC Buck Converter (Lucanu et al., 2017).

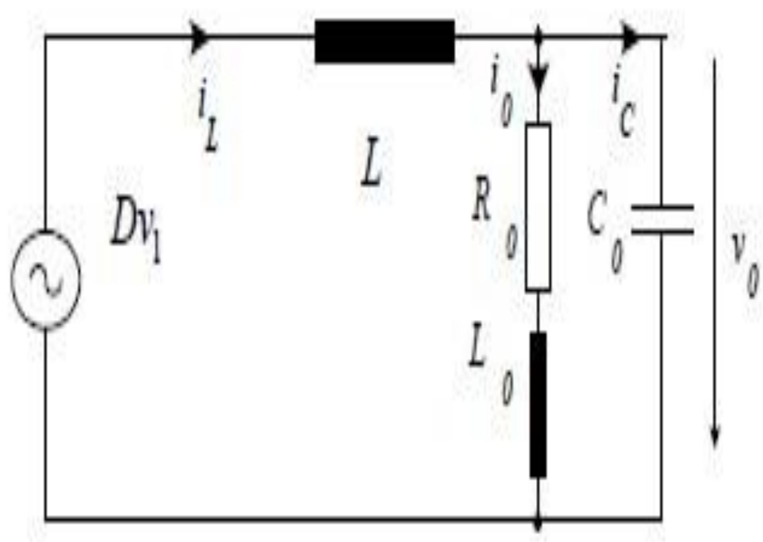

The equivalent circuit equation where $L = L_1 = L_2$ and $i_L = i_{L1} + i_{L2}$:

$$DV_1(t) = L\frac{di_L}{dt} + v_0(t) \quad (1)$$

The distortion of the current waveform resulting from the absorption of grid current will be prevented by:

$$C_0 = \frac{L_0}{R^2 + (\omega L_0)^2} \quad (2)$$

The output circuit of the converter will be as an equivalent resistance:

$$R_{0e}\frac{R_0^2 + (\omega L_0)^2}{R_0} \quad (3)$$

The input voltage varies between the limits:

$$V_{I(min)} \leq V_I \leq V_{I(max)} \quad (4)$$

The output voltage varies between the limits:

$$V_{0(min)} \leq V_0 \leq V_{0(max)} \quad (5)$$

Maximum value for duty cycle D:

$$D_{(max)} = \frac{V_{0(max)}}{V_{I(min)}} \quad (6)$$

Minimum value for duty cycle D:

$$D_{(min)} = \frac{V_{0(min)}}{V_{I(max)}} \quad (7)$$

Ripple current flowing through L_1 and L_2:

$$\Delta i_L = D(1 - D)\frac{V_1}{LF_s} \quad (8)$$

Maximum Ripple current flowing where $L_1 = L_2$:

$$I_{0(max)} = \frac{V_{0(max)}}{\sqrt{R_0^2+(\omega L_0)^2}} \quad (9)$$

Figure 2.2:

Image Showing Detailed Circuit of The Suggested AC-AC Buck Converter (Lucanu et al., 2017).

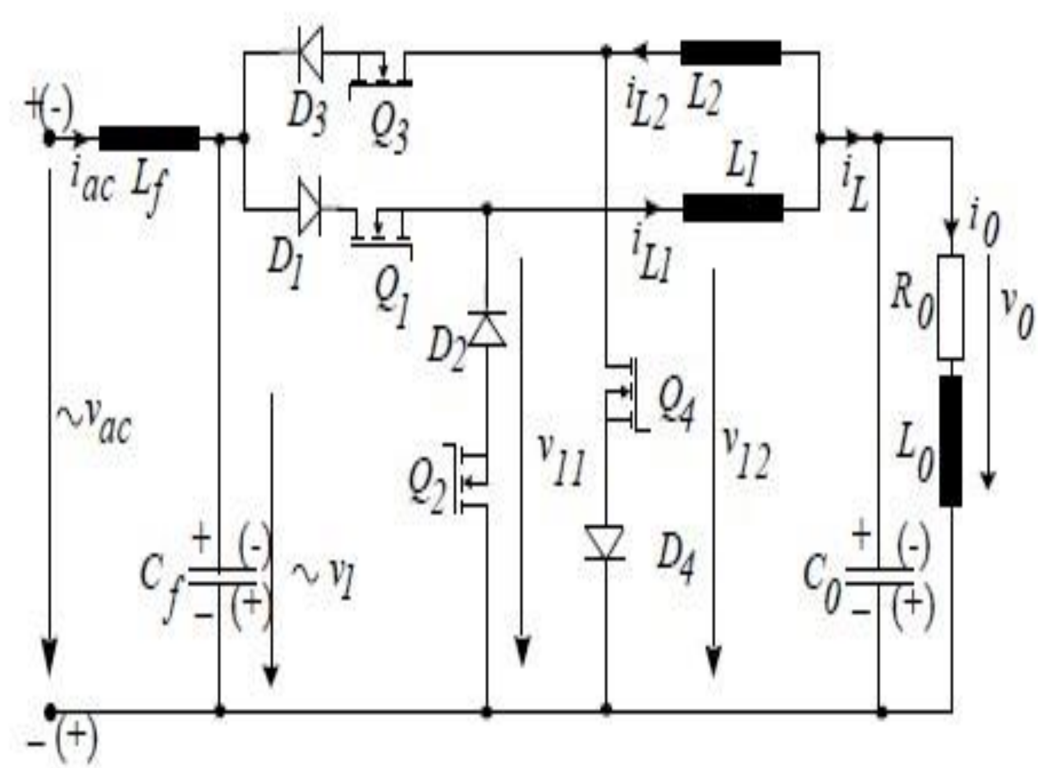

In this circuit the dual buck inductors L_1 and L_2 are controlled by the switching frequency denoted as fs while the grid frequency (input) of 50 Hz is involved in the control of transistors Q_2 and Q_4. The transformer's inductors L_f and capacitor C_f are a part of the grid filter and are applied for refining the power transmission while C_2 is additional to that, R_0 and L_0 are wavelengths to show the load impedance of the network**.** The input variable is registered at Q_2 and is then compared with the threshold voltage (set by the bandgap voltage reference) at Q_3. The output will be high or low depending upon the comparison. It is very simple that the main role of a digital filter would be to avoid the loss of the current waveform characteristic to preserve and maintain the integrity of the signal. With the AC grid being the provenience of the voltage, its period has to be in harmony with that of the grids. It is either by properly tuning the output capacitor C_0 or simply through the selection of the filter. An i_L current transducer signal should be applied at the reversing input of C_p if the R_0/L_0 ratio is significant during the operation. In this case, the variability of the duty cycle D has no effect on the phase shift/difference (Fig. 2.4). hence, the semiconductor material used carries current that directs conduction switching between Q_2 and Q_4 in a contrary direction when crosses the 0 value. On the other hand, parallel inductances L_1 and L_2 in the L filter (fig 2.1) cause a decline in both current shapes and voltage fluctuations. The series resonant power converter design permits to spread of the inductance coefficient between two components and as a result the current waveforms become ceteris paribus, this architecture reaches lower harmonic distortion and consequently, the power losses during conversion are reduced (Lucanu et al., 2017). Additionally, because of the converter operating control which is usually done through the use of pulse width modulation (PWM) techniques. Theoretically, this control mechanism provides optimum torque by accurately switching the transistors at the converters with specific switching frequency (f_s) and synchronizes the switch operation with the constant frequency of the AC grid (input). As such, it provides grid operators with real-time tracking and monitoring of actual power flows and facilitates the smooth incorporation of renewables into existing power infrastructures (Aurasopon & Khamsen., 2013).

Figure 2.3:

Waveforms of The Voltage V_1, V_{11}, V_{12}, i_{L1}, i_{L2} (Lucanu et al., 2017).

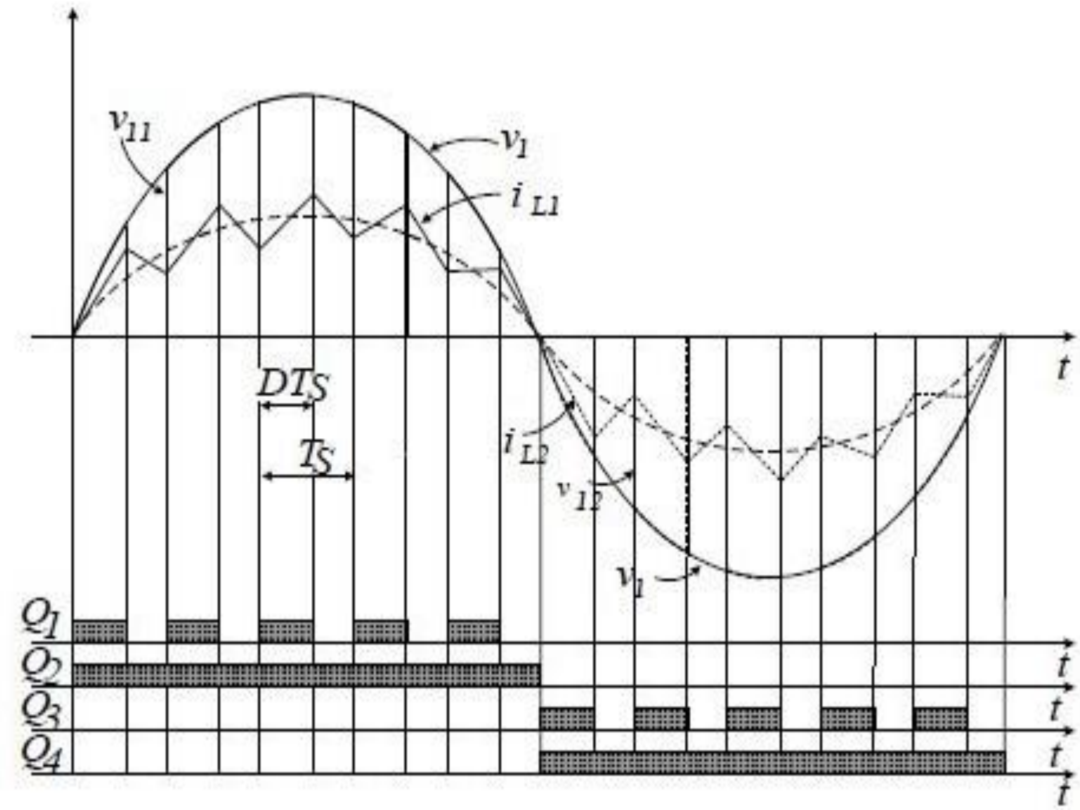

Figure 2.3 shows the voltage V_1 at the converter input, as well as the voltages of the buck inductance throughout the grid's positive V_{11} and negative V_{12} alternations when they are connected in series with the load impedance. It also displays the controlling signals for the four MOSs and the currents flowing via the buck inductances i_{L1} and i_{L2}. The structure of the logic gate as well as the four MOSs control signals, the voltage waveforms of V_1 at the converter input, along with the voltages across the buck inductance connected in series with the load impedance referring to the both positive alteration V_{11} and negative alternations V_{12} of the grid (Lucanu et al., 2017).

Figure 2.4:

Control Circuit of The Suggested AC-AC Single-Phase Buck Converter (Lucanu et al., 2017).

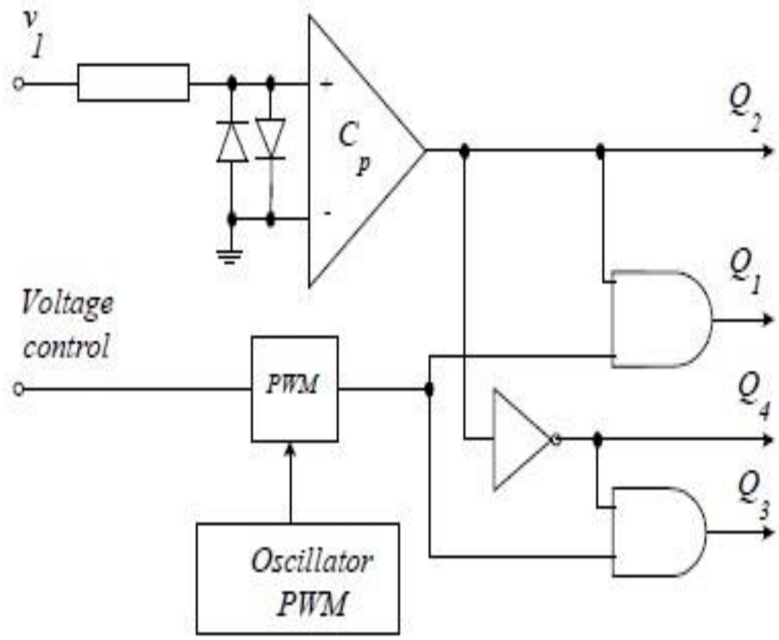

During positive phase of V_1, function of continuous conduction mode is set to Q_2, whereas Q_1 receives PWM control, and the converter's operating frequency is determined by the sawtooth oscillator (shown in Figure 2.4) by $f_S = 1/T_S$. In the positive phase the MOS Q_3 and Q_4 are off. Subsequent, in the negative phase of voltage V_1, MOS Q_4 continuously conducted, while Q_3 is controlled by pulse width modulation, and Q_1 and Q_2 are off. The control method just built is effective because two buck DC-DC converters are working in an antiparallel way, getting only power through two diodes in one phase of voltage V_1. This mode of operation allows the AC-AC converters to approach the efficiency of the DC-DC converters very closely (Lucanu et al., 2017).

Figure 2.5:

Waveform of The V_{ac} Voltage, V_0 Voltage Current and i_0 Current, For D = 0.3 (Lucanu et al., 2017).

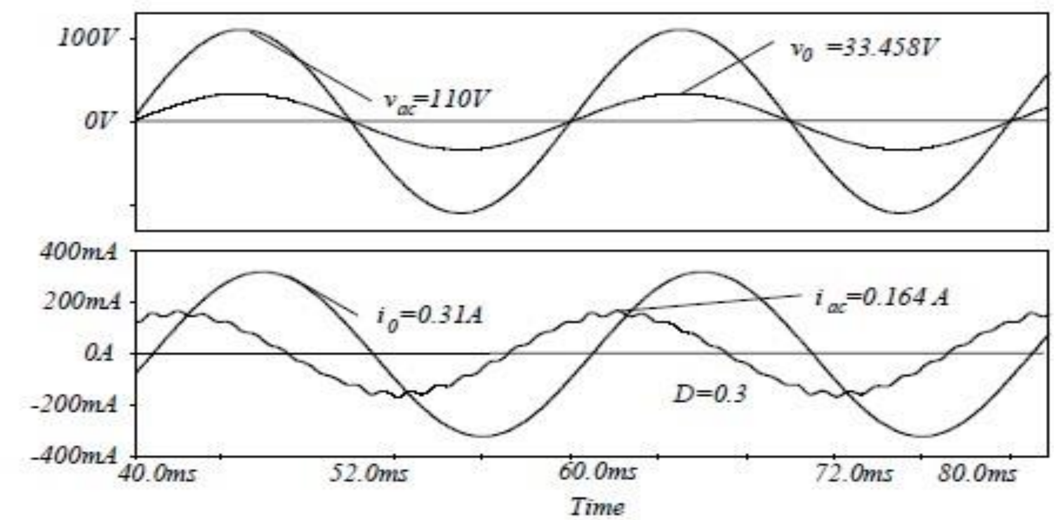

Figure 2.6:

Waveforms of The V_{ac} Voltage, V_0 Voltage, i_{ac} Current and i_0 Current, For D = 0.5 (Lucanu et al., 2017).

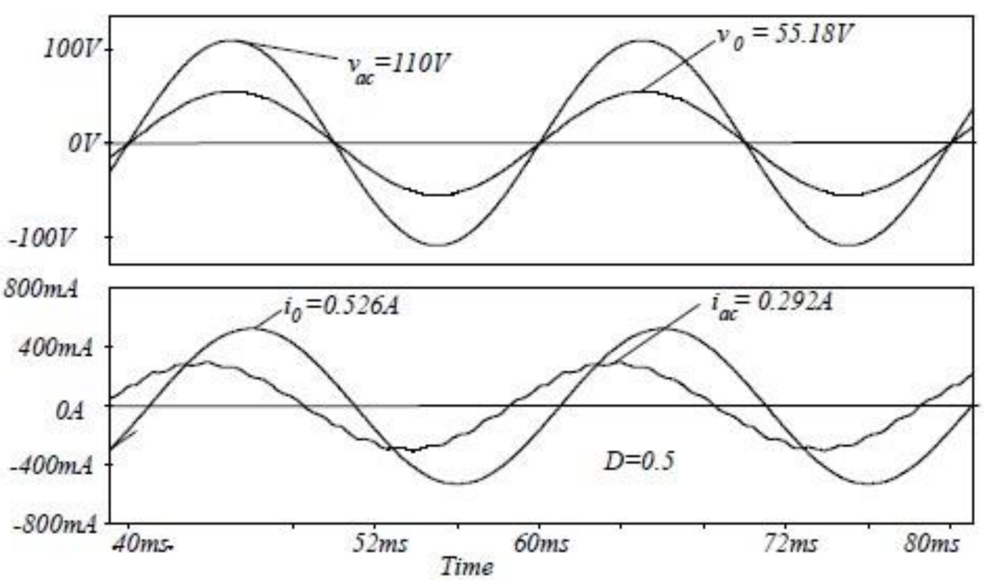

Figure 2.7:

Waveforms of The V_{ac} Voltage, V_0 Voltage, i_{ac} Current and i_0 Current, For D = 0.7 (Lucanu et al., 2017).

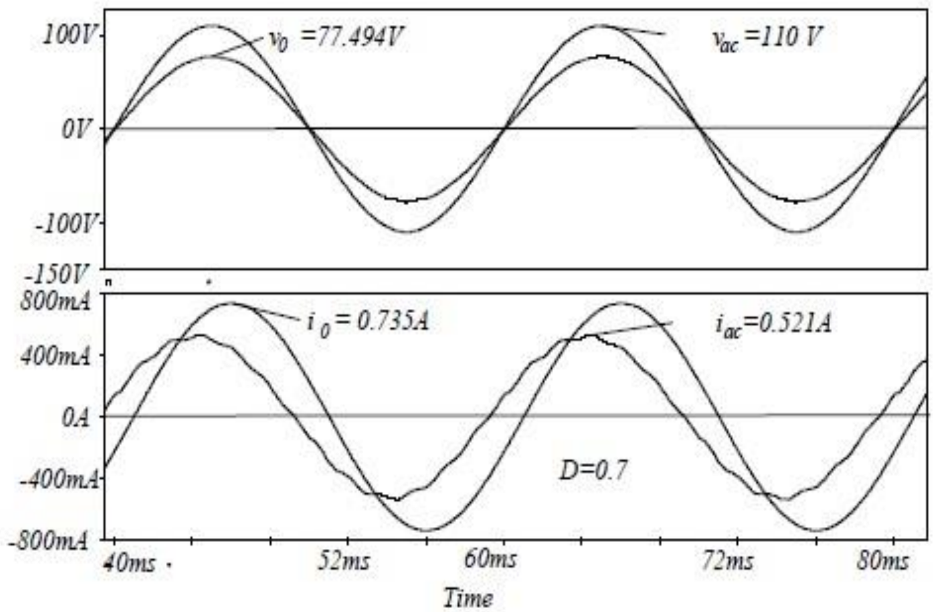

Regarding the result integrity of the circuit operation, it was checked by simulation which was performed in a resistive load R_0 = 100 ohm and an inductance L_0 = 100 mH. Inductor L_f input = 7 mH, capacitor C_f = output capacitor C_0 = 3.5 uF, : 10uF, the buck inductances L_1 = L_2 = 1.5 mH. The grid voltage amplitude is 110 V and the switch frequency corresponds to f = 40 KHz. The calculations were made for the following set of variables: cycle: D = 1/3, 1/2, and 2/3. The paper includes just few retrieved of waveforms, which include those that are the most indicative. In this case, the graph in Fig. 2.5 shows that the waveforms of operation are that of the Vac voltage at the grid side and the V_0 load voltage with the corresponding period and zero crossing. waveforms are the overall system frequency of the i_{ac} current and the i_0 load current. D = 0.3 (Lucanu et al., 2017).

2.3. AC Boost Voltage Regulator Transformer Less Based on Z-Source Network

This Z-source architecture is a main feature, which, beside capacitors, inductors and switches, includes a specific topology. This mesh network is all about semi-conductors, isolation and impedance matching capabilities for error-free power flow at both directions while also boosting the system's voltage at varying voltage ranges (Adel et al., 2023). The operations of the Z-source network are actively controlled through high-frequency switching devices MOSFETs and or IGBTs, which emit the controlled input signals resulting in the obtainment of the desired output power in efficiency. The controller achieves this through the switching frequency variety which is the function of adjusting the duty cycle of the switch. It has bidirectional power flow ability where the voltage is always regulated to meet load requirements in a wide range of input voltages. This capability is due to its suitability for applications in places where there is a likelihood of varying input voltages. The main point is that this device does not require transformers, hence it also eliminates power drops that usually appear during the process of voltage raise with the assistance of a typical transformer. As a consequence, the regulator is making the system up to 16% more efficient. Some examples are mobiles, electric vehicles or emergency supplies. Z-source power regulator in brief, displays its high features throughout power factor making it the efficient alternative for magic angle with other traditional AC-DC-AC converters. The results are of interest to engineers in power electronics technologies considering the prospects related to future applications and developments of this perhaps still nascent technology (Mousavi et al., 2022).

Figure 2.8:

Image Showing Block Diagram of The System Shown in (a). Switches as a Bi-polar Combination of Two IGBTs are Shown in (b) (Sonar et al., 2013).

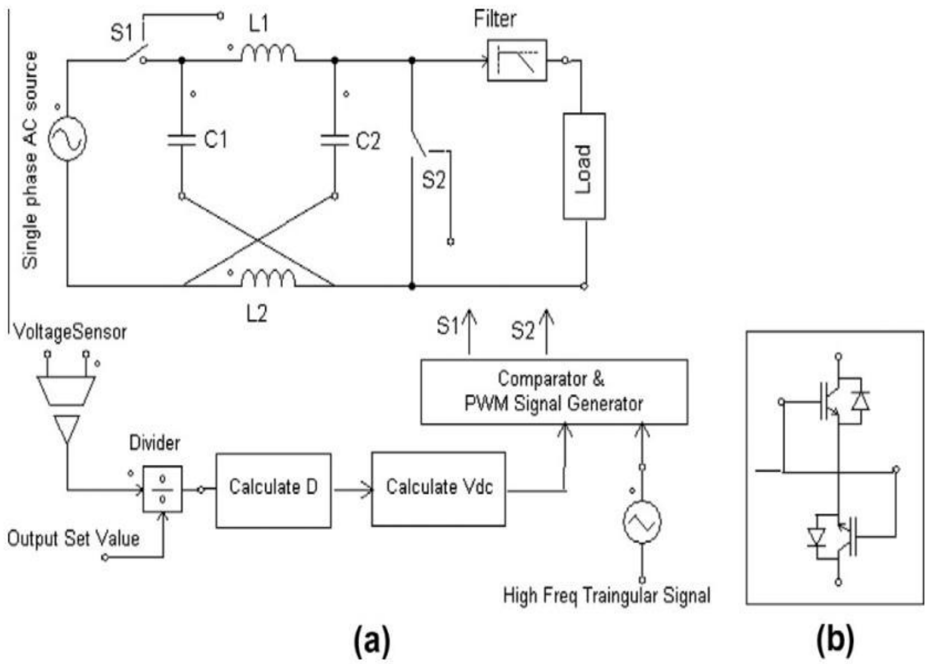

The regulator based on the Z-sources network has wide range voltage ac boost derived using single phase transformers less regulates the input voltage with high efficiency. The Z-source network is the central element of its function as its circuit composed of a capacitor, inductor, and switch set in an already-defined pattern. Power interchange in this network is twofold and is useful in transferring energy from the input side of the regulator to the output side. Thus, the input voltage is controlled by MOSFETs, IGBTs and pulse-width modulation to provide the desired output level with high accuracy (Sonar et al., 2013). The Z-source network utilize capacitors and inductors specifically for energy storage and energy transferral as well as voltage and current waveform control. The control algorithms of the advanced controller are monitoring the performance of the regulator, which is within the range of the voltage output and changing the states of the switches accordingly to meet the outcome it desires. This allows the feedback to be adjusted very easily and rapidly over a wide input voltage range and hence the type of regulator is suitable for a broad range of applications. In general, the converter covers the original features of the Z-source network besides sophisticated control approaches to yield more efficient, reliable, and versatile voltage regulation that not be too bulky and complicated as traditional transformer-based systems do (Wijekoon et al., 2008). Z-source network has a different circuit layout application which ensures that power can flow both backwards as well as forward and Boosting property of voltage can also be obtained. While a conventional voltage regulator, which across current direction only allows power flow, a Z-connected configuration-based voltage regulator provides a natural choke on the power values transferred between the input and output side with bidirectional functionality, applications that require energy feedback or generation such as regenerative brakes could be done, which is useful in electric vehicles (Mousavi et al., 2022).

Figure 2.9:

Equivalent Circuit During State 1 (a), and During State 2 (b) (Sonar et al., 2013).

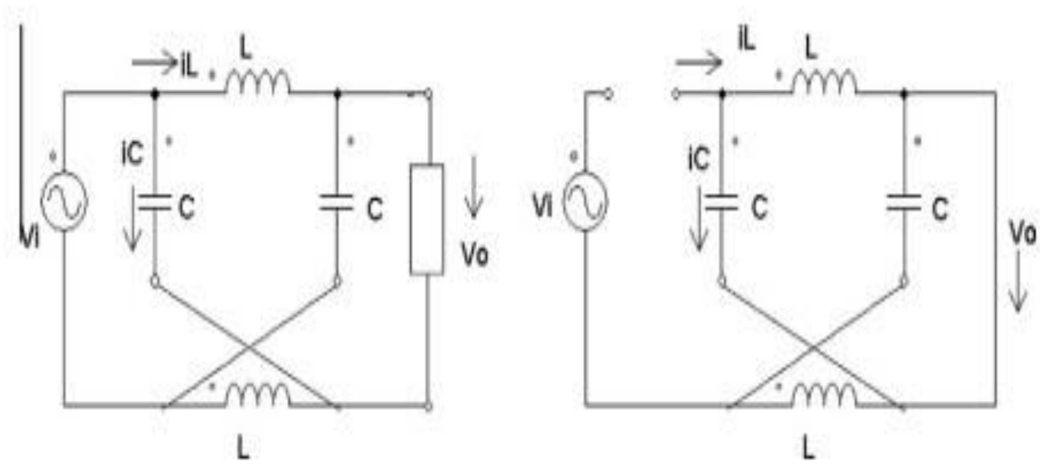

(a) (b)

In steady conditions, the Vav of the coil inductors during one cycle:

$$V_L = \overline{V_L} = \int [V_c . DT + (V_i - V_c)(1 - D)T]dt = 0 \quad (1)$$

Assuming that filter inductors and impedance inductors have very small value with no drop voltage across it, then the voltage across(Vo) will be the same as that across the capacitor (V_C) of the Z-network:

$$V_0 = \left|\frac{1-D}{1-2D}\right| V_i \quad (2)$$

Expressing duty cycle as a function of gain:

$$D = \frac{G-1}{2G-1} \quad (3)$$

The conceptual idea of operation of a bidirectional single –phase AC-AC converter is as a result of the AC input line signal, the z-network component, two switches, filter as well as the command unit. In this specification, it is possible to observe the load of the R–L series. The emphases lie here on the symmetrical Z-network, which can be assembled by connecting two inductors and two capacitors. With it, the basic working principle is to deal with the energy storing and releasing according to needs of the circuit till it has a smooth operation. Instead of the actual basic circuit with two switches and a control circuit, the substituted circuit was electronically installed to the main chip circuit through the PWM signal transmission route, which provides the main chip circuit with information regarding the upcoming voltage status (Vargas et al., 2009). S_1& S_2 (fig 2.9) are the switches that now make it possible to alternate the conduction of the current and the blocking of voltage in both directions. Thus, these two switches tag team each other with them being switched on and off. This therefore indicates that if you turn S_2 on with the duty cycle D, then you can turn S1 on with the duty cycle 1-D. Here, two IGBTs are arranged in the emitter-back-to-back mode in a common emitter configuration and two diodes are positioned, as depicted in Fig. 2.8 (b). Such an array of diodes is going to be employed to give the breakthrough function. The fundamental 'LC type' filter is the basic filtering, which obstructs or filters out the output voltage. In this case, the circuit has two possible states: one is called on-state and another as off-state. As well, fig. 2.9 (a) and (b) demonstrate the parallel and series circuits models and the configurations of such processes. Thus, utilizing both the infinity of the induction of L as well as C, the Z-Network would be of the same dimensions as the two segments L and C in isolation. As it is with the case of the state 1 with the duty cycle (1-D)T, where D is the duty ratio of switch S2 and T is the time for the switching cycle At this moment S1 is operating as a bi-directional switch and is turned on while S2 is turned off hence charging of the network capacitors is done through the ac source and the charge is transferred to the load through the inductors. (Mousavi et al., 2022).

Figure 2.10:

Generated Pulse Width Modulated Signal (Sonar et al., 2013).

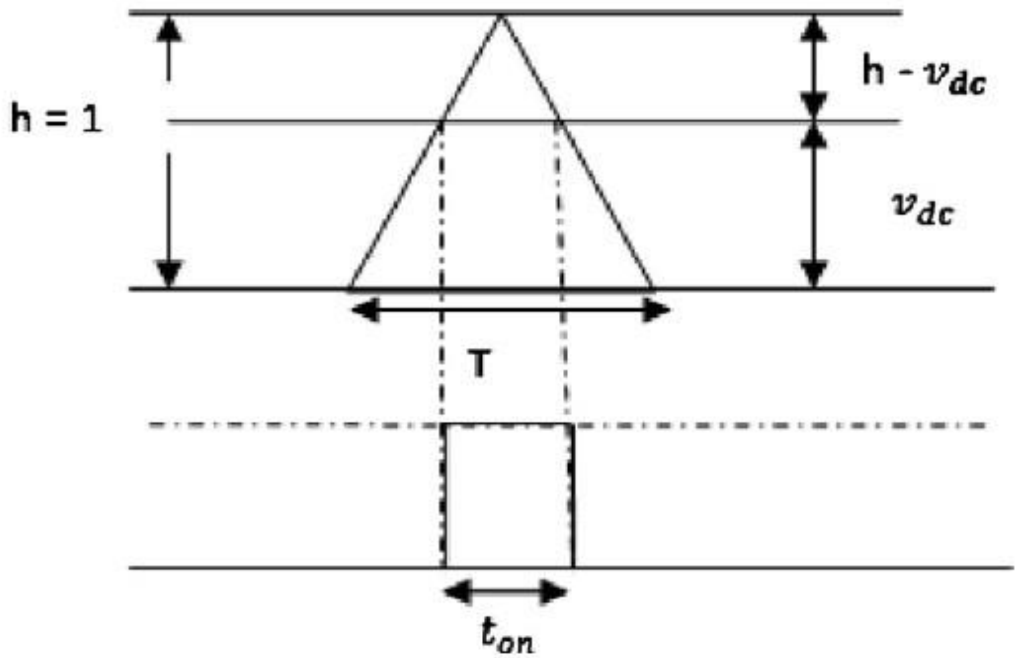

PWM signal is generated by applying triangular and dc signal comparison method

$$\frac{h}{T} = \frac{h - V_{dc}}{t_{on}} \quad (4)$$

$$V_{dc} = 1 - \frac{t_{on}}{T} \quad (5)$$

If peak value is unity.

$$V_{dc} = 1 - D \quad (6)$$

This category of converters operates based on increasing voltage performance leading to the best voltage step-up effect with the output voltage being higher than the input one. This is a quality that is particularly mind-blowing in the instances where the voltage at the output side is required to be greater than the voltage at the input side. It operates without traditional transformers as compared to the ordinary regulators that use transformers in their voltage conversion, (Peng et al., 2003). The absence of transformers allows the size, weight and cost of the inverter to be reduced. The end product is a compact and inexpensive method of power inversion which is crucial. To impose control over electric currents, the regulator employs active switching elements, such as MOSFETs or IGBTs to control the flow on a dual active bridge and Z-source network seamlessly. This is where these modular devices can make a difference because they switch with such speed; for effective voltage regulation. PWM is the control techniques whereby the output voltage of the given regulator is controlled through the act of controlling the switching devices' duty cycle. Therefore, through controlling the width of the switching pulses, the regulator might be able to regulate the amount of the output voltage adequately (Zarei et al., 2023). Professional capacitors and inductors are considered as the most crucial part of the Z-Network due to the functions of power storage, voltage and current control, respectively. Capacitors act as electrical energy rechargeable chambers that charges and discharges electricity serving it as a reservoir and Inductors margin out variations in currents and offer resistance to control currents. The Z-source voltage controller, therefore, enable conversing of a big range of input voltage magnitudes into reduced variations in the output voltage. This makes it's easy to implement in applications where the input voltage follows a low periodicity, for example in renewable energy systems or those with structures based on unstable gridlines This enables efficient voltage adjustment across a large range of input voltage (Babaei et al., 2015). With reduced size, weight, and cost compared to transformer-based regulators when adapted regulator makes possible smaller, lighter and cheaper system compared to the conventional system whose transformers are quite bulky, this has the advantage of making it more compact, lightweight, and cheaper because the chance of damage or defect is minimized, especially in applications where space or weight is crucial. With the utilization of complex control algorithms and PWM methods (Pulse Width Modulation), the regulator can obtain the accurate management of voltage level. It guarantees operation to be consistent and reliable, although the load is varying and the input voltage is fluctuating.

The system shown is flexible and also has economic features that complete the modern electricity systems. Voltage regulation efficiency can be improved and energy consumption can also be reduced by eliminating old-fashioned, bulky and very demanding devices such as transformers. Such advantages move in the direction of energy efficiency. It is crucial in lowering greenhouse gas emissions and energy consumption, which lessens the impact on the environment (Mousavi et al., 2022).

2.4. AC–AC Converter Without Commutation Problem

The single-phase AC-AC converters of high-efficiency type without commutation problem give a meaningful advancement to power electronics, at least in the AC voltage conversion where there are no downsides of commutation. These converters have several advantages such as better efficiency, less complexity and reliable performance. Such converters differ from the traditional AC-AC converters by eliminating commutation which functions via a commutation process involving switches or diodes to preserve the correct polarity of voltages and phase synchronization. Unlike other types, these conversions neither require a commutator nor diodes. This condition eliminates switching losses connected with a full unity power factor operation, causing no significant power loss (Khan et al., 2016). In many cases, highly efficient single-phase AC-AC converters using direct conversion techniques, which make commutation problems redundant, are a bad choice. The latter benefits of this method are facilitated by the fact that it reduces the number of converter components and therefore both involved complexity and cost which make a direct conversion approach. It improves power conversion efficiency by eliminating low power dissipation at commutation and can achieve higher overall efficiency than and play design of modern power filters (Ahmed et al., 2019). The significance of this lies in the fact that it is useful where energy efficiency is vital, for example, in renewable energy systems, motor drives, and power supplies. Enhanced reliability by a simple configuration combined with less component quantity that improves reliability and robustness. The number of system components that might fail is decreased which inevitably leads to the minimizing of the need for inevitable downtime and maintenance. Therefore, the system's uptime and lifecycle duration are extended (Colak & Yildirim., 2010). This opens a wide range of applications like energy saving, single-phase AC-AC converters that do not have a commutation problem, which find areas of use in industry, consultation, and so on. Appliances, HVAC systems, lighting controls, industrial automation, and grid-tied inverters for renewable energy. Top-rated AC-AC single-phase converters without commutation problems are a perfect solution for multiple industries and sectors. They are commonly employed in consumer electronics and energy systems (e.g., grid-tied inverters and solar inverters), industrial automation (PLCs), uninterruptable power supplies (UPS), and EV charging stations. These magnetic devices often use sophisticated control methods like pulse width modulation (PWM), phase shifting modulation, or resonant clipping that enable the fine-tuning of the voltage, and help to achieve high efficiency. This regulating role of these devices guarantees constant and consistent performance under different load conditions and input voltage fluctuations (Liu et al., 2012). This converter act as the key element in the smart grid power conversion approach. This refers to their ability to transmit power without communication effects makes them work well when interconnected to ultimately the grid, and microgrid systems. Thanks to them smart grid systems become more reliable in combining renewable energy sources with grid stability improvement and the creation of efficient energy management solutions. These technologies allow for integrating their operations with the grid which involve a grid-tied mode of operation, voltage regulation, frequency control, and power quality improvement thereby contributing to the overall reliability and sustainability of the grid (Colak & Yildirim., 2010).

Figure 2.11:

Image Showing Different kinds of Traditional Converter: (a) DC-DC, (b) AC-AC and (c) AC-AC Switching Cell (Khan et al., 2016).

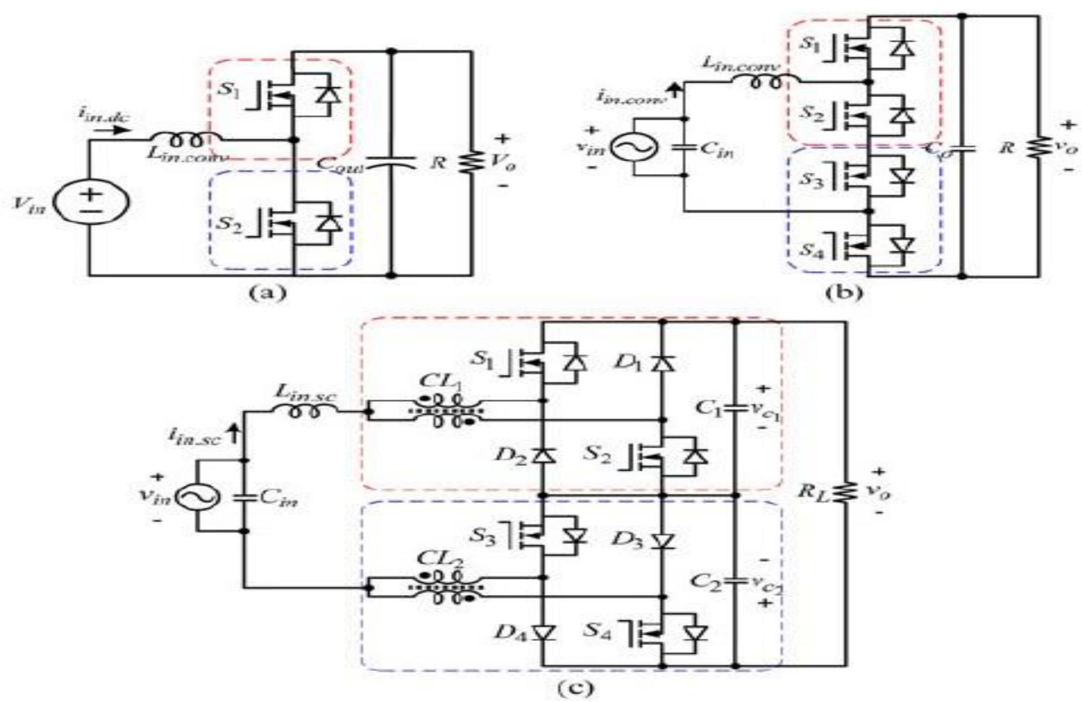

The direct PWM AC-AC converters are categorized into the direct topologies and placed in the simplest category of converters. Despite the fact that they were obtained from the basic DC-DC converters through adaptations, the use of AC switches caused them. The single-phase boost type DC-DC converter is shown in the Fig 2. 11 (a); the Single-phase AC- AC type converter is depicted by Fig 2. 11 (b). Nevertheless, the switches of this converter are series-connected, still they are of invalid operation under commutation trouble. The switches ((S_1, S_4), (S_2, S_3)) are controlled on/off complementarily like that the gates of a converter being always with ideal inputs and it will operate properly, otherwise commutation problem will occur (Fig.2.11 and Fig.2.12). However, the non-drifting of drive circuits and switch devices is overlaid in another. This will lead to jumps (di/dt) and voltage spikes (dv/dt) due to overlapping period and the dead zone shown in (Fig. 2.12(a)) and (Fig. 2.12(b)) respectively which result in damaging the semiconductor devices. Hence, the overlap and no-load situation of the switches is one of those factors which maintains the low efficiency of traditional AC– AC converter and therefore its use is very needed. In general, AC-AC power converters without commutation problems of high-efficiency single-phase type give a tremendous impact to the power electronics technology, resulting in increasing efficiency, reliability, and versatility for many applications. Research and development of this field are predicted to go on for a long time and at the end of it all, better performance and applicability of the converters in future energy systems can be expected. Regarding commutation mechanism, conventional AC-AC converters process commutes using usually used switches or diodes to guarantee the right voltage polarity and phase synchronization. These converters contrary to commutation problem status, a commutation mechanism is neglected, either through the use of alternative circuit topologies or through control strategies that do not require switching between different components.

Figure 2.12:

(a) Commutation Problem in Overlap Time. (b) Commutation Problem in Dead Time (Khan et al., 2016).

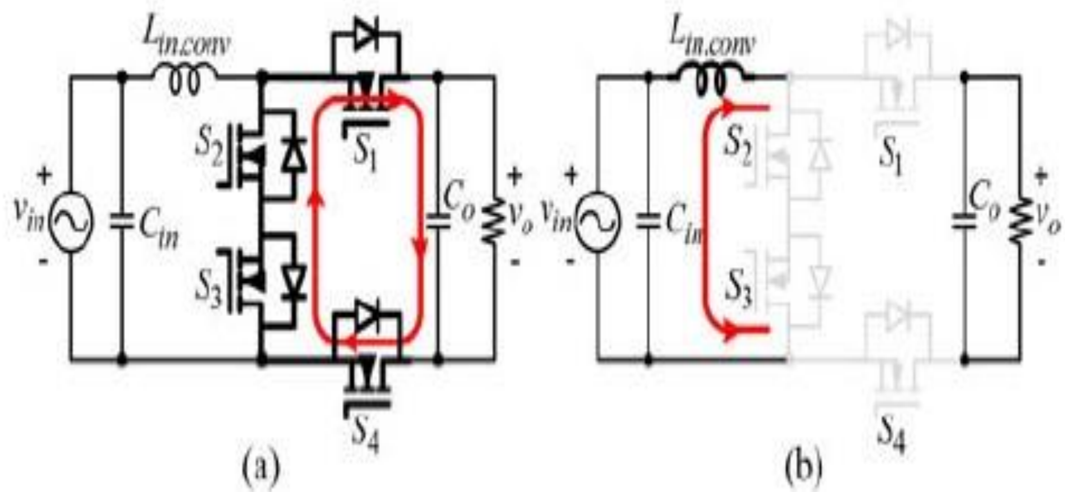

Besides, in such circuits, only those circuits which do not contain a commutation free circuit with a good or geometric circuit are used. Some of these might be; restructure of resonant converters, direct AC-AC conversion or topological structures involving PWM or phase shift modulation. This is to mean that advance control keeps the voltage in a desirable range near the amount of voltage needed to sustain the operation and shocking without commutation (Lucanu et al., 2014). Maybe it could do so in a way that it regulates or maintains other characteristics such as output voltage, frequency, and phase angle constant then ensure that in the event it is presented with varied levels of loads and several voltage conditions, it enjoys sufficient stability. Such components as switch, capacitor and Inductor are switched in a certain extent for this special role of commutation free operation as stated above. The On/off time and the on-state voltage drop are reflected as parameters of power dissipation which are still possible to minimize by the components that are aimed to help to achieve the maximum efficiency of the system (Babaei et al., 2023).

Figure 2.13:

(a) Buck-Type AC–AC Converter with Reverse Recovery Problem. (b) Occurred Problem When Switch S_1 is on (Khan et al., 2016).

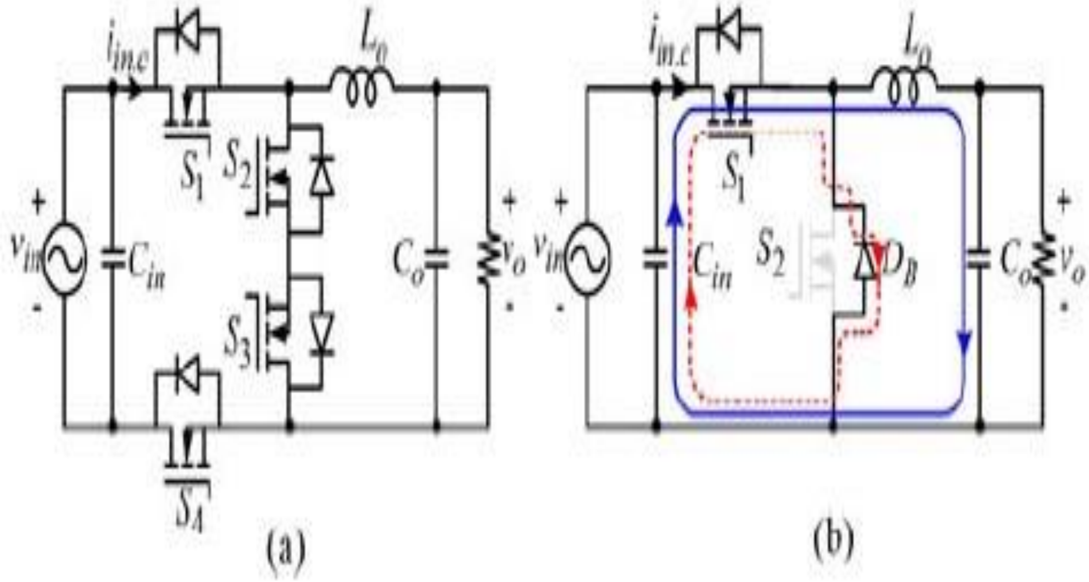

Figure 2.14:

Two Types of SCs (Khan et al., 2016).

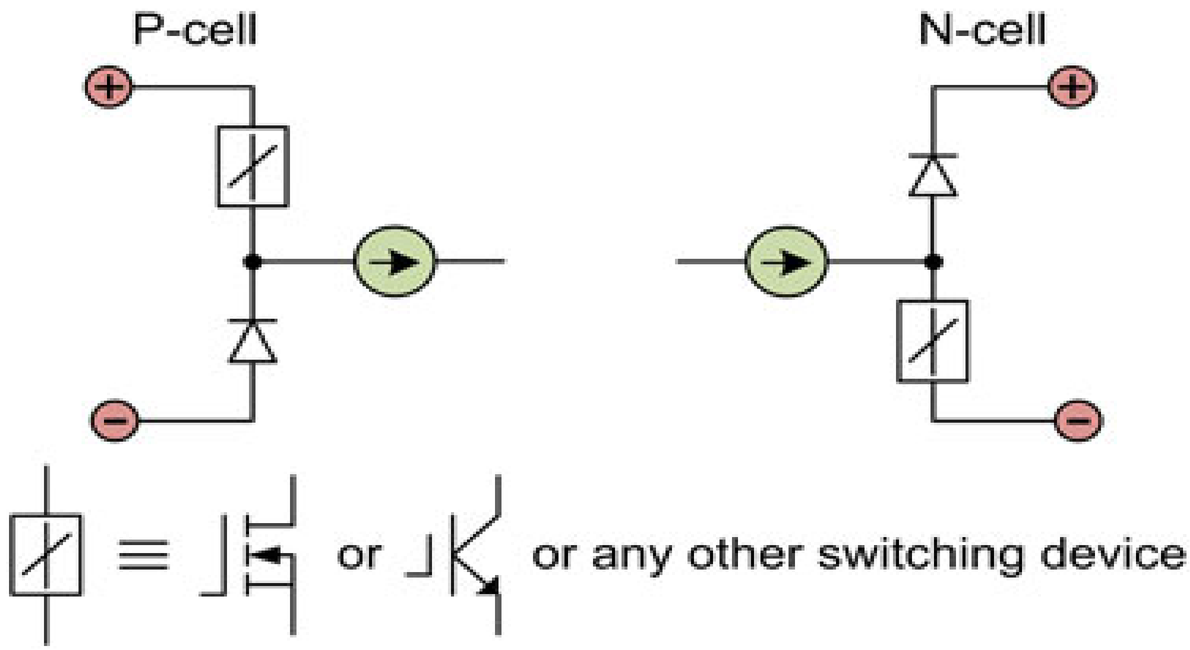

The SC construction demonstrated in Fig. 2.14 could eliminate this issue from its root. As shown in Fig. (2.14) P and N-type semiconductors are the two types of SCs. The IGBT and the MOSFET act as the switching devices, whereas the freewheeling diode is connected in series to an inputted external diode. In the case of P-type SCs, the positive terminal of either the current source or inductor is connected to the common point where in N-type SCs it is the opposite, the negative terminal is connected to the common point. Thus, making use of the SC structure for producing converters will help get rid of the current shoot-through issue. This current sustainable shift is made possible by soft conversion techniques have been investigated to see if they provide a possibility of safety commutation and do not have lossy snubber circuits. Voltage-current sensing modules are used in these methods to enable the switch devices to function as intended. On the other hand, the sensing modules just lead to an increase in expenses, and the controller needs to be more complicated overall and continue to influence the degrees of dependability and safety particularly when the distortion input voltage is cut off next to the zero-crossing line. Similarly, built-in protection cannot be supplied for this type of approach either, since the protection provided is the same as that of RC snubbers. To shoot through at low current power where signals have been misread as a result of radio interference, the body diodes are parallel or antiparallel with the metal-oxide-semiconductor (MOS) while the latter proves to be not dense enough to achieve the required accuracy and true signal required for neural networks (Li et al., 2012). Within its outstanding features, it includes what's known as the recharge component that leads to the lower capacitance when the voltage is to transition; as a result, the insulated gate like IGBTs (gate bipolar junction transistors) are the choice options that is used in hard switching instead of environmentally obsolete devices. Seeing Fig. 2.14, it interprets the reverse recovery effect, the converter rectifies the AC on the output side with the help of the body diode of the MOSFET, which is a classical buck-type converter. Switches S_3 and S_4 are activated for the secure passing when $v > 0$. To avoid the shuttle, there is a finite dead time between S_1 and S_2 to work and the current flows of inductor in the body diode DB of S_2 during the dead time. As for S_1, it takes more time after the deadtime to turn it on due to reverse recovery current of DB during this period which is shown in Fig. 2.13(b). For that reason, the synchronous buck converter switches and the diodes operate with over-current spikes. The functioning of the current transformer (CT) consists of shorting out the current through the secondary during the initial period after the system upset is experienced, during which, the S_1 is activated at the same instant the polarity of the system source is reversed (recovery process is indicated in Fig. 2.13(b)). This is why the case of a reverse recovery has to be factored in. Fig. 2.14. Converters are particular in terms of how they operate, such as reaching a specified voltage, efficiency, and power factor correction. They are designed to provide a constant voltage output having ideal distortion figures and low harmonic content while having an efficient transfer of energy. As aside of perks, these converters could also encounter difficulties like affordability, complexity and reliability issues. Both the converter's topology and implementation technique are critical, requiring attention regarding the choice of component, the control strategy, and thermal management, to ensure efficiency and reliability (Vargas et al., 2009). Thus, narrowing down the AC-AC converters might be figured out by increasing the efficiency, compressing the costs and expanding the application area. This may bring about the designing of novel semiconductor materials, improved control methods and highly innovative circuit structures that will change the way the limitations of energy conversion and management are seen, thus resulting to the unleashing of new opportunities.

2.5. Z-Source PWM AC-AC Converters

The single-phase AC-AC Z Source PWM type is an improved answer regarding power electronics engineering because it is a more efficient and adaptable solution for voltage transmission using single-phase AC systems. This source of energy utilizes a unique circuit arrangement of a Z-source network with the support of PWM technology which facilitates the bidirectional power flow with a precise voltage control. Essentially the backbone of this converter is the Z-Source network that consists of capacitors, inductors and switches which are positioned at key places for bidirectional energy flow to be feasible. In comparison to the topologies of conventional converter networks, the Z-Source network allows energy to flow in both directions between the input and the output sides, which not only offers versatile applications, but also enables energy feedback, or regeneration, as in the case of electric vehicles (Li et al., 2012). Capacitors and inductors are vital parts of the Z-Source network that not only supply the energy but also smoothen the voltage and the current. Besides, capacitors store and discharge power, whereas inductors regulate current motions to control energy and reduce losses, allowing a progressive energy transformation. The utilization of PWM control methods becomes critical for the transformation of the converter output voltage. Thanks to the variable duty cycle of the PWM signal that is applied to the Z-Source network microprocessor-controlled switches, the converter can change the output voltage with high precision. This type of control realized the purpose of effective and precise regulation of the voltage usually over a broad range of inputs and outputs, leading to a wide improvement in functional aspects (Fang et al., 2005).

The advent of single-phase Z-source PWM AC-AC converters demonstrates the high level of engineering competence in the field of power electronic engineering, as it proposes a highly advanced solution for fine and efficient AC voltage regulation or control in single-phase AC systems. These converters feature advanced designs which are carefully configured to take advantage of the Z-Source network together with Pulse-Width Modulation (PWM) control techniques. Hence, the resultant system not only enables a bidirectional flow of power but also ensures perfect voltage regulation under varying conditions (Fang et al., 2005).

Figure 2.15:

(a) Voltage-Fed Single-Phase Z-Source AC–AC Converter, (b) Current-Fed Single-Phase Z-Source AC–AC Converter (Fang et al., 2005).

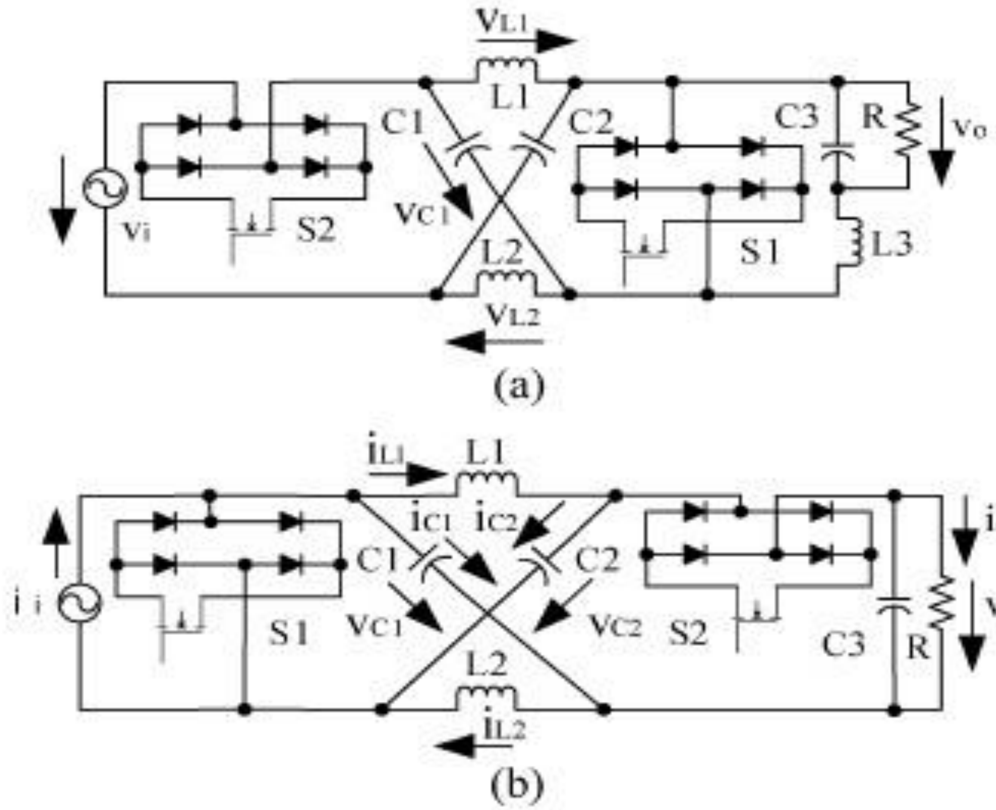

Fig.2.15 (a) and (b) include the Z-source voltage-fed or current fed single-phase PWM Buck-Boost as well as the typical Buck-Boost converter. On the other hand, both modes of operation have two active elements (i.e., S_1 and S_2), their ranges of operation are expanded with the use of the full bridge diode which serves as a bi-directional voltage barrier and current path. They are tiny for the elimination of ripples arising from possible unexpected shifts in load demand. Symmetrical Z-source network AC-AC converter is single-phase with a transmission unit built of two inductances with two capacitors as an AC frequency controller. The frequency switching of inverter is high and lap power capacitance and inductance of inductors and capacitors are inversely national (Fang et al., 2005). With the help of the PWM duty ratio, the proposed AC-AC converters may carry out almost the same level of precision as the standard DC-DC converters. Figure 2.16 shows the common switching functions of the grouped AC-DC converters, S_1 and S_2 are flipped by complement as shown in Fig 2.15 and Fig. 2.17. This little snubber circuit

should be added because it helps the commutation and reduces the excepted switching losses and error.

Figure 2.16:

Duty-Ratio Control of Z-Source AC–AC Converters (Fang et al., 2005).

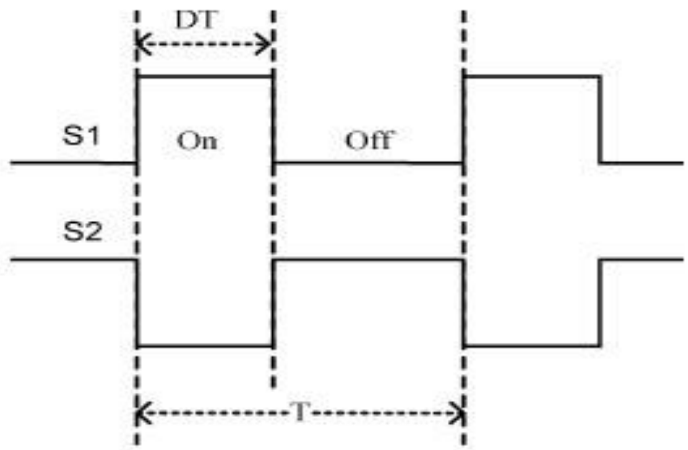

Figure 2.17:

(a) State 1. (b) State 2 (Fang et al., 2005).

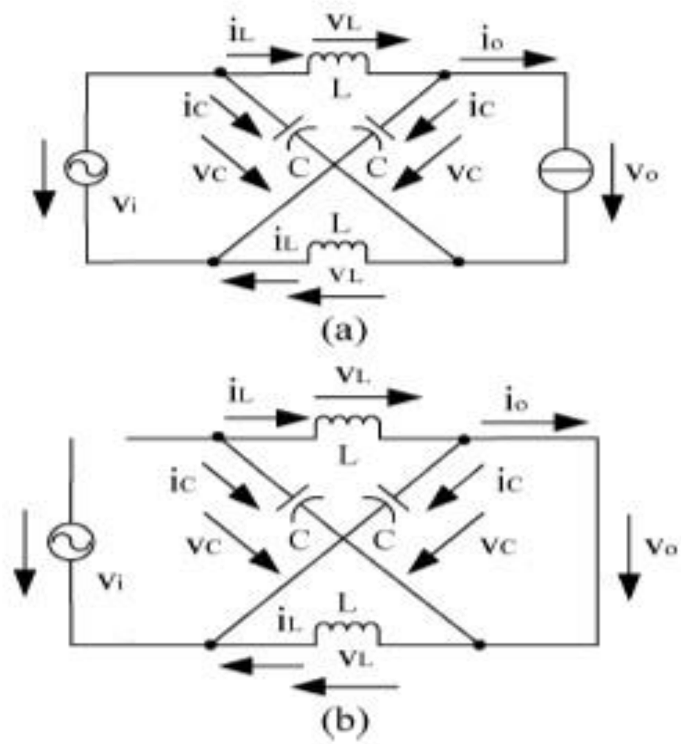

In State 1, the bidirectional switch S_1 is in an off condition and S_2 is in an on condition. An AC source that is utilized for charging the Z network capacitors, whereas inductors discharge and deliver energy to the load. Duty cycle of the converter is expressed as (1-D)T, where T is the successive toggling period and D is the duty ratio of switch S_1 shown in Fig.2.17(a).s

$$V_c = V_i - V_L \quad V_0 = V_i - 2V_L \tag{1}$$

In state 2, S_1 is turned on and S_2 is turned off. But as inductors charge and collect the energy, the Z-network capacitors discharge their own. As seen in Fig. 2.17(b), the period of the operation stage when the converter is in this mode is DT.

$$V_C = V_L\,,\ \ V_0 \tag{2}$$

Ignoring the basic voltage loss, the average voltage of the inductors for one AC line period in steady condition should be zero.

$$\frac{V_C}{V_i} = \left|\frac{1-D}{1-2D}\right|, \text{ when } D < 0.5,\ \emptyset_c = 0, \text{ and when } D > 0.5,\ \emptyset_c = \pi \tag{3}$$

Taking into account the smallness of the filter and the inductor of the Z-network and also the lack of any line frequency drop voltage over the inductor, the load voltage must be the same as Vc, the voltage across the Z-network's capacitor.

$$V_0 = \left|\frac{1-D}{1-2D}\right| V_i,\ \emptyset_0 = 0 \text{ For } D < 0.5\text{ ,and}\emptyset_0 = \pi \text{ For } D > 0.5 \tag{4}$$

In the end as a result

$$V_0 = \frac{1-D}{1-2D} V_i \tag{5}$$

The Z-Source network which is meant to be the core of these converters is an intricately designed circuit arrangement that has capacitors, inductors, and switches organized in a strategic position. This network replaces the classical approach in power conversion by allowing the exchanging of energy, not only from input to output but also in the opposite direction and stands out with the impedance networks that help either voltage boost or buck, depending on the needed one. Therefore, such two-way characteristics are critical, especially in applications where the energy feedback or regeneration is essential like regenerative braking systems for electric tramways or renewable energy systems. Also, the feature of PWM control systems to regulate the voltage precisely, makes these converters even more functional and efficient. In the microsecond scale, by defining the duty cycle of the PWM signals transmitted to the switches in the Z-Source network, the converter can precisely set the output voltage level to meet the needs of the load. It not only gives all the efficiency but also enables the system to manage fluctuations in input voltage and load conditions that result in the symphony of the overall system (Geng et al., 2013).

PWM control methods are subject to major pinpointing applications in managing the output voltage from the converter with the provision of programmable accuracy. Adjusting the duty cycle of PWM signals sent to the switches that are part of the Z-Source network will enable modulation of the voltage level emitted to the required levels. This has the effect of voltage regulation that is economical and helps to achieve high precision and selectivity for a wide range of input voltages and power conditions. To compensate for the high-speed switching, there are MOSFETs or IGBTs within the Z-Source network, which regulate the course of electrical energy flow. They are rightly employed to do PWM control and subsequently enable power flux in both directions. Relying on dedicated algorithms that are meant to observe and control the following parameters, the output voltage, the output current, and the frequency as well. The control algorithm continuously adjusts the instructions to the switches based on the incoming sensor signals. Since computations deal with load requests and utter volatility of input, the system maintains stability and reliability even under changing load conditions and fluctuating input levels (Adel et al., 2023). Most importantly, the strategic layout and the optimization of the Z-source network topology play a huge role in achieving an efficient and secure operation. Taking into account such factors as cut-off rate, control and strength of the system component is necessary for maximizing overall system output. Thereby, minimization of power waste is one of the main goals to be accomplished during the design process. Modulation Techniques: On an additional note, in addition to PWM other modulation techniques like phase shift modulation or resonant modulation can also be considered in the quest to find the right balance between efficiency and performance. These techniques are constituted by varying the timing or phase angle so that the signals are being exactly in phase to achieve particular control goals (Adel et al., 2023). Through the completion of these functions and methods, this converter is capable of providing efficient, adjustable, and reliable voltage regulation within single-phase AC systems. A remarkable trait of the Z-Source PWM AC-AC converters is their ability to adapt to different voltage ranges as far as input and output are concerned. These converters are suitable in all the applications where there is need of a constant and quality power supply since they control the voltage boosting or bucking without needing other controls through the usage of the Z-Source network. In addition, the matter of applying the simplified topology and the reduction in the number of components consolidates the reliability and sturdiness of the unit in a very significant manner that it can be capable of carrying out the function regardless the conditions of the environment in which it finds itself even if such environment is highly dangerous. The discussed converters can be used in a number of areas including renewable energy sectors, grid connected power converters, induction motor drives, UPS systems, and electric vehicle charger systems. Such fixed characters as efficiency, reliability, and flexibility embedded in their engineering system permits them to occupy the hill of the most advanced power systems hence, outfitting them to address the requirements of the evolving energy market. This single-phase Z-Source PWM AC-AC converter creates a number of systems and apparatus that precisely regulate the voltage in and within the unipolar AC matrix by using power conversion and control techniques. Some of the advantageous properties of converters include the following: Single phase Z-Source PWM AC-AC converters can be designed and planned manually depends on the different input and output voltage levels. Moreover, due to these interlinking structures and fewer elements integrated in the circuit, the failure ratio and life span of these regulators are affected. Based on this, their engineering ability together with other attributes of power system elements such as efficiency, reliability and flexibility can position them as the dominant elements in the structure of modern power system that is in line with the requirement of energy today's world as we continue from day today.

CHAPTER III

Proposed Topology and Simulation Results

3.1.Introduction

A well-known AC-AC converter with an integrated Z source and buck-boost works great by converting power using impedance networks that have a very special effect. Different than the traditional one-way AC-AC converters that exist currently, this algorithm stands as bidirectional which means that it can both step up the revenue of the input and also step it down. This part including the configuration of Z-source converter focus on unique properties like the impedance and wide voltage variations. Also talk about the control algorithms that are in place to regulate the operation of the converter which involves modulation techniques for attaining the desired output voltage and current waveforms and describe how the control system checks the duty cycle of the switching signals and determines if the output voltage and current levels are appropriate, during the same instant ensuring efficient transfer of energy between the input and output. Moreover, it shows modeling and simulation of the converter system using PSCAD by providing the needed process. This makes the next vital stage to ensure a proper implementation of different duty cycle and frequency. Elaborate the results obtained for the experiments testing the active duty of AC-AC Z source with buck-boost functionality. Verification of results by testing various techniques and evaluation both efficiency, reliability and performance. Show the results of the experiments, by comparing the measured performance metrics (e.g. efficiency, voltage regulation, and harmonic distortion), from the theory and the real-life values, to evaluate the accuracy of the model.

3.2.Power Circuit.

The circuit configuration of the proposed converter under name: single-phase AC-AC z-source converter with buck-boost capabilities is illustrated in Figure (3.1). It comprises two primary components: the impedance block and the H-bridge cell, along with the power supply link. This configuration contains four identical inductors (L_{1N}, L_{2N}, L_{1P} and L_{2P}), three capacitors (C_N, C_P and C_L), six controlled switch (S_{1N}, S_{1P}, S_1-S_4) and ten diodes (D_{1N}-D_{5N}, D_{1P}-D_{5P}) connected together. The converter source network is an essential element in the process of voltage regulation, both providing the potential boosts and bucks in the voltage regulation scheme. It's divided into two segments: the N-Z_{AC} and the P-Z_{AC}. Elements of the N-Z_{AC} and P-Z_{AC} networks can be seen in Figure (3.1). These networks being the operating forces are responsible for the triggering of positive and negative responding elements in the process of internal cycles perception. Consequently, the basic cell of the H-bridge is connected to the positive and negative terminals of the output impedance source (J_1 and J2) via low-frequency switching. At this instance, the output terminals are demonstrated and is shown in Figure (3.1), the H-bridge cell. Inductions L+ and L- are not only safe release paths of capacitances C_N and C_P but also are involved in load current keeping the current on both sides of system current continuous.

Figure 3.1:

Power Circuit of Impedance-Source AC-AC Converter (Rahman et al., 2019).

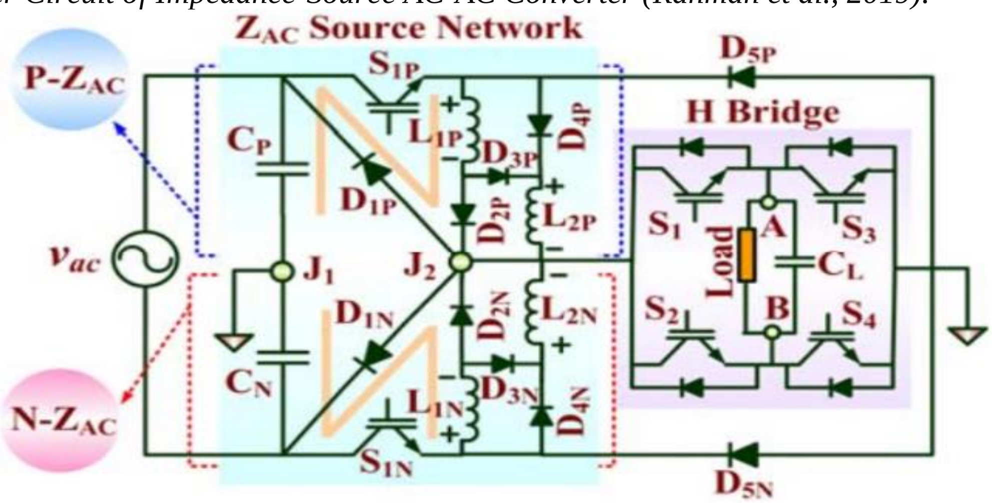

3.3. Switching Logic and Operational Principle

Figure (3.2) shows the actual way of logic switching being used in order to generate voltage at the output side with same,double or half of the input frequency. Here, it is supposed that the load is linked to terminals A and B, exhibiting [V_0,V_{AB}] for the voltage at the output side. To get two logic levels for switches S_{1N} and S_{1P}, a high frequency triangle carrier waveform which is compared to another will be used. Thus, the periods of output can adjust to either be identical or different to the periods of the input by N times or 1/N times respectively. Working at lower switching frequency, S_1 and S_4 are operating like S_2 and S_3 which are complementing each other to transform the input waveform into the desired output frequency. Thus, we would consider the methods of the output voltage producing at the same switching frequency (F_S) as the input. In this regard also makes sense the method of generation and the output voltages through different frequencies. The converter operation is the repeated switching of positive or negative pulses of the voltage at the output side (at any frequency), which is demonstrated by the given logic switching as shown in the figure (3.2).

Figure 3.2:

Logic Diagram For The Switching of The Converter Presented (Rahman et al., 2019).

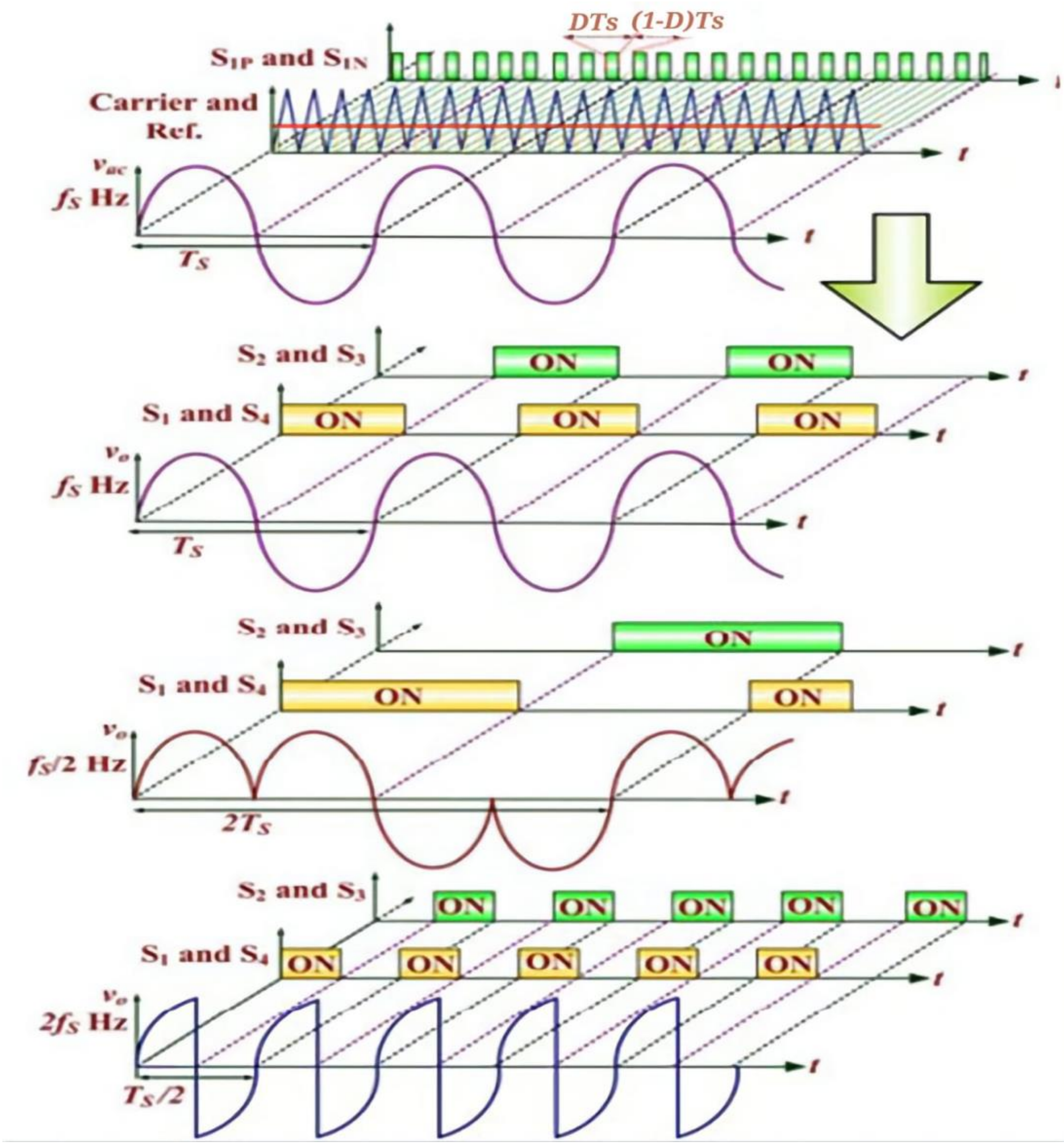

3.2.1. Generating The Positive Part Of The Cycle

The positive cycle of the output voltage V_0 is generated by turning on switches S_1 and S_4 while keeping S_2 and S_3 OFF, where switch S_{1P} controls the voltage range of V_0. Under the positive cycle's there are two modes of operation:

A. **Mode 1:** During a DT_S period where switch S_{1P} is turned on.

B. **Mode 2:** During a $(1\text{-}D)T_S$ period where switch S_{1P} is off.

The input voltage is during the positive part of the cycle (V_{AC}>zero).

A. Mode 1:

Figure (3.3.a) represent the corresponding circuit for mode 1. Inductors L_{1P} and L_{2P} with parallel connection with the input voltage are being charged and diodes D_{1N}, D_{2P}, and D_{4P}

are forward-biased when switch S_{1P} is turned on. The paths V_{AC}-S_{1P}-D_{4P}-L_{2P}-D_{1N}-V_{AC} and V_{AC}-S_{1P}-L_{1P}-D_{2P}-D_{1N}-V_{AC} are used to charge inductor L_{2P} and L_{1P}, respectively. Switches S_1 and S_4 are switched on simultaneously, and capacitors C_N and C_P discharge the energy they have stored across the terminals A and B (output).

Applying KVL to the equivalent circuit of mode one, the mathematical expressions for the voltages across the inductors and capacitors are as follows:

$$v_{L,1p} = v_{L,2p} = v_{ac} \quad (3.1)$$

$$-v_{C,p} + v_{L,1p} + v_o = 0 \quad (3.2)$$

$$-v_{C,n} - v_{ac} + v_{L,1p} + v_o = 0 \quad (3.3)$$

By substituting equation (3.1), the following relationships are obtained

$$v_{C,p} = v_{ac} + v_o \quad (3.4)$$

$$v_{C,n} = v_{C,L} = v_o \quad (3.5)$$

We can write after applying (KCL) to the equivalent circuit of the first operating mode the corresponding equation:

$$i_{C,n} = i_{C,p} = i_C \quad (3.6)$$

$$i_{ac} = i_C + 2i_{L,2p} \quad (3.7)$$

$$i_{L,1p} = i_{L,2p} \quad (3.8)$$

$$i_{C,L} = i_o = -\frac{v_o}{R} \quad (3.9)$$

B. Mode2:

Figure (3.3-b) represent the corresponding circuit for mode 2. Inductors L_{1P} and L_{2P} are discharged in series across switches S_1 and S_4, diodes D_{3P} and D_{5P}. Diodes D_{3P}, D_{5P}, and D_{1N} works as forward-biased when switch S_{1P} is off. Capacitors C_N and C_P are simultaneously charged by the series connection of L_{1P} and L_{2P} across diodes D_{1N}, D_{3P}, and D_{5P}.

Applying KVL to the equivalent circuit of mode two, the mathematical expressions for the voltages across the capacitors and inductors L_{1P} and L_{2P} are as follows:

$$v_{L,1p} + v_{L,2p} = -v_o \quad (3.10)$$

$$v_{L,1p} = v_{L,2p} = -\frac{v_o}{2} \quad (3.11)$$

$$v_{C,p} = v_{ac} + v_o \quad (3.12)$$

$$v_{C,n} = v_o \quad (3.13)$$

We can write after applying (KCL) to the equivalent circuit in the second operating mode the corresponding equation:

$$i_{L,1p} = i_{L,2p} = i_{C,L} + \frac{v_o}{R} \tag{3.14}$$

$$i_{C,n} = i_{C,p} = i_C = i_{ac} \tag{3.15}$$

Figure 3.3:

Equivalent Circuit of The Impedance-Source Converter For The Positive Part Of The Cycle Operation; (a) Mode 1, (b) Mode 2 (Rahman et al., 2019).

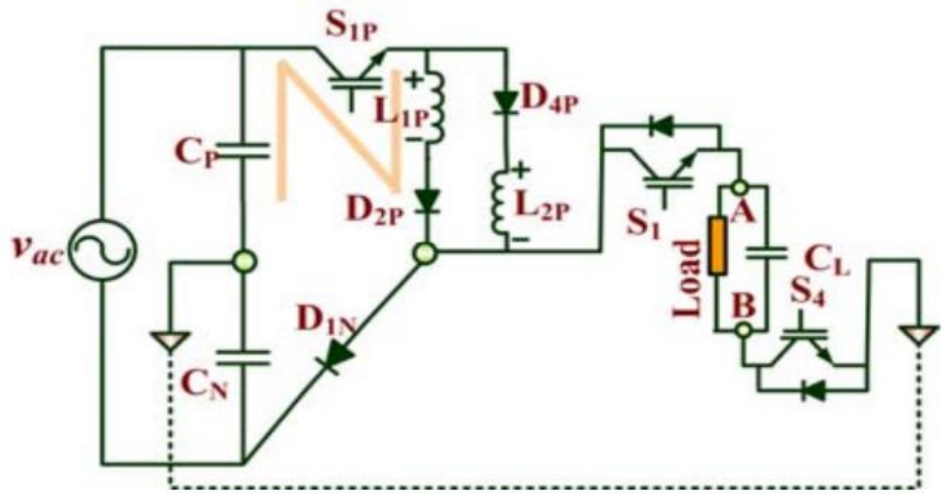

(a)

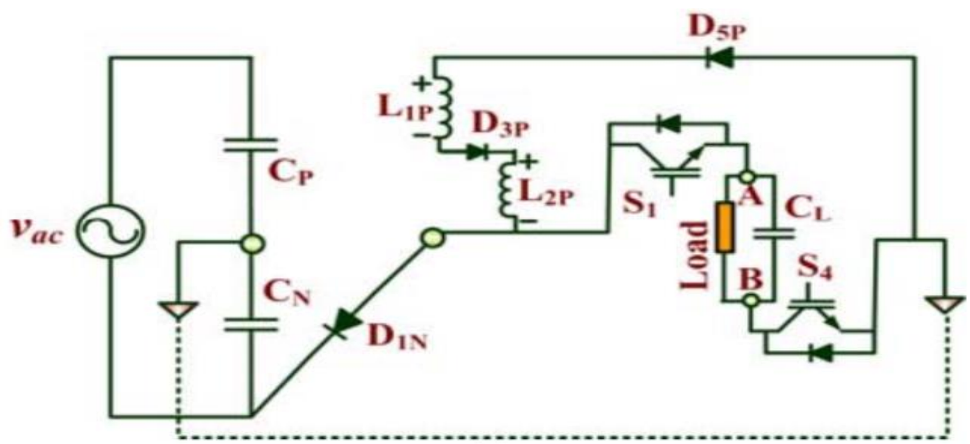

(b)

3.2.2. Generating The Negative Part Of The Cycle

The output voltage V_O is produced by turning on switches S_2 and S_3, where switch S_{1N} is responsible to regulates the voltage range of V_O. During the negative cycle $V_{AC}<0$ and two mode of operation is obtained:

C. **Mode 3:** When switch S_{1N} is activated for a period of time during DT_S.
D. **Mode 4:** When switch S_{1N} is off for a period $(1\text{-}D)T_S$.

C. **Mode 3:** Figure (3.4.a) represents the corresponding circuit for mode 3. When switch S_{1N} is turned on, the input voltage charges inductors L_{1N} and L_{2N} in parallel with equal voltages, diodes D_{1P}, D_{2N}, and D_{4N} are working in forward-biased. The paths V_{AC}-S_{1N}-D_{4N}-L_{2N}-D_{1P}-V_{AC} and V_{AC}-S_{1N}-L_{1N}-D_{2N}-D_{1P}-V_{AC} are used to charge inductor L_{2N} and L_{1N}, respectively. Switches S_2 and S_3 are switched on simultaneously, and capacitors C_N and C_P discharge their energy across the terminals A and B (output).

Applying KVL to the circuit of the converter during mode three in Figure (3.4.a), the mathematical expressions for the voltages across the capacitors and inductors L_{1P} and L_{2P} are as follows:

$$v_{L,1n} = v_{L,2n} = -v_{ac} \tag{3.16}$$

$$v_{C,n} - v_{L,1n} + v_o = 0 \tag{3.17}$$

$$v_{C,p} + v_o = 0 \tag{3.18}$$

These are the mathematical expressions obtained by substituting Equation (3.10):

$$v_{C,n} = -(v_{ac} + v_o) \tag{3.19}$$

$$v_{C,p} = -v_o \tag{3.20}$$

After applying (KCL) to the circuit of the converter during mode three in Figure (3.4.a) corresponding equations came out:

$$i_{ac} = i_C - 2i_{L,2p} \tag{3.21}$$

$$i_{L,1p} = i_{L,2p} \tag{3.22}$$

$$i_{C,L} = i_o = -\frac{v_o}{R} \tag{3.23}$$

D. Mode 4: Figure (3.4.b) represents the corresponding circuit for mode 4. Inductors L_{2N} and L_{1N} are discharged in series across switches S_2 and S_3, also across diodes D_{3N} and D_{5N}. Diodes D_{1P}, D_{3N}, and D_{5N} works as forward-biased when switch S_{1N} is set to off state. Capacitors C_N and C_P are simultaneously charged by the series connection of L_{2N} and L_{1N} across diodes D_{1P}, D_{3N}, and D_{5N}.

Applying KVL to the circuit of mode four in Figure (3.4.b), the mathematical expressions for the voltages across the inductors L_{1P} and L_{2P} are as follows:

$$v_{L,1n} + v_{L,2n} = v_o \tag{3.24}$$

$$v_{L,1n} = v_{L,2n} = \frac{v_o}{2} \tag{3.25}$$

By applying KVL to the same circuit, the voltages across the capacitors are obtained as follows:

$$v_{C,n} = -(v_{ac} + v_o) \tag{3.26}$$

$$v_{C,p} = -v_o \tag{3.27}$$

By applying KCL to the same circuit, we can write:

$$i_{C,n} = i_{C,L} = i_C = i_{ac} \tag{3.28}$$

$$i_{L,1P} = i_{L,2P} = i_{C,L} + \frac{v_o}{R} \tag{3.29}$$

With respect to the current balance law for capacitor C_L and according to equations (3.9) and (3.14), we can write:

$$D\left(-\frac{v_o}{R}\right) + (1 - D)\left(i_{L,1P} - \frac{v_o}{R}\right) = 0 \tag{3.30}$$

After simplifying the equation, we get:

$$i_{L,1P} = i_{L,2P} = \frac{1}{1-D}\frac{v_o}{R} \tag{3.31}$$

According to the current balance law for capacitors C_P and $C_{N,}$ and according to equations (3.7) and (3.15) it can write:

$$D(i_{ac} - 2i_{L,1P}) + (1 - D)i_{ac} = 0 \tag{3.32}$$

By simplifying the above equation, we can write:

$$i_{ac} = 2Di_{L,1P} \tag{3.33}$$

Considering equations (3.31) and (3.33), the following relationship can be obtained:

$$i_{ac} = \frac{2D}{1-D}\frac{v_o}{R} = \frac{P_O}{V_{ac}} \tag{3.34}$$

Figure 3.4:

Equivalent Circuit For The Negative Part of The Cycle Operation of The Impedance Source Converter; (a) Mode 3, (b) Mode 4 (Rahman et al., 2019).

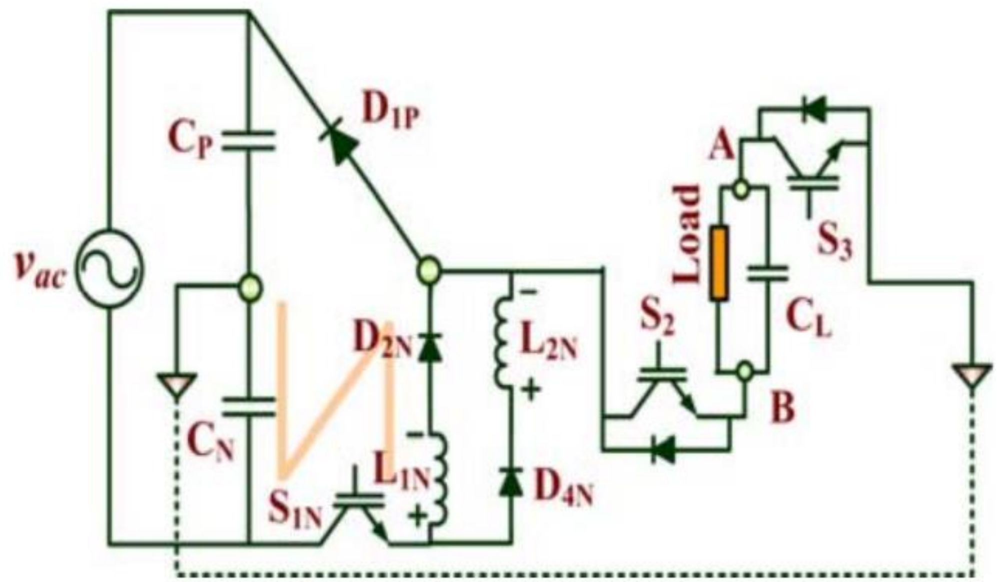

(a)

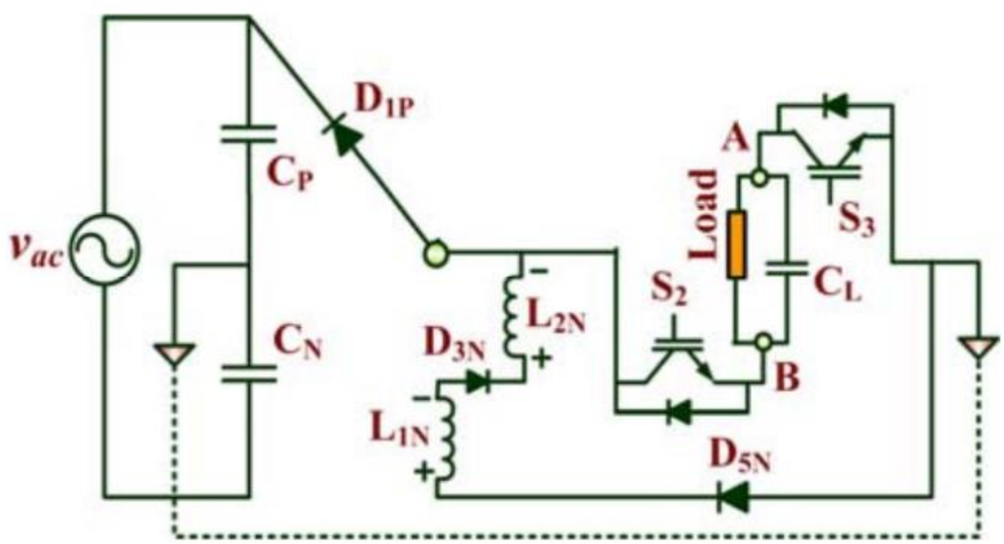

(b)

The law of voltage balance during the positive working cycle for coils L_{1P} and L_{2P} is applied as follows:

$$DT_S v_{L,1p} + (1-D)T_S v_{L,1P} = 0 \quad (3.35)$$

$$DT_S v_{L,2P} + (1-D)T_S v_{L,2P} = 0 \quad (3.36)$$

According to equations (3.1), (3.7), (3.19), and (3.20), the following equation can be written:

$$DT_S v_{ac} - T_S \frac{v_o}{2} + DT_S \frac{v_o}{2} = 0 \quad (3.37)$$

With simplification, it can be written as:

$$\frac{v_o}{2}(1-D) = Dv_{ac} \quad (3.38)$$

Applying the voltage balance law during the negative working cycle for coils L_1 and L_2 we can write:

$$DT_S v_{L,1N} + (1-D)T_S v_{L,1N} = 0 \quad (3.39)$$

$$DT_S v_{L,2N} + (1-D)T_S v_{L,2N} = 0 \quad (3.40)$$

According to equations (3.10), (3.16), (3.39), and (3.40), and applying the voltage balance law, the following equations are obtained:

$$-DT_S v_{ac} + T_S \frac{v_o}{2} - DT_S \frac{v_o}{2} = 0 \quad (3.41)$$

The voltage gain can be obtained as follows using equation (3.38).

$$\frac{v_o}{v_{ac}} = \frac{2D}{1-D} \quad (3.42)$$

Calculating the current efficiency:

If the converter is considered ideal: $V_i I_i = V_o I_i$, Therefore:

$$\frac{v_o}{v_{ac}} = \frac{i_{ac}}{i_o} \quad (3.43)$$

With the above conclusion and equation (3.42), the conversion ratio is as follows:

$$\frac{i_o}{i_{ac}} = \frac{1-D}{2D} \quad (3.44)$$

Figure 3.5:

A Graph Showing The Ratio of Voltage Conversion In Proportion To The Duty Cycle Plot. A: Presented Impedance Source Converter AC-AC. B: Buck-Boost AC-AC Converter (Rahman et al., 2019).

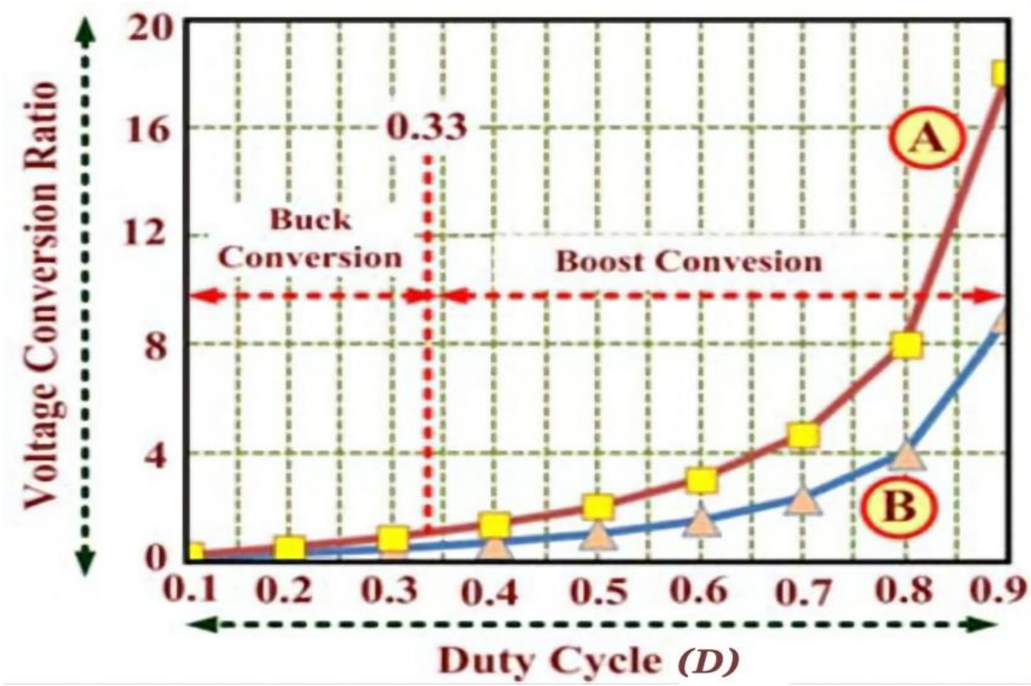

In particular, the voltage conversion ratio of the Z- source converter is double of that of the usual buck-boost topology. Furthermore, it is appreciated that the control of switches S_{1N} and S_{1P} determines the switching modes that dictates the magnitude of the wave form; where if D<0. 33, the converter operates in a buck mode; while if D>0. 33, the converter operates in a boost mode. Furthermore, the frequency of the switching output can also be easily changed by changing the states of the H-bridge switches. Therefore, the present multiple switches states can be employed to control the frequency and the magnitude individually so that the desired shape of the wave is obtained.

3.4. Design Losses and Analysis

The four inductors of the P-Z_{AC} and N-Z_{AC} switching inductors source networks are the same, meaning that $L_{1N} = L_{2N} = L_{1P} = L_{2P} = L$. Inductors are made with their highest allowable current ripples in the circuit. Suppose that the inductor's current ripple is represented by Δi_L. Inductor current fluctuations are equal to r% of peak current ($i_{L,\ peak}$). The proper value of the inductors can be chosen by this equation:

$$L = \frac{\Delta v_L \Delta t}{\Delta i_L} \quad (3.45)$$

Based on equations (3.1) and (3.16), the following relationship can be derived:

$$L = L_{1,N} = L_{2,N} = L_{1,P} = L_{2,P} = \frac{V_{ac,peak} D T_S}{\Delta i_L} \tag{3.46}$$

Given that $V_{ac,peak} = \sqrt{2V_{ac,rms}}$ the magnitude of L is obtained as follows:

$$L = \frac{\sqrt{2} v_{ac,rms} D T_S}{\Delta i_L} \tag{3.47}$$

The ripple current of the coil Δi_L can be obtained using equation (3.31) and the following equation:

$$\Delta i_L = (r\% i_{Lpeak}) = (r\%) \frac{\sqrt{2}}{(1-D)} i_{o,rms} \tag{3.48}$$

The peak current through the coils can be obtained as follows:

$$i_{L,peak} = \frac{\sqrt{2}}{(1-D)} i_{o,rms} \tag{3.49}$$

Assuming capacitors, C_N and C_P have the same properties, meaning C_N=C_P=C the ripple voltage across the capacitors (R%) is equal to the peak voltage. The values of the capacitors can be obtained as follows:

$$C = \frac{\Delta i_C \Delta t}{\Delta V_C} \tag{3.50}$$

According to equation (3.15), we can write:

$$C = \frac{i_{ac,peak}(1-D) T_S}{\Delta V_C} = \frac{\sqrt{2} i_{ac,rms}(1-D) T_S}{\Delta V_C} \tag{3.51}$$

The ripple voltage across capacitor ΔV_c can be obtained as follows:

$$\Delta V_C = (R\%) V_{C,peak} \tag{3.52}$$

Considering equations (3.4) and (3.42), the maximum capacitor voltage can be obtained as follows:

$$V_{C,peak} = V_{C,P,peak} = V_{ac,peak} + V_{o,peak} = \sqrt{2} \frac{(1+D)}{(1-D)} V_{ac,rms} \tag{3.52}$$

3.4.1. Selecting The Maximum Voltage For Semiconductor Element.

In the second operating mode, switch (S_2) is off, so we can write:

$$-V_{ac} + V_{S,1P} + V_{L,1P} + V_{L,2P} = 0 \tag{3.53}$$

According to equation (3.10), we can write:

$$V_{S,1P} = V_{ac} + V_o \tag{3.54}$$

According to equation (3.42), the following relationship is obtained:

$$V_{S,1P} = V_o \left(\frac{1+D}{2D}\right) \tag{3.55}$$

The switch S_{1N} is turned off in the fourth mode of operation; therefore, we can write:

$$-V_{ac} - V_{L,2N} - V_{L,1N} - V_{S,1N} = 0 \tag{3.56}$$

Based on equation (3.25), we can write:

$$V_{S,1N} = -(V_{ac} + V_o) \tag{3.57}$$

According to equation (3.42), the following relationship is obtained:

$$V_{S,1N} = -V_o\left(\frac{1+D}{2D}\right) \tag{3.58}$$

According to equations (3.55) and (3.58), the maximum voltage required for the switches and the impedance source networks (S_{1P} and S_{1N}) is obtained as follows:

$$V_{S,1p}, V_{S,1N} > \frac{\sqrt{2}(1+D)v_{o,rms}}{2D} \tag{3.59}$$

During the positive working cycle, switches (S_3) and (S_2) are off, and (S_1) and (S_4) are turned on. Therefore, it can be written:

Applying KVL to Figure (3.1), we can write:

$$V_{S3} = V_o \tag{3.60}$$

$$V_{S2} = V_o \tag{3.61}$$

During the negative working cycle, switches (S_1) and (S_4) are off, and switches (S_3) and (S_2) are on. Therefore, it can be written:

Applying KVL to Figure (3.1), we can write:

$$V_{S1} = -V_o \tag{3.62}$$

$$V_{S4} = -V_o \tag{3.63}$$

Therefore, the maximum required voltage for the switches from bridge H can be obtained as follows:

$$v_{S1}, v_{S2}, v_{S3}, v_{S4} > \sqrt{2}v_{o,rms} \tag{3.64}$$

Therefore, according to the first operating mode and by applying KVL in Figure (3.1), we can write:

$$V_{D,1p} = V_{D,3p} = -V_{ac} \tag{3.65}$$

$$V_{D,5p} = -\left(V_{L,2p} + V_o\right) \tag{3.66}$$

By substituting equation (3.1) into the above equation, we can write:

$$V_{D,5p} = -(V_{ac} + V_o) \tag{3.77}$$

According to equation (3.42), we can write:

$$V_{D,1p} = V_{D,3p} = \sqrt{2}\frac{1-D}{2D}V_{o,rms} \tag{3.68}$$

$$V_{D,5p} = -\sqrt{2}\frac{1+D}{2D}V_{o,rms} \tag{3.69}$$

By applying KVL in the second operating mode, we can write:

$$V_{D,2p} = V_{L,2p} \tag{3.70}$$

$$V_{D,4p} = V_{L,1p} \tag{3.71}$$

According to equation (3.11), we can write:

$$V_{D,2p} = V_{D,4p} = -\frac{V_o}{2} \tag{3.72}$$

According to equation (3.42), we can write:

$$V_{D,2p} = V_{D,4p} = -\sqrt{2}\frac{V_{o,rms}}{2} \tag{3.73}$$

Therefore, according to the third operating mode and by applying KVL (Kirchhoff's Voltage Law) in Figure (3.1), we can write:

$$V_{D,1N} = V_{D,3N} = V_{ac} \tag{3.74}$$

$$V_{D,5N} = V_o - V_{L,2N} \tag{3.75}$$

which, according to equation (3.16), can be written as:

$$V_{D,5N} = V_o + V_{ac} \tag{3.76}$$

According to equation (3.42), we can write:

$$V_{D,1N} = V_{D,3N} = \sqrt{2}\frac{1-D}{2D}V_{o,rms} \tag{3.77}$$

$$V_{D,5N} = \sqrt{2}\frac{1+D}{2D}V_{o,rms} \tag{3.78}$$

Therefore, by applying KVL in the fourth operating mode, we can write:

$$V_{D,2N} = V_{L,2N} \tag{3.79}$$

$$V_{D,4N} = V_{L,1N} \tag{3.80}$$

According to equation (3.25), we can write:

$$V_{D,2N} = V_{D,4N} = \sqrt{2}\frac{V_{o,rms}}{2} \tag{3.81}$$

3.4.2. Selecting The Currents of The Switches

By applying KCL in the first mode and utilizing equation (3.8), we can write:

$$i_{S,1p} = 2i_{L,1p} \tag{3.82}$$

By applying KCL in the third operational mode and utilizing equation (3.22), we can express:

$$i_{S,1N} = 2i_{L,1N} \tag{3.83}$$

By applying KCL in the second and fourth operational modes, we can write:

$$i_{S1} = i_{S2} = i_{S3} = i_{S4} = i_{CL} + i_o \tag{3.84}$$

In many ways, the suggested converter works better. Other than having fewer switches built in than some other AC-AC converters, the converter come with a built-in ability to manage inductors currents ripples. By adding capacitors to the input, the converter becomes independent of time-wasting circuits and serves as an input filter as well. The converter that is being provided has the greatest contribution in terms of efficiency. Indeed, one can state that, in terms of the efficiency coefficient, there is no other circuit that can be as efficient as this one within the given field. This converter is useful in applications that require High voltage AC.

Switching losses are the loses that incurred by the switches of the given impedance converter. The conduction losses were dependent with current through the IGBT and the voltage drop across the switches in the direct conduction state. Switching has two types the following are the changeover losses which is mainly acquired when the switches change their state from ON to OFF and also from OFF to ON. This depends with the kind of converter that is in use and the switching frequency of the converter. Conduction losses that rise up from the average current generated by the switch and the voltage drop through the switch in the direct conduction state are written as follows: Using the switch current average value and the voltage rise through the switch in the direct conduction state the conduction losses are expressed as follows:

$$P_{con,loss} = V_{ce} I_{cn} d_n + V_{fn} I_{fcn} d_n \tag{3.85}$$

Here V_{ce}, V_{fn} is the saturation voltage or the collector-emitter voltage and I_{cn} is the collector current and the forward voltage drop of the diode which exists in the on state.

Similarly, switching losses can be calculated as follows: Likewise, the switching losses include the following:

$$P_{sw,loss} = f_s . E_{loss} \tag{3.86}$$

Therefore, the switching power losses result from the switching frequency and the energy losses within one pulse. The total converter losses comprise the sum of conduction losses and switching losses. Thus:

$$P_{loss} = P_{con,loss} + P_{sw,loss} \tag{3.87}$$

The converter efficiency can be written as follows:

$$\eta_{con} = \frac{P_o}{P_{ac}} = \frac{V_o I_o \cos(\varphi_o)}{V_{ac} I_{ac} \cos(\varphi_{ac})} \tag{3.88}$$

3.5. Simulation Results

The performance of the proposed converter is verified with the help of the simulation of a single-phase AC-AC converter with a 500W source in PSCAD/EMTDC software. The frequency of the switching F_{SW} is set to 100 kHz. A converter with two duty ratios of 0.6 and 0.3 is simulated, the first one for the boosting mode (D=0.6) and the second one for the bucking mode (D=0.3) The output waveform is obtained for different frequencies: 50 Hz, 25 Hz, and 100 Hz.

Table 3.1:

Numerical Values of The Parameters Used in The Simulation

Parameter	value
Peak input voltage	73.5v
Duty cycle	0.6,0.3
Switching frequency (F_S)	100KHz
Output frequency	25Hz,50Hz,100Hz
C_P=C_N	220µF
C_L	4.5µF
L	3.5mH
Load impedance (R)	52Ω

3.5.1. Boost Mode With a Frequency of 50Hz

Shown in the figure (3. 6) below is the boost mode function of the converter at the frequency 50Hz where the duty cycle is set at 0. 6 as shown below: Waveform of the input voltage that provides a maximum amplitude of 73. 5V is shown in figure (3. 6. a) and is of sinusoidal type. The waveform of the output voltage which is obtained is as shown in figure (3. 6. b) and it is 223V. As it can be accepted from the equation (3. 42), the maximum value of the main component of the output voltage is 220. 5 V. With the anticipated analysis, input voltage of 73. 5V rises to the output voltage of 220. 5V. Therefore, the above-said analysis supports that when the duty cycle is 0. 6, the presented converter works in boost mode with boost ratio of third. However, the THD of the output voltage waveform as shown in the figure (3. 6. B) is 11. 36.

Figure 3.6:

Waveforms of The converter Voltages At The Input and Output sides In Boost Mode; (a) Input Voltage; (b) Output Voltage

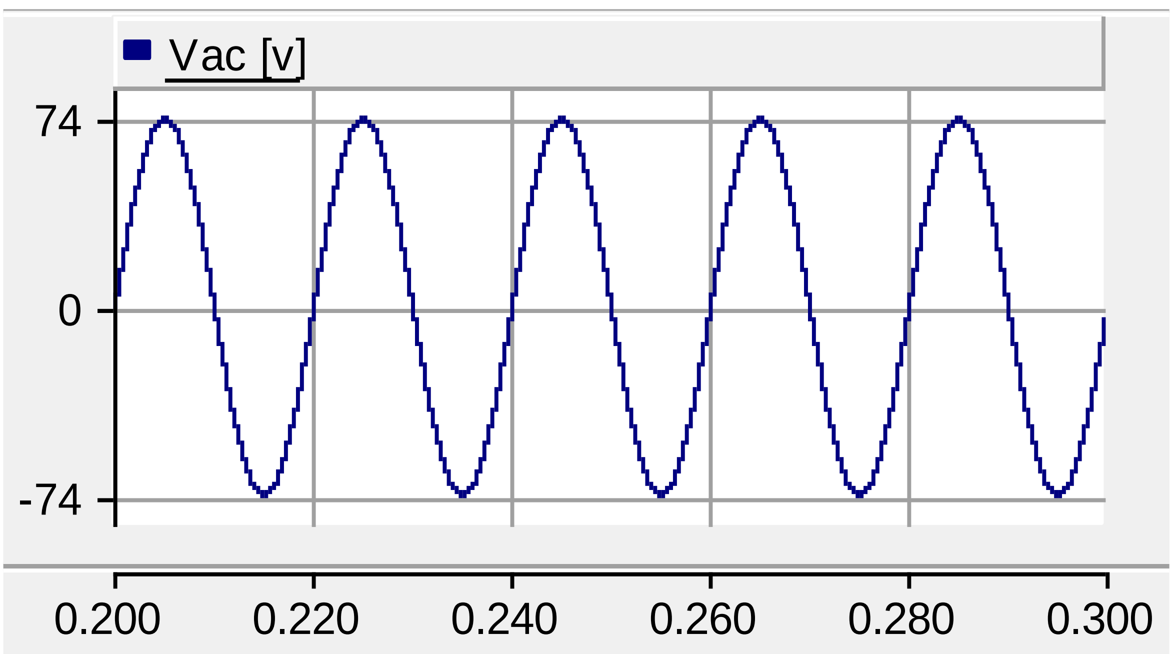

(a)

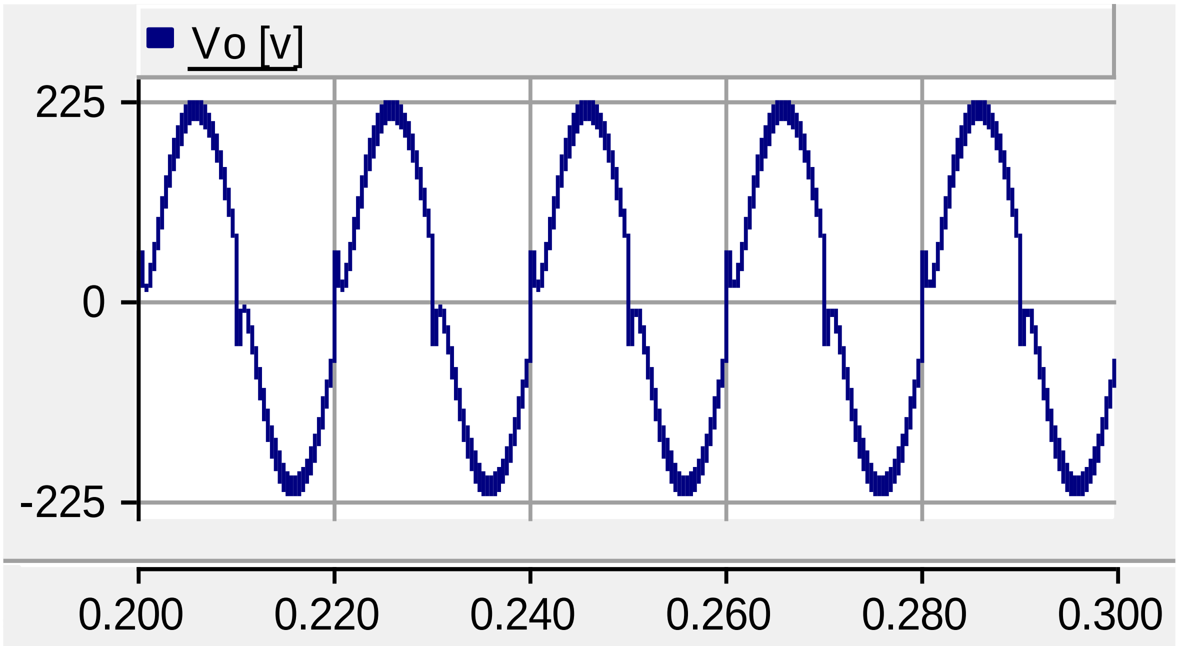

(b)

Figure (3.7) illustrates the currents waveforms at the input and output sides when the converter operates with a duty cycle of 0.6 at a frequency of 50Hz. In Figure (3.7.a), the waveform of the input current is depicted, with its main peak value being 23A. Theoretical calculation, based on equation (3.88) and assuming ideal converter behavior, yields a peak input current value of 22.72A. Figure (3.7.b) shows the waveform of the output current, with its peak value being 4.3A. According to equation (3.9), the theoretical peak output current value is 4.2A.

Figure (3.7):

Currents Waveforms At The Input and Output Sides of Converter In Boost Mode; (a) Input Current; (b) Output Current.

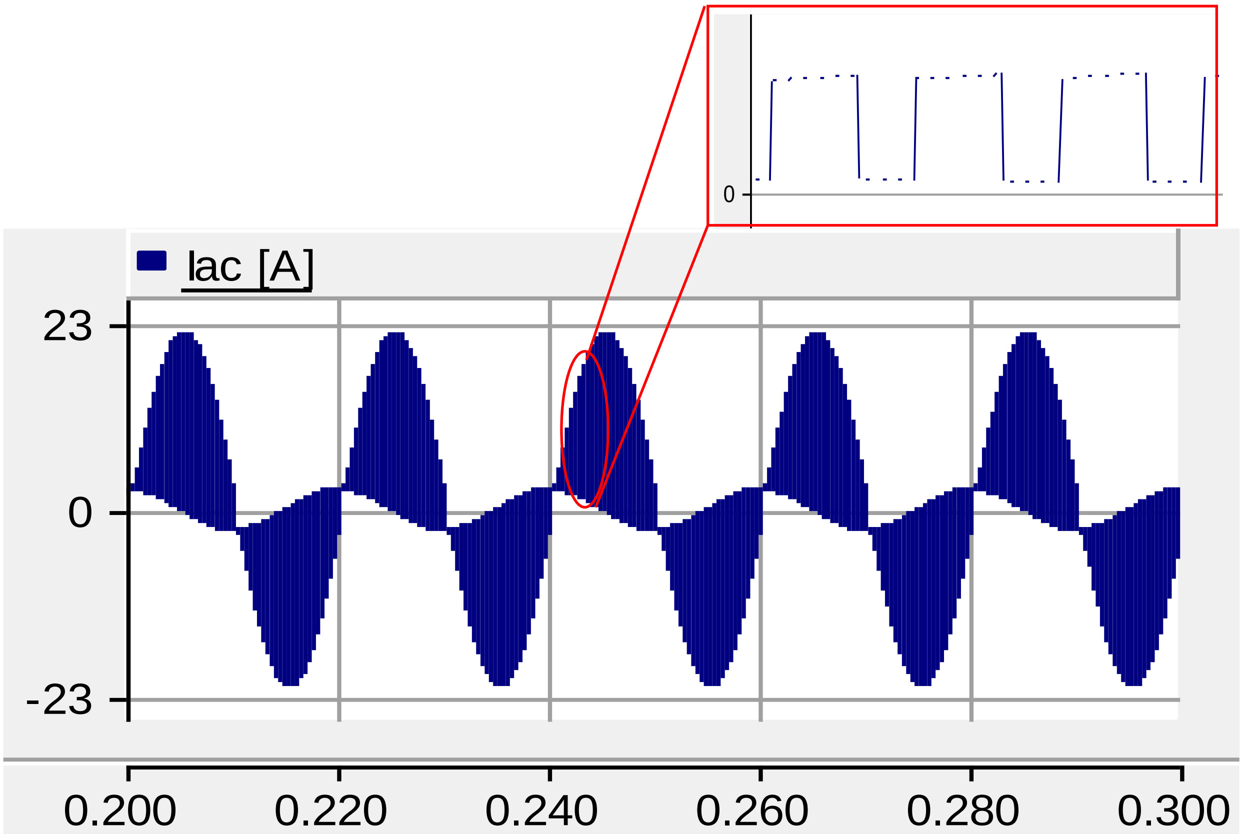
Iac [A]
23
0
-23
0.200
0.220
0.240
0.260
0.280
0.300
0

(a)

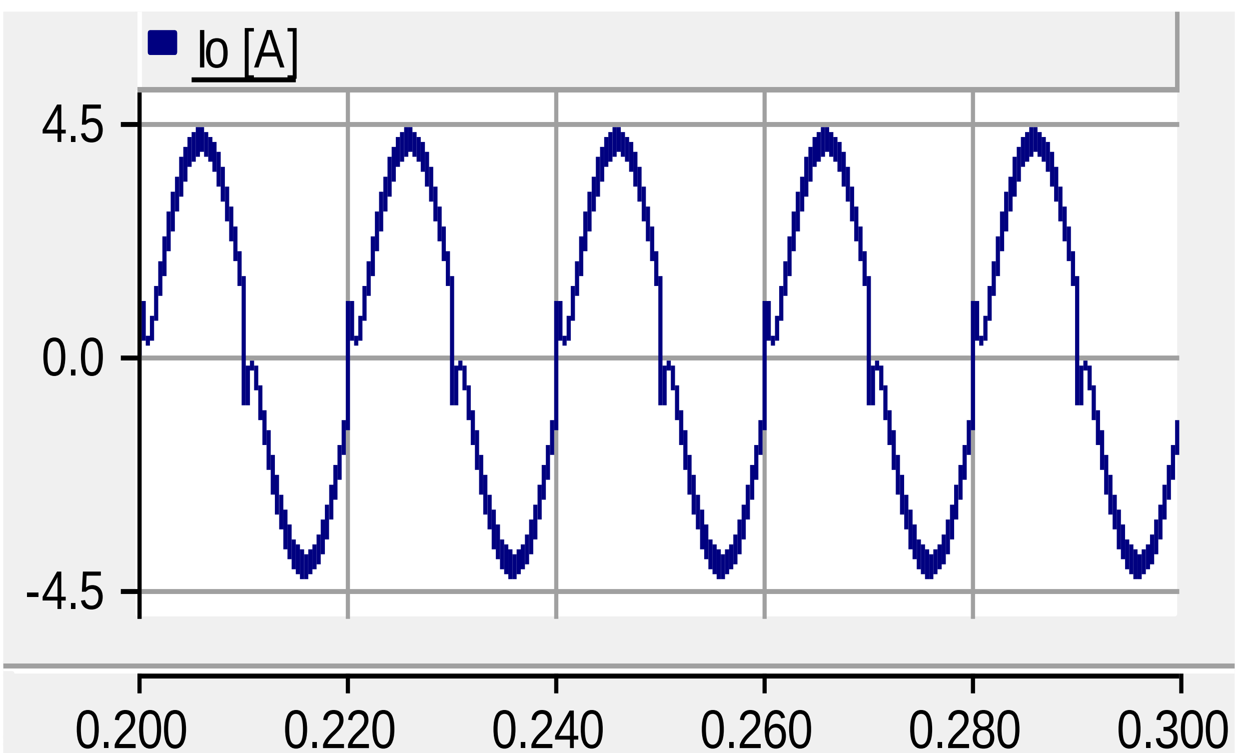
Io [A]
4.5
0.0
-4.5
0.200
0.220
0.240
0.260
0.280
0.300

(b)

Figure (3.8) illustrate the voltage waveforms in boost mode across the switches for a duty cycle of D=0.6. Considering Figure (3.8.a), the maximum voltage across switches S_{1N} and S_{1P} is 300V. According to the theory derived in (3.59), this value equals 324.4V. Regarding Figure (3.8.b), the maximum voltage across switches S_1, S_2, S_3, and S_4 is 226V. As per the theory derived in (3.64), this value is 224V.

Figure (3.8):

Voltage Waveforms Across The Terminals of The Switches For The Presented Converter In The Boost Mode; ***(a)*** *Voltage Across The Terminals of Switches S_{1P} and S_{1N};* ***(b)*** *Voltage Across The Terminals of Switches S_1, S_2, S_3, and S_4*

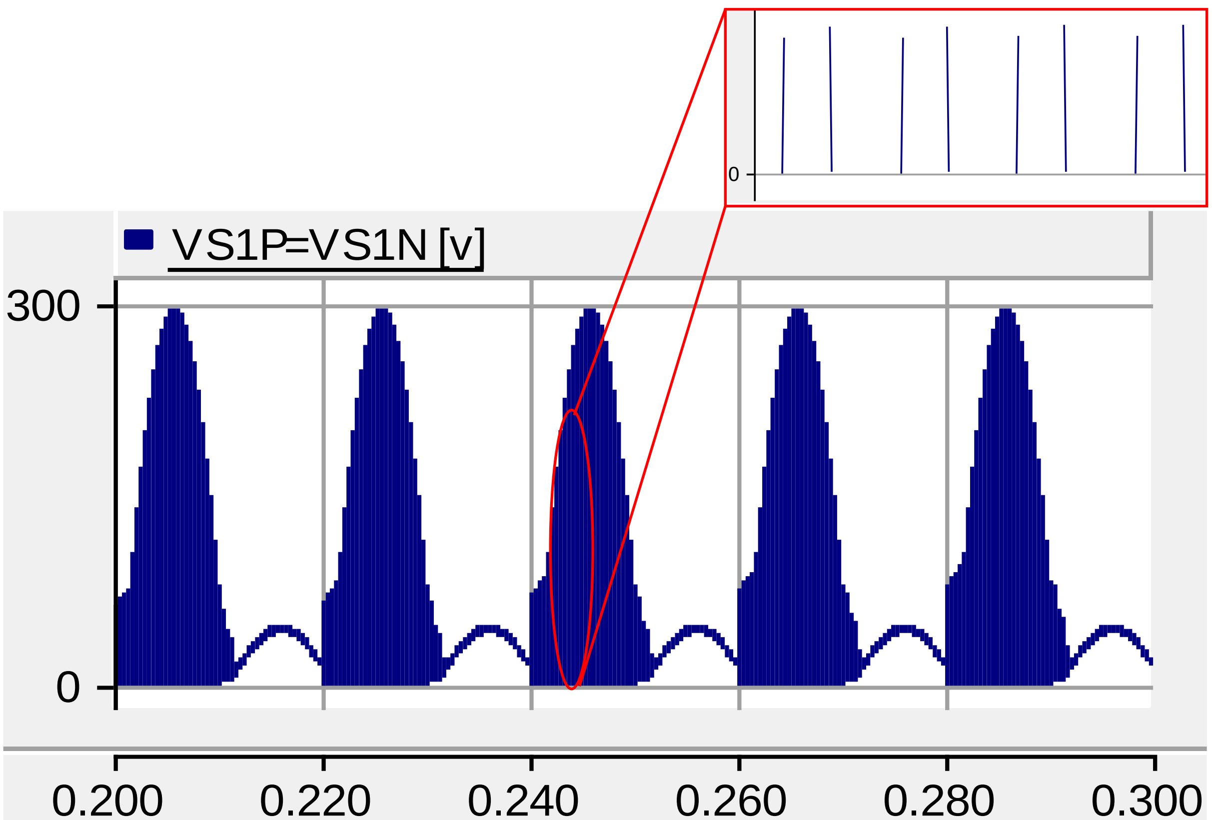

(a)

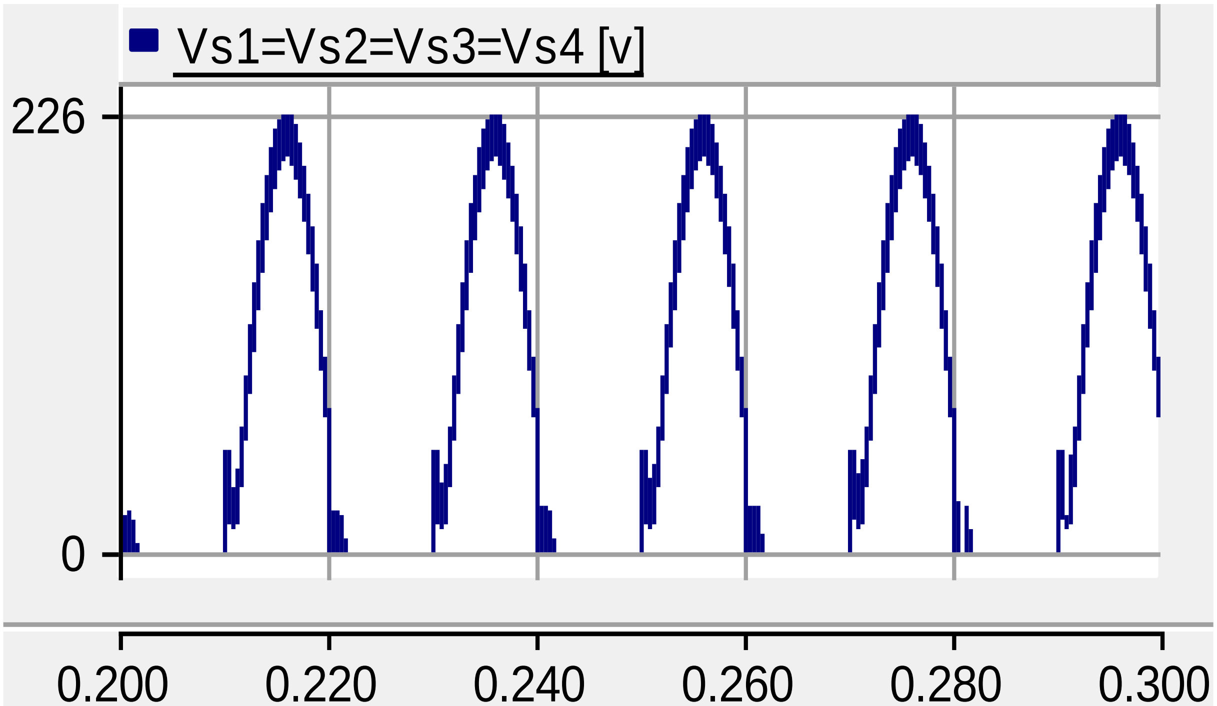

(b)

Figure (3.9) depicts the current waveforms across the terminals of the switches in the boost mode for a duty cycle of D=0.6. According to Figure (3.9.a), the maximum current through switch S_{1P} is 22.2A, which, according to the theoretical equation derived in (3.82), is equal to 21.2A. Similarly, in Figure (3.9.b), the maximum current through switch S_{1N} is 22.2A, which, according to the theoretical equation derived in (3.83), is equal to 21.2A. Finally, according to Figures (3.9.c) and (3.9.d), the maximum current through switches S_1, S_2, S_3, and S_4 is 10.8A, which, according to the theoretical equation derived in (3.84), is equal to 10.6A.

Figure (3.9):

Current Waveforms of The Switches in The Boost Mode; (a) Waveform of S_{1P}, (b) Waveform of S_{1N}, (c) Waveform of S_1 and S_2, (d) Waveform of S_3 and S_4

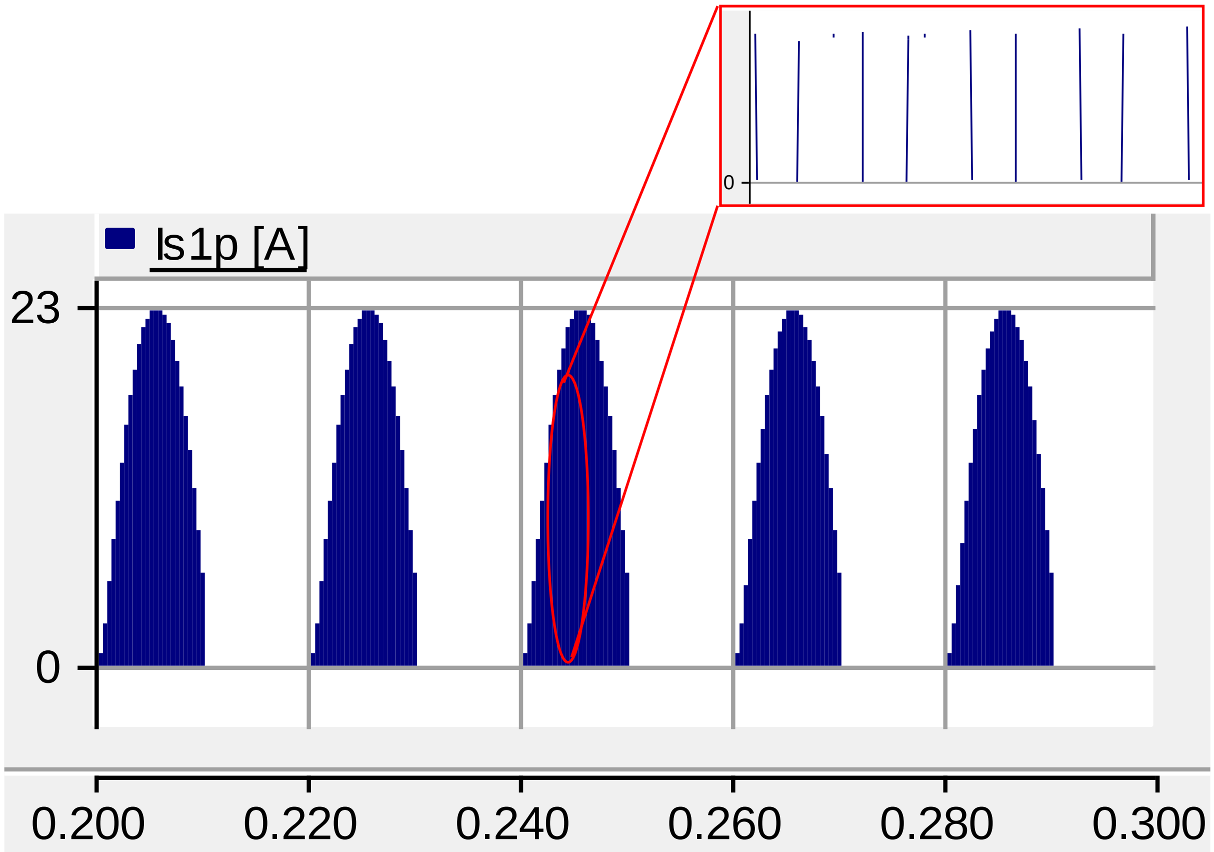
0
Is1p [A]
23
0
0.200
0.220
0.240
0.260
0.280
0.300

(a)

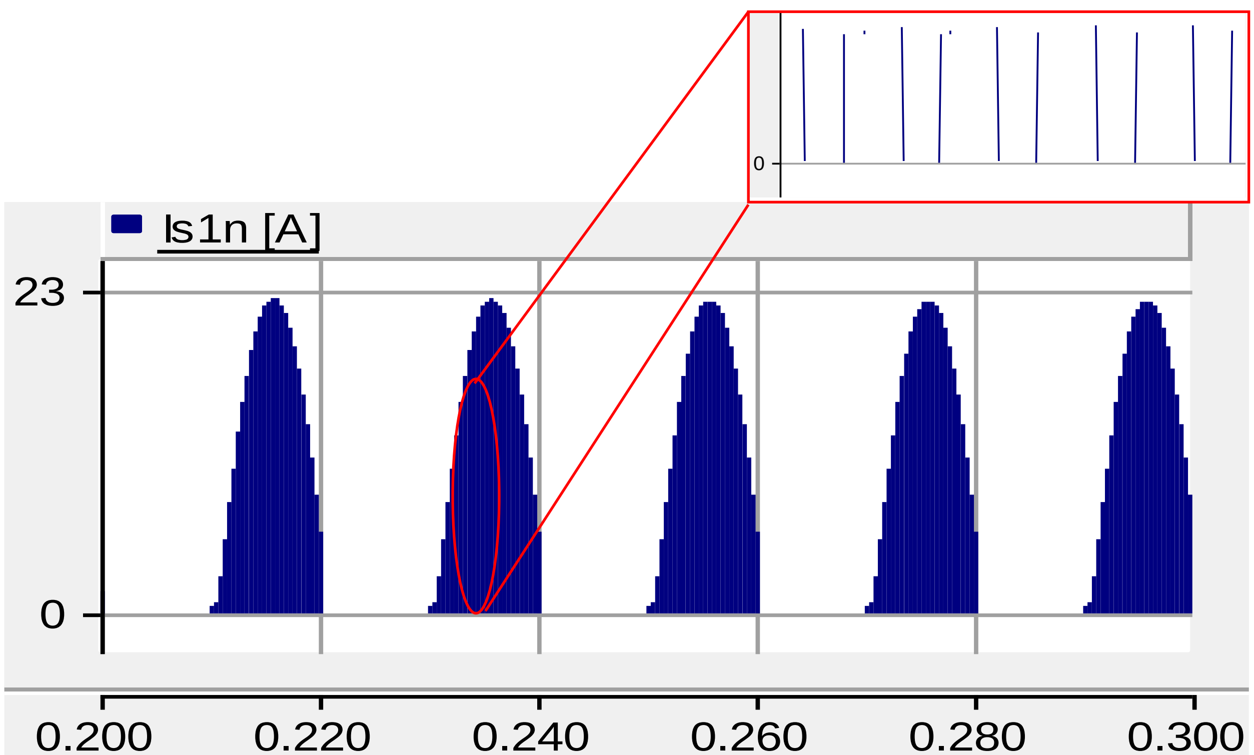
0
Is1n [A]
23
0
0.200
0.220
0.240
0.260
0.280
0.300

(b)

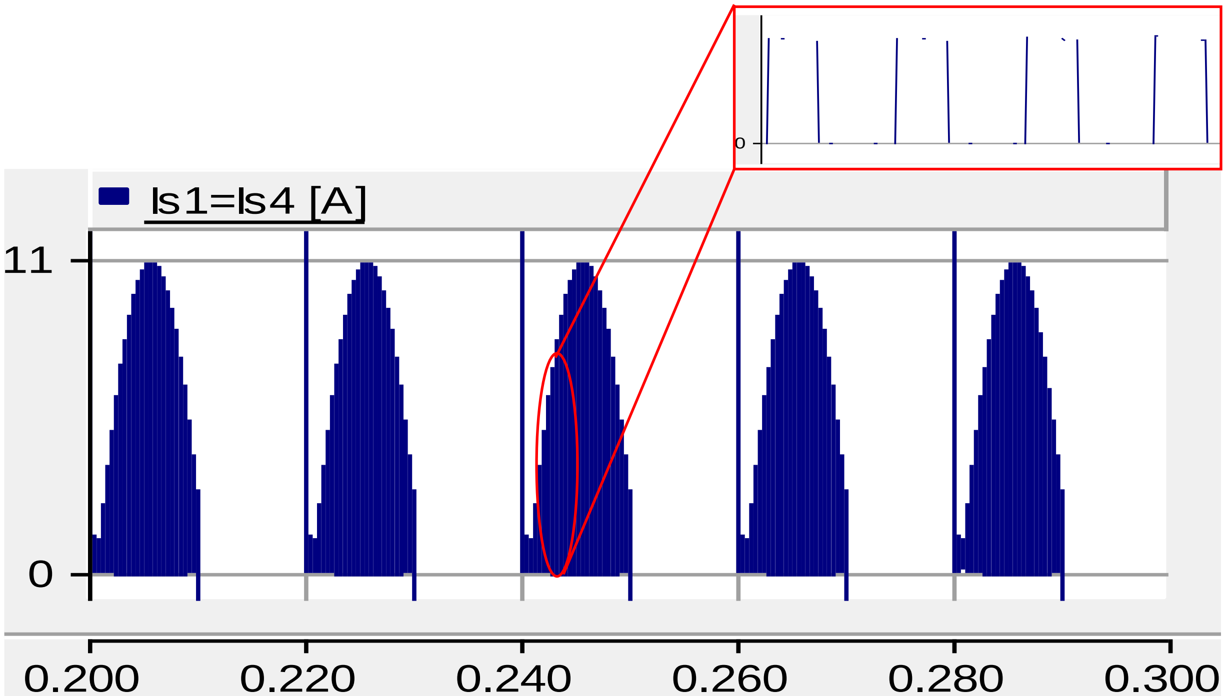
Is1=Is4 [A]
11
0
0.200
0.220
0.240
0.260
0.280
0.300

(c)

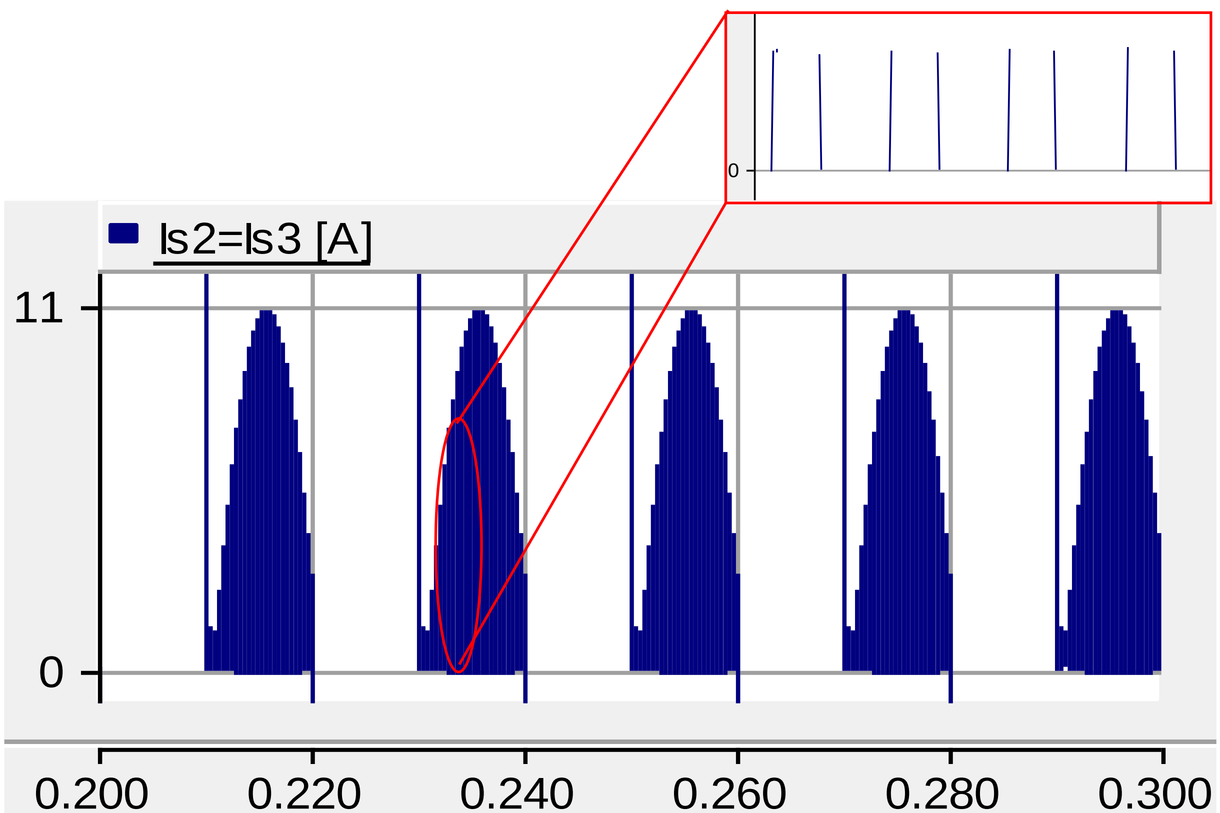
Is2=Is3 [A]
11
0
0.200
0.220
0.240
0.260
0.280
0.300

(d)

Figure (3.10) illustrates the voltage waveforms across the capacitors at a frequency of 50 Hz and a duty cycle of D = 0.6. In Figure (3.10.a), the peak voltage of the main component of capacitor C_N is 124V. According to equation (3.53), the peak voltage across capacitor C_N is calculated to be 294V. In Figure (3.10.b), the peak voltage of the main component of capacitor C_P is 124V. According to equation (3.53), the peak voltage across capacitor C_P is calculated to be 294V.

Figure (3.10):

Voltage Waveforms Across The Capacitors in The Boost Mode; (a) Voltage Waveform Across Capacitor C_N; (b) Voltage Waveform Across Capacitor C_P

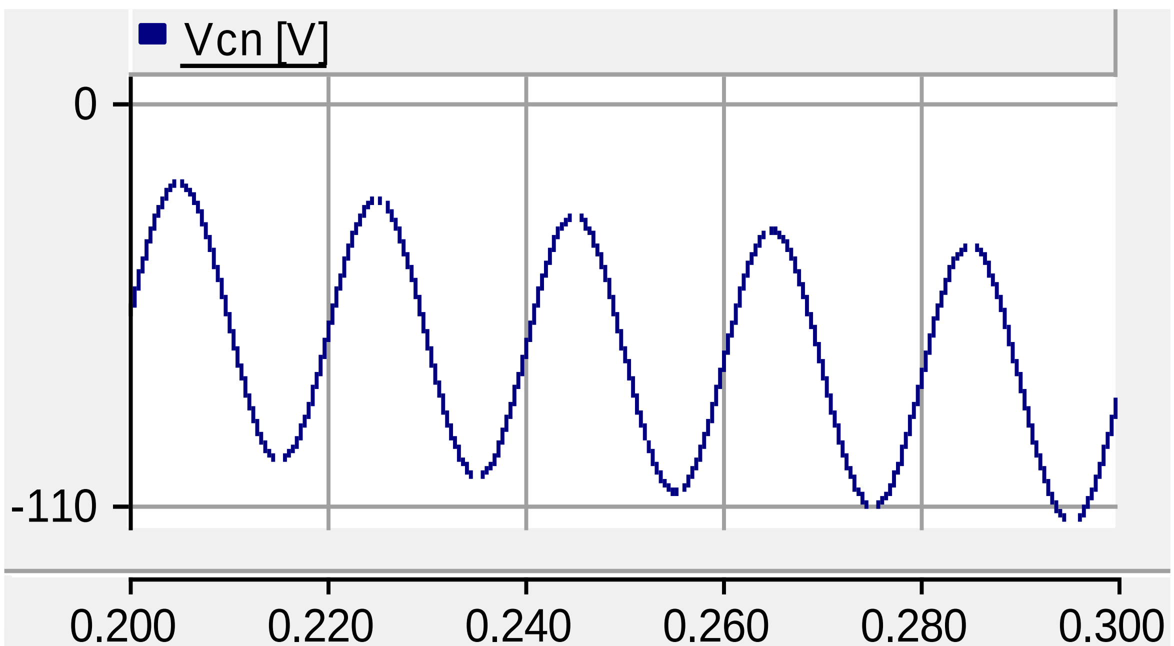

(a)

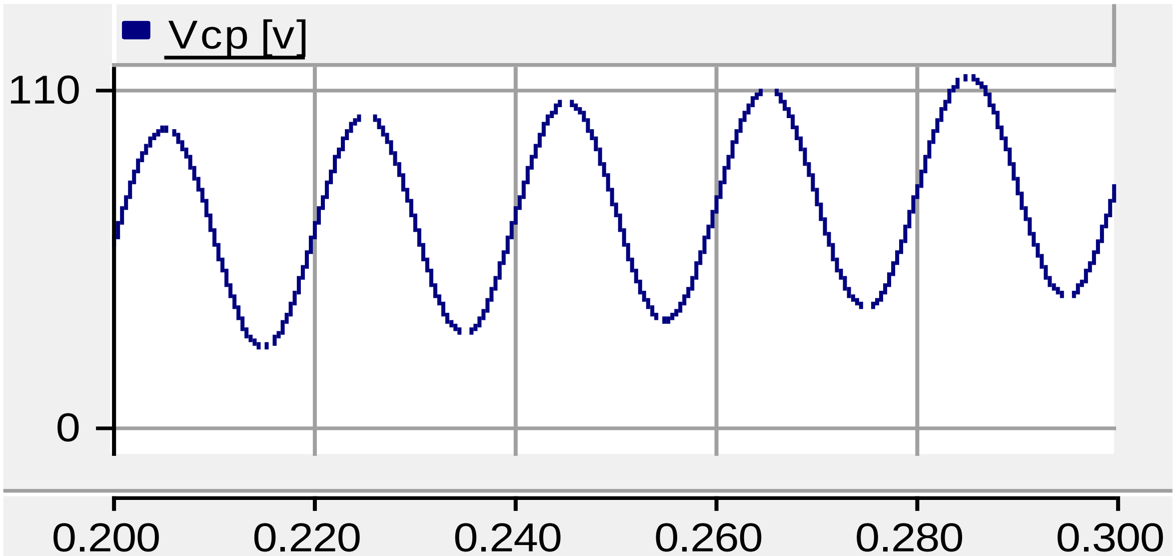

(b)

Figure (3.11) illustrates the current waveforms across capacitor C_L in the boost mode at a frequency of 50Hz and duty cycle D=0.6. In this figure, the main component peak current of capacitor C_L is 4.5A in mode 1 and 6.8A in mode 2. According to equation (3.9), the peak current across capacitor C_L in mode 1 is 4.24A, and according to equation (3.14), in mode 2, it is 6.36A.

Figure (3.11):

Current Waveform Across Capacitor C_L in The Boost Mode

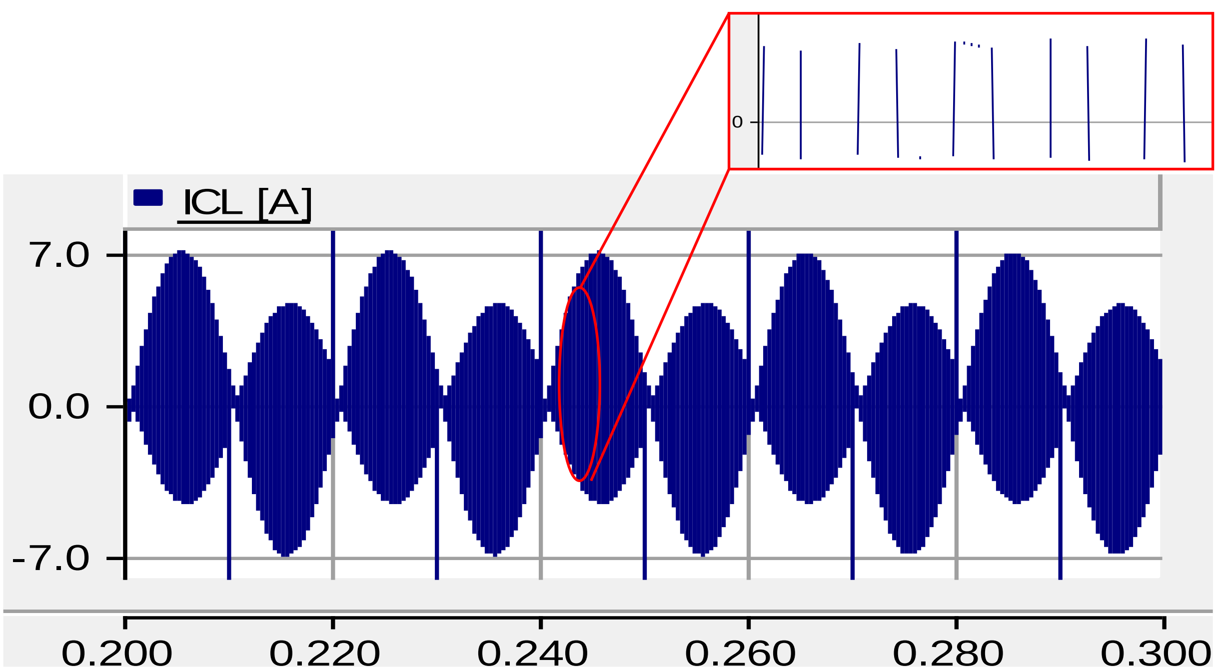

Figure (3.12) illustrates the current waveforms across coils with equal magnitudes at a frequency of 50Hz and a duty cycle of D=0.6. According to the figure, the peak current value across the coils is 11A, which, based on the theoretical equation derived in (3.49), corresponds to a peak coil current value of 10.6A.

Figure (3.12):

Waveforms of The Current Across The Coils in The Boost State; (a) Waveform of The Current Across Coils L_{1P} and L_{2P}; (b) Waveform of The Current Across Coils L_{1N} and L_{2N}

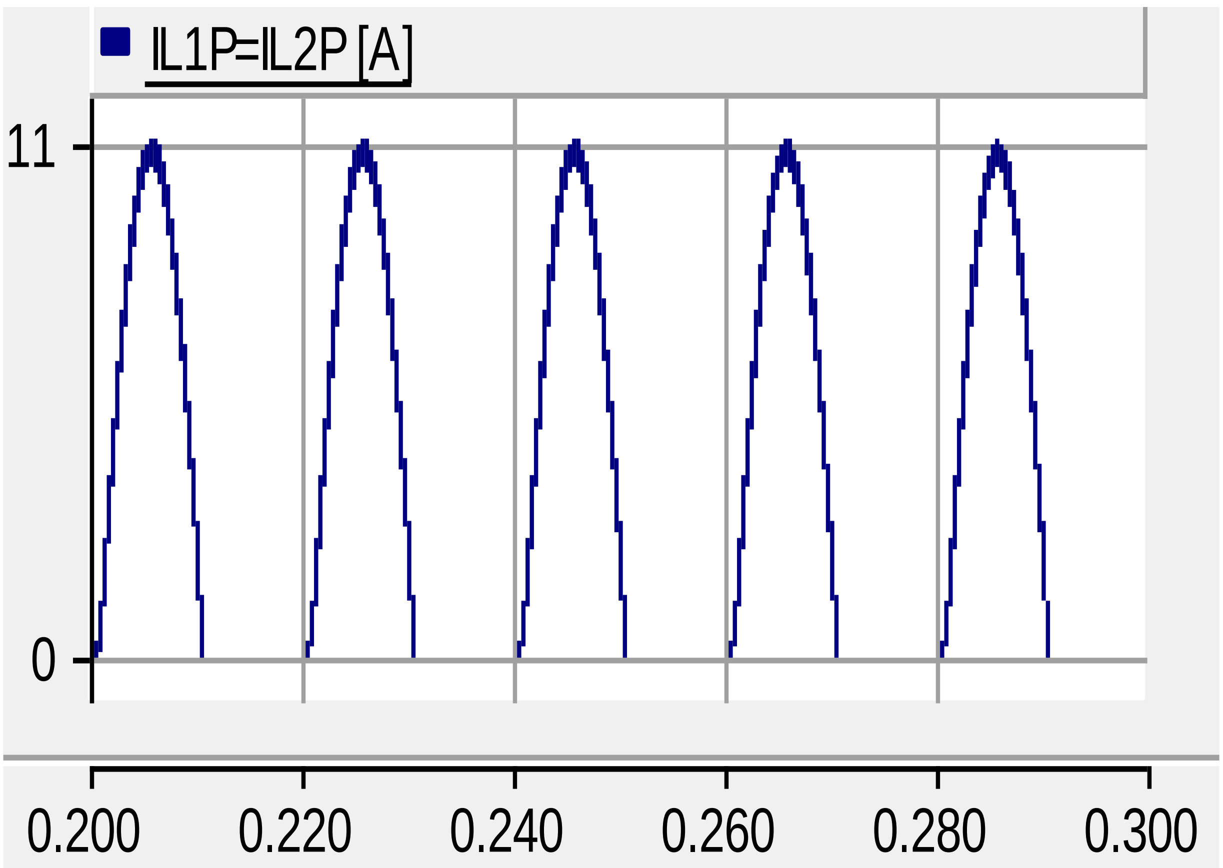

(a)

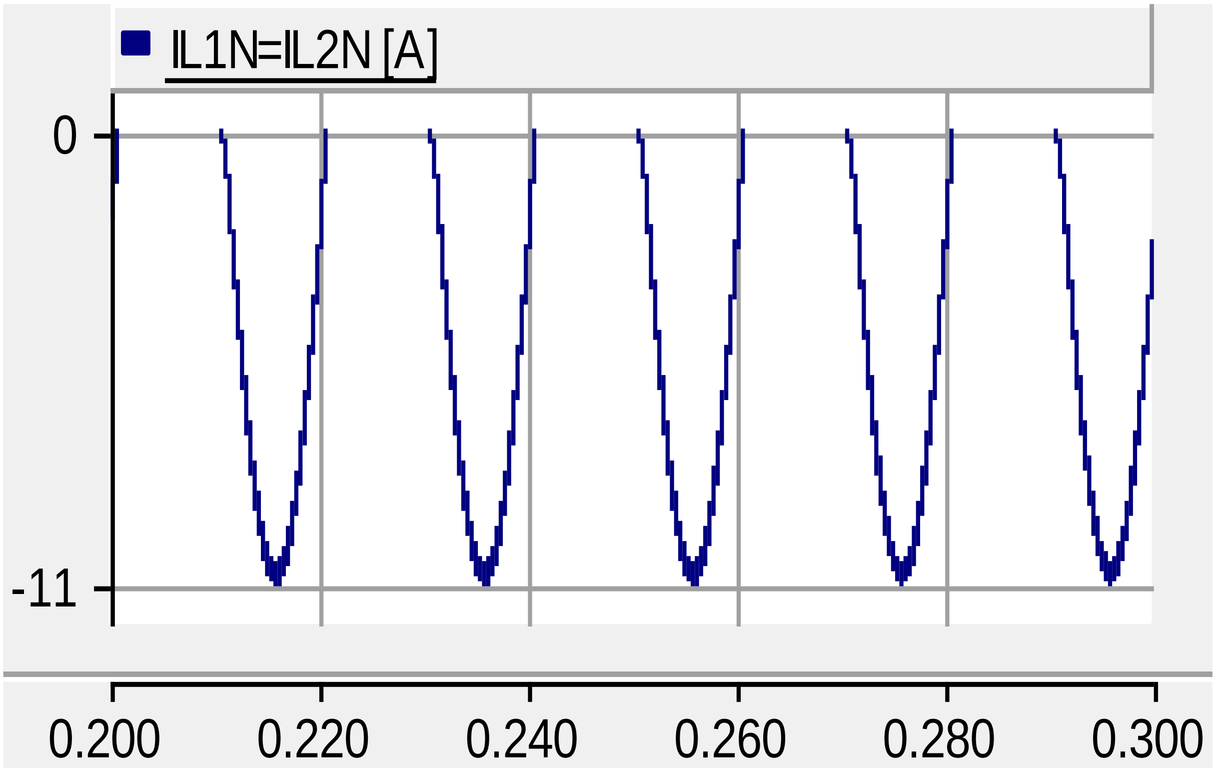

(b)

Figure (3.13): Waveforms of the voltage across the coils in the boost state, where coils have equal sizes, at a frequency of 50Hz and a duty cycle of D=0.6. According to Figure (3.13.a), the peak voltage across coils L_{1P} and L_{2P} in the first mode is 73V, and in the second mode is 111.6V, which according to the theoretical equation (3.1), the peak voltage of these coils in the first mode is 73.5V, and in the second mode is 112.25V. According to Figure (3.13.b), the peak voltage across coils L_{1N} and L_{2N} in the third mode is 73V, and in the fourth mode is 111.6V, which according to the theoretical equation (3.16), the peak voltage of these coils in the third mode is 73.5V, and according to equation (3.25), in the fourth mode is 110.25V.

Figure (3.13):

Voltage waveforms across the coils in the boost state; (a) Voltage waveform across coils L_{1P} and L_{2P}, (b) Voltage waveform across coils L_{1N} and L_{2N}.

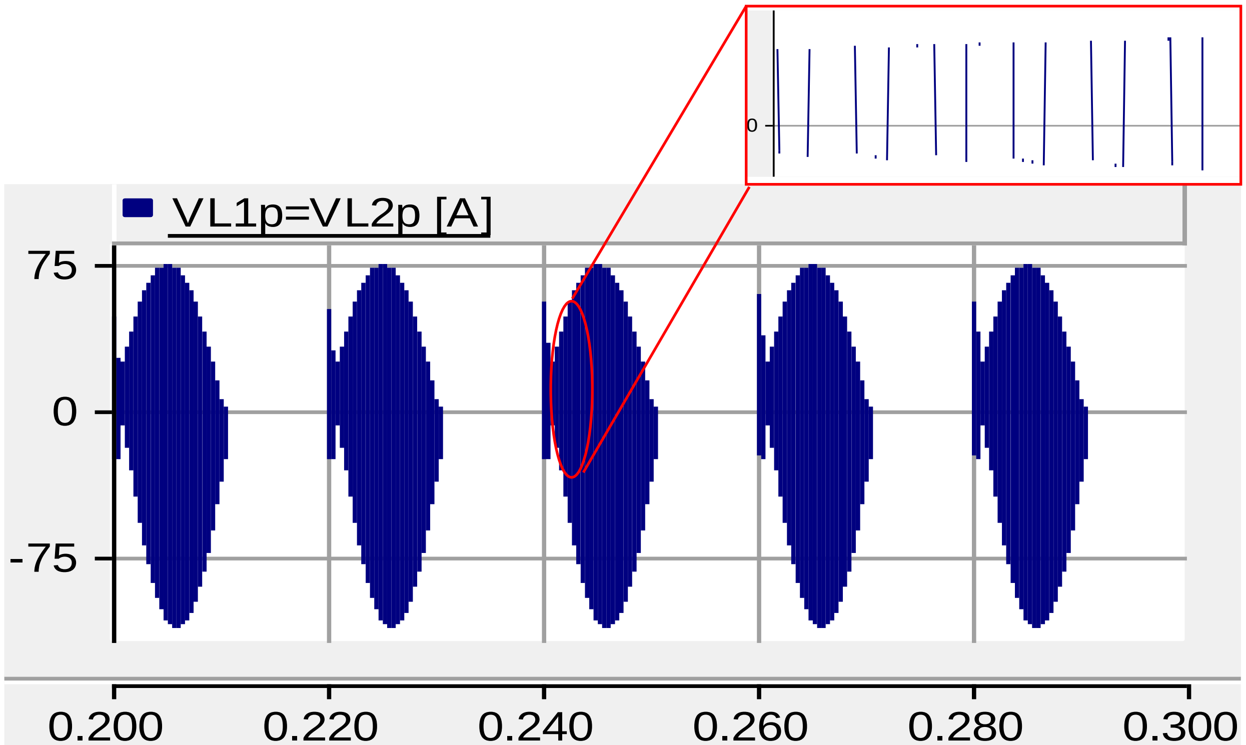
VL1p=VL2p [A]
75
0
-75
0.200
0.220
0.240
0.260
0.280
0.300

(a)

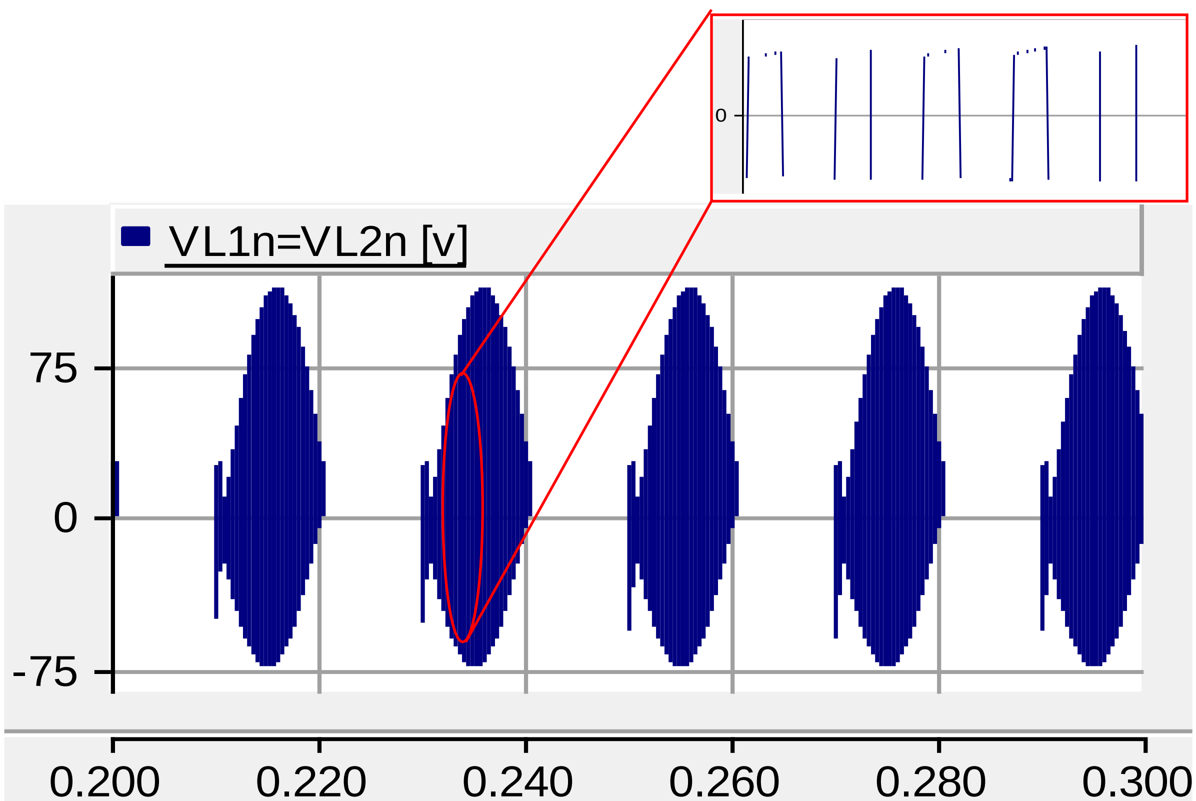
VL1n=VL2n [v]
75
0
-75
0.200
0.220
0.240
0.260
0.280
0.300

(b)

Figure (3.14) illustrates the voltage waveforms across the diodes at a frequency of 50Hz and a duty cycle of D=0.6. According to waveforms shown in figures (3.14.a) and (3.14. b), the peak voltage across diodes D_{1P}, D_{3P}, D_{1N}, and D_{3N} is 73.6V, which, according to equations (3.68) and (3.77), equals 73.5V. According to waveforms shown in figures (3.14.c) and (3.14.d), the peak voltage across diodes D_{2P} and D_{2N} is 111.6V, and according to equations (3.73) and (3.81), it equals 110.25V. According to waveforms shown in figures (3.14.e) and (3.14.f), the peak voltage across diodes D_{5P} and D_{5N} is 294.4V, which, according to equations (3.69) and (3.78), equals 294V.

Figure (3.14):

Voltage Waveforms Across The Diodes in Boost Mode; (a) D_{1P} and D_{3P}; (b) D_{1N} and D_{3N}; (c) D_{2P} and D_{4P}; (d) D_{2N} and D_{4N}; (e) D_{5P}; (f) D_{5N}

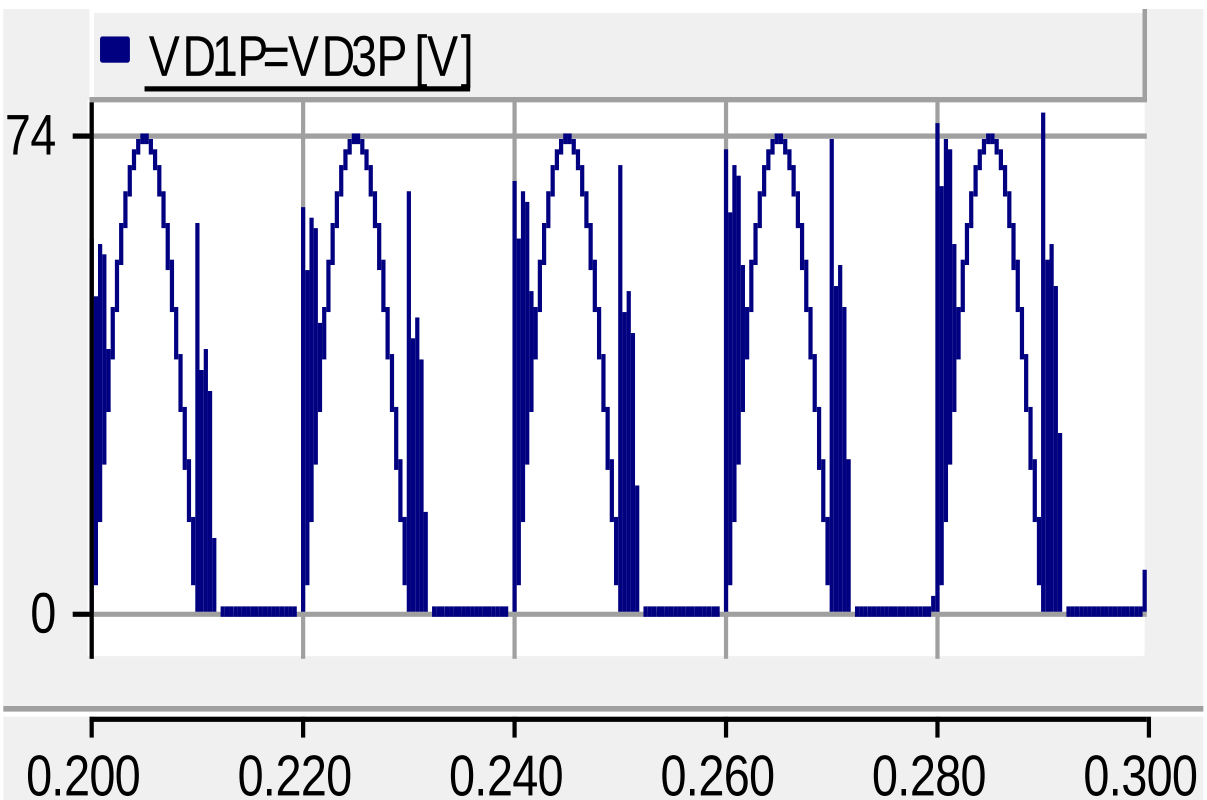

(a)

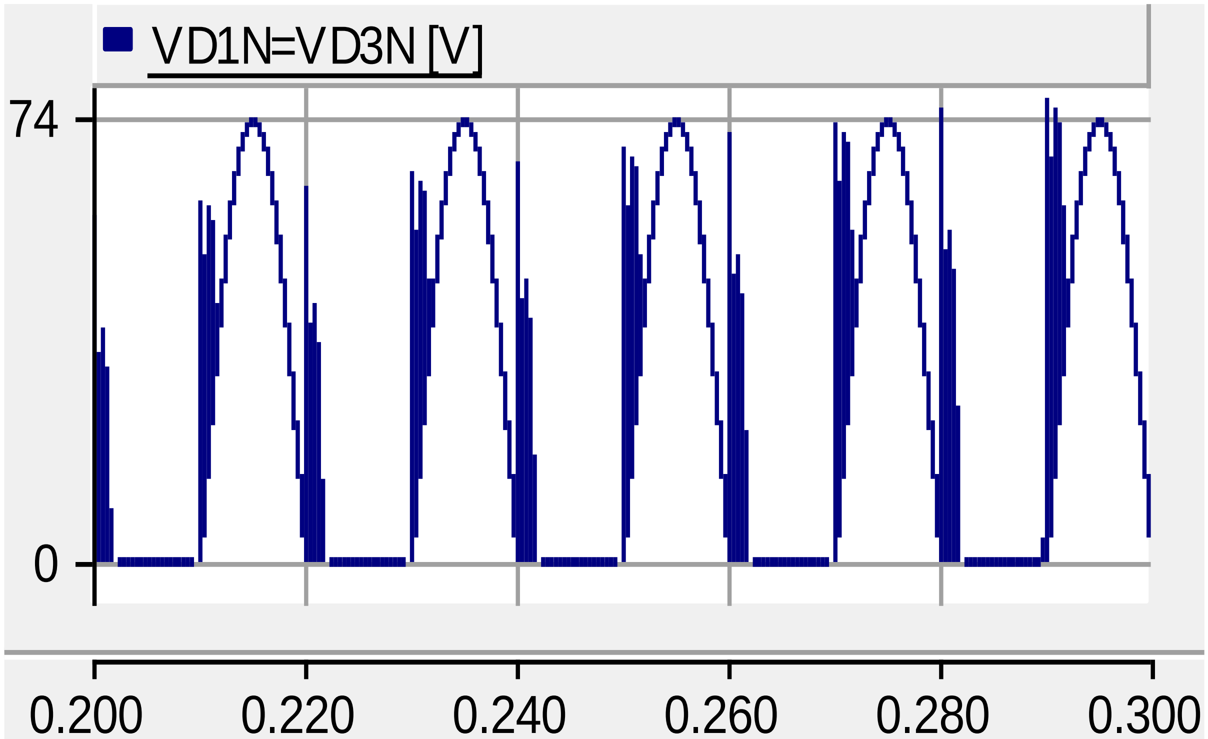
VD1N=VD3N [V]
74
0
0.200
0.220
0.240
0.260
0.280
0.300

(b)

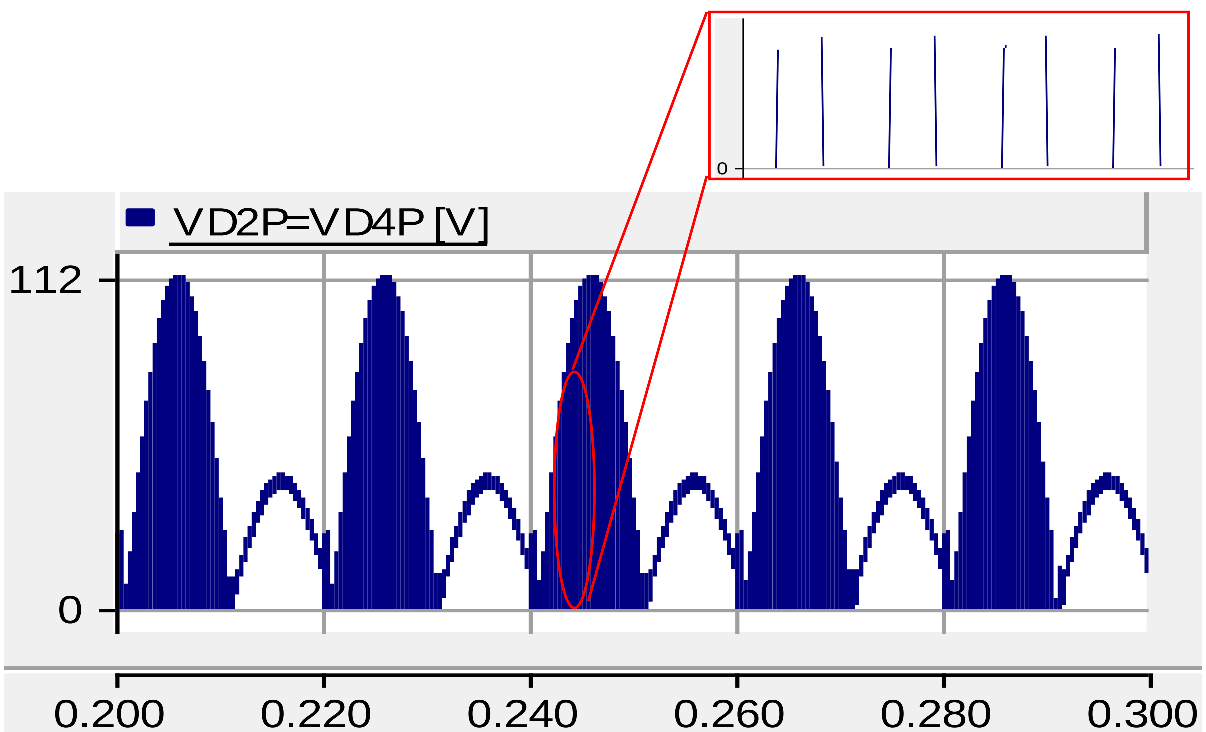
0
VD2P=VD4P [V]
112
0
0.200
0.220
0.240
0.260
0.280
0.300

(c)

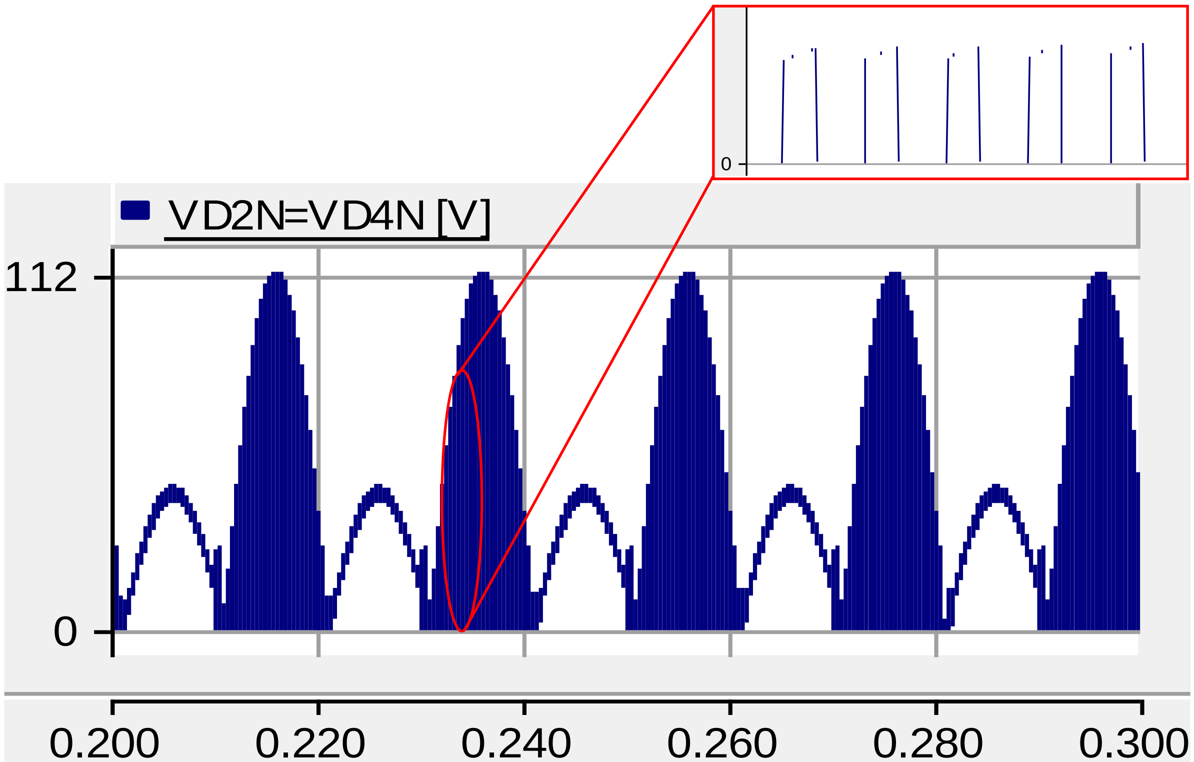
VD2N=VD4N [V]
112
0
0
0.200
0.220
0.240
0.260
0.280
0.300

(d)

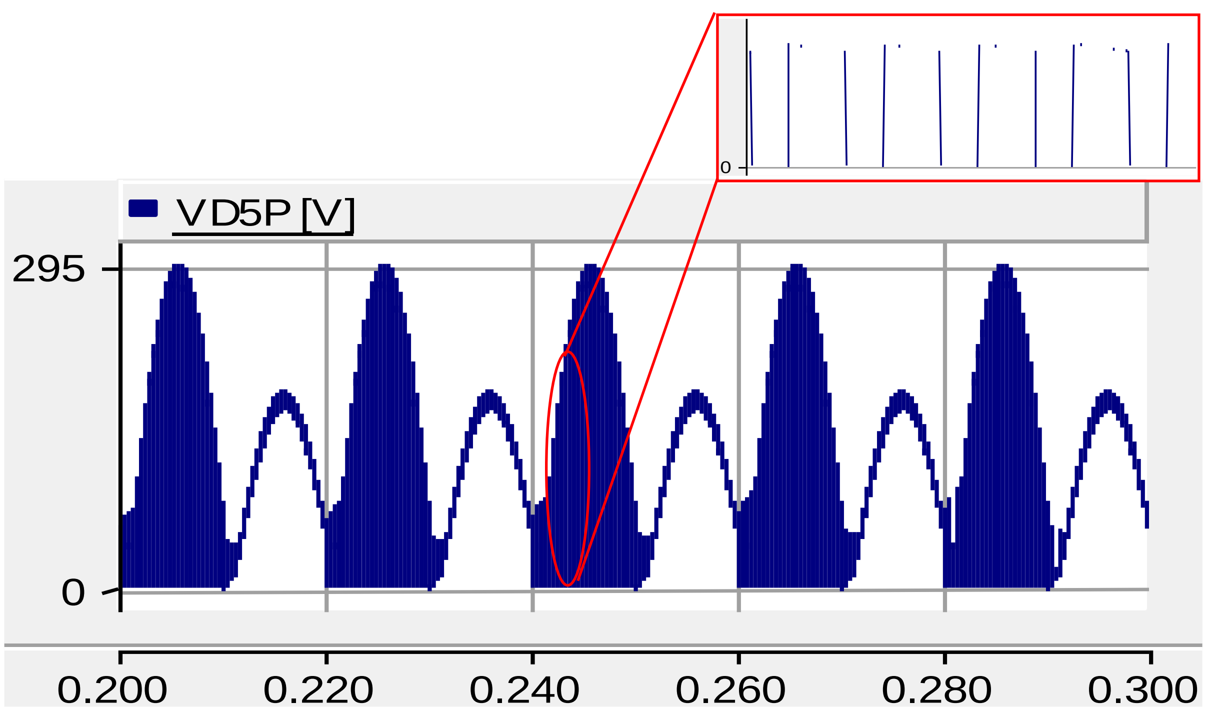
VD5P [V]
295
0
0
0.200
0.220
0.240
0.260
0.280
0.300

(e)

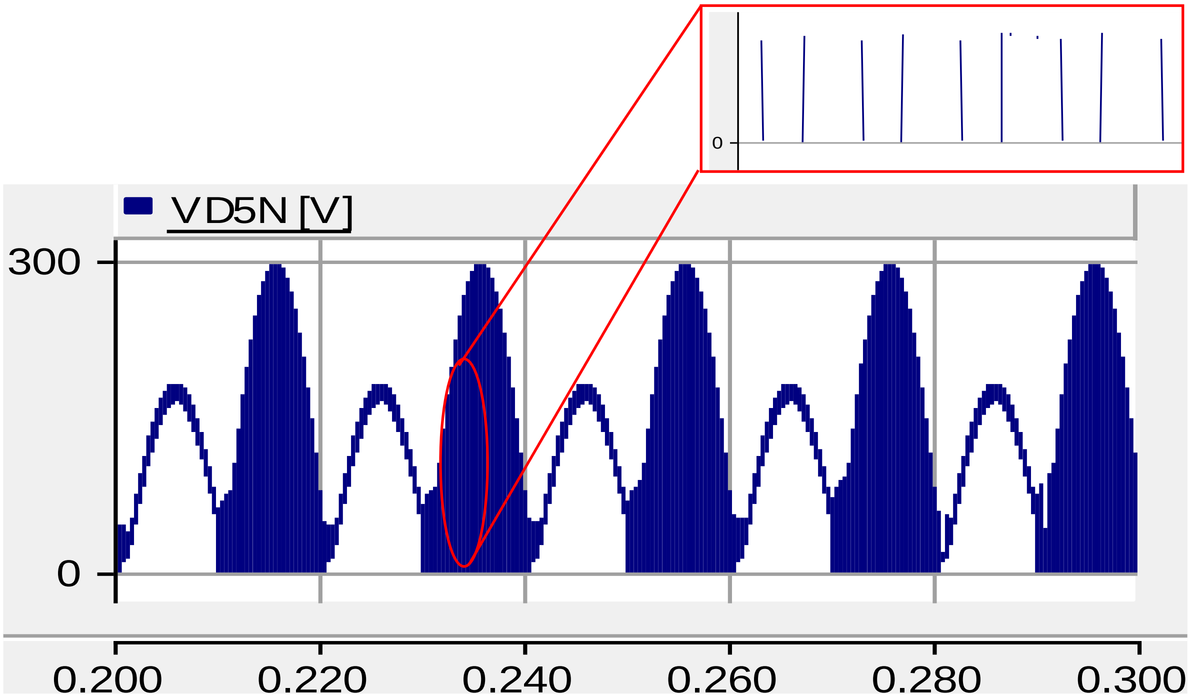

(f)

3.5.2. Buck Mode With a Frequency of 50Hz

The oscillograms of voltage at the input and output side at a frequency of 50 Hz and with the regulation of the converter's duty cycle at the level of 0. 3 are shown in figure (3. 15). In reference to Figure (3. 15. a), the input voltage waveform can be observed which is in the form of a pure sinusoid with a peak value of 73. 5V. The output voltage waveform is evident from figure (3. 15. b) and it is 64V. Thus, using the second half of the Fourier series, obtained according to equation (3. 42), the note is the fundamental component of the output voltage with a note of 63V. According to the linearity of the waveforms received the input voltage of 73. 5V is reduced to an output voltage of 63V. Hence, it is concluded that for the operating duty cycle of 0.3, the converter is in the buck mode with voltage gain of approximately 0. 86. However, the THD of the voltage waveform at the output side in Figure (3. 15. b) is 1. 48 It can be concluded from the above analysis that the operation of the proposed method is without any issues and produces output voltage waveform with acceptable THD.

Figure (3.15):

Voltage Waveforms of The Converter in Buck Mode; (a) Input Side; (b) Output Side.

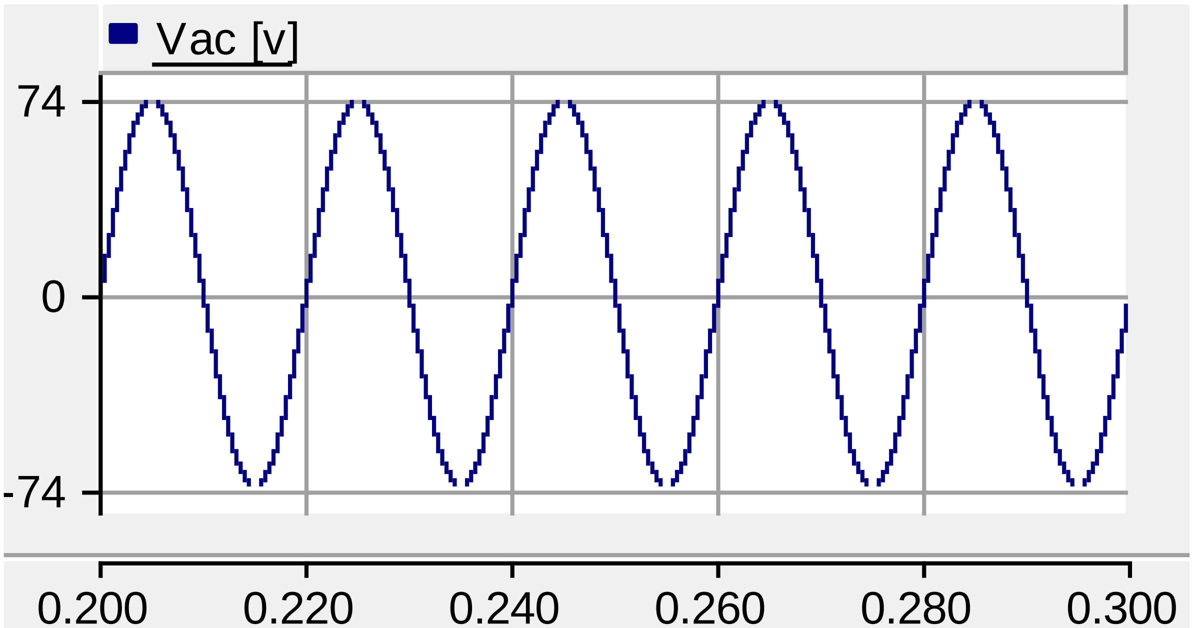

(a)

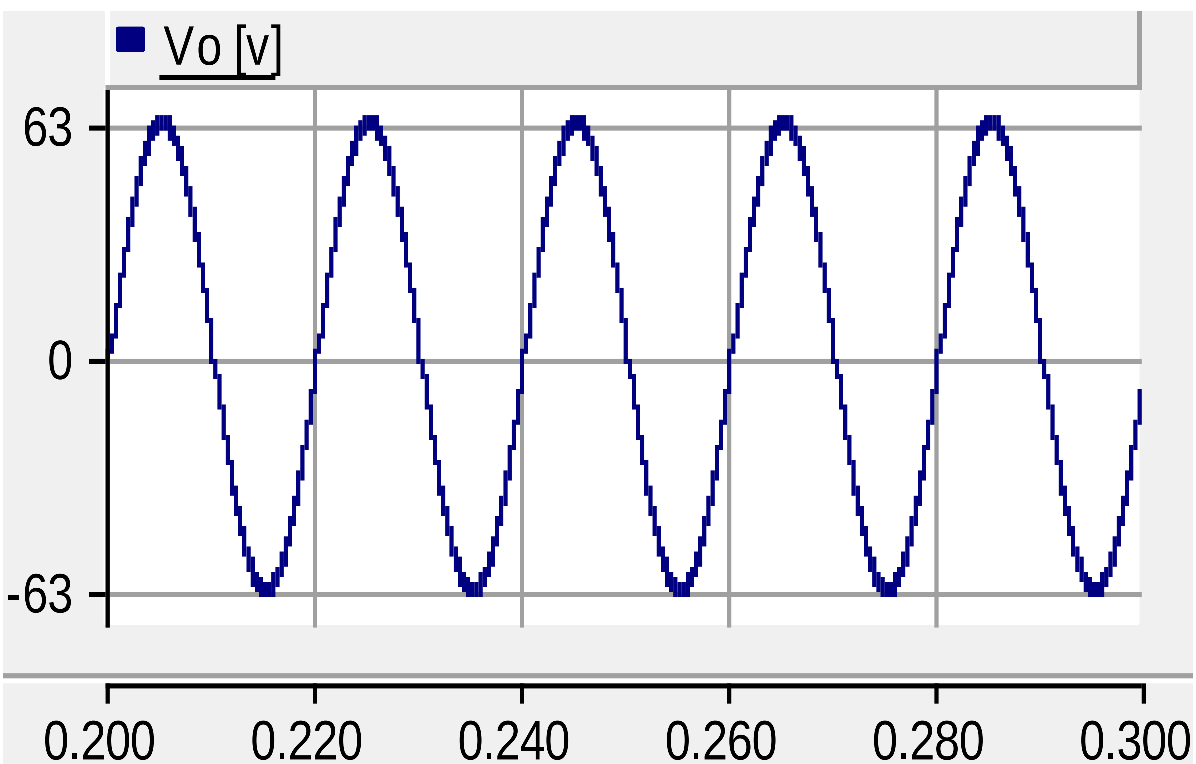

(b)

Figure (3.16): Currents waveforms of input and output side of the converter in step-down mode; (a) Input current waveform, showing a peak value of 1.3A. The theoretical peak value of the input current, assuming ideal converter operation, is 1.03A according to equation (3.88). (b) Output current waveform, with a peak value of 1.3A. The theoretical peak value of the output current is 1.2A according to equation (3.9).

Figure (3.16):

Waveforms of The Converter in Buck Mode; (a) Input Current Waveform, (b) Output Current Waveform

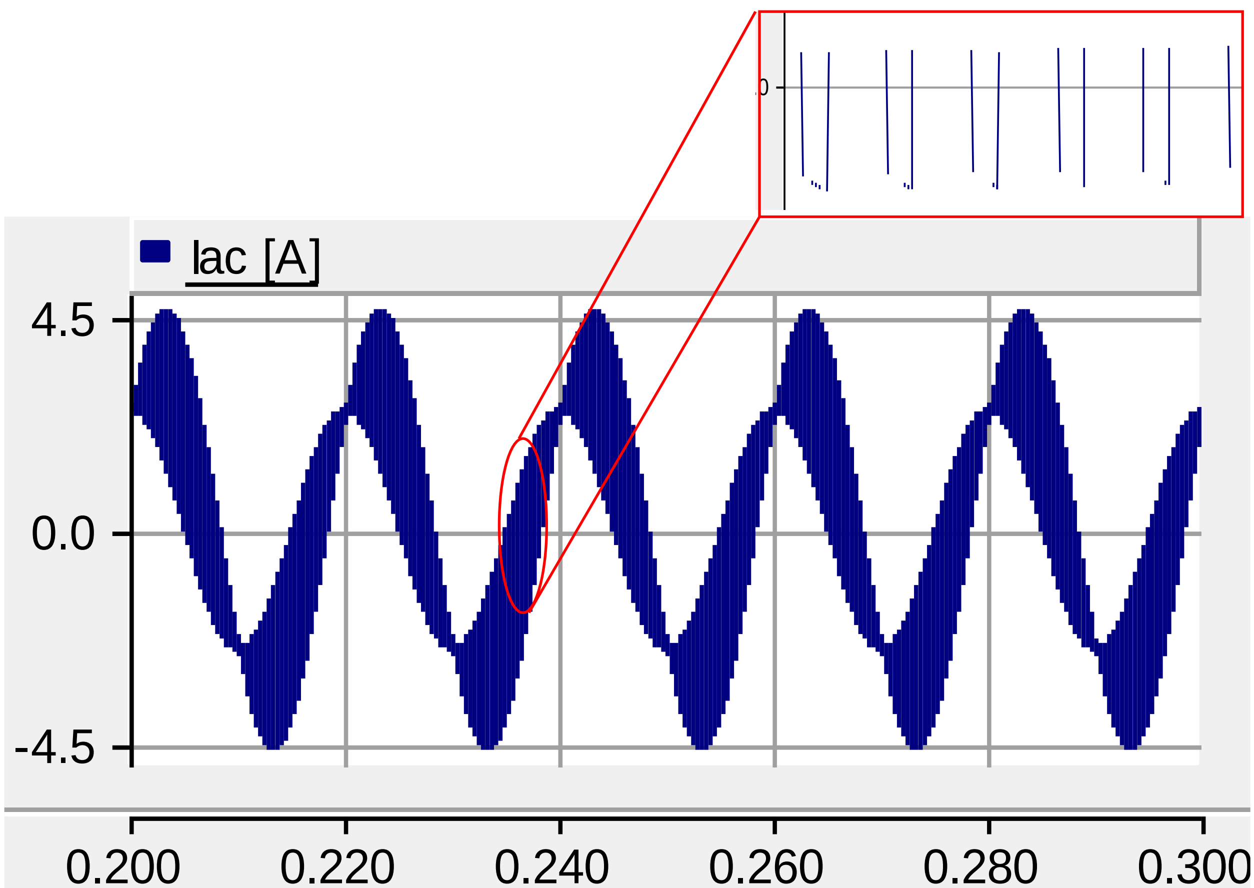

(a)

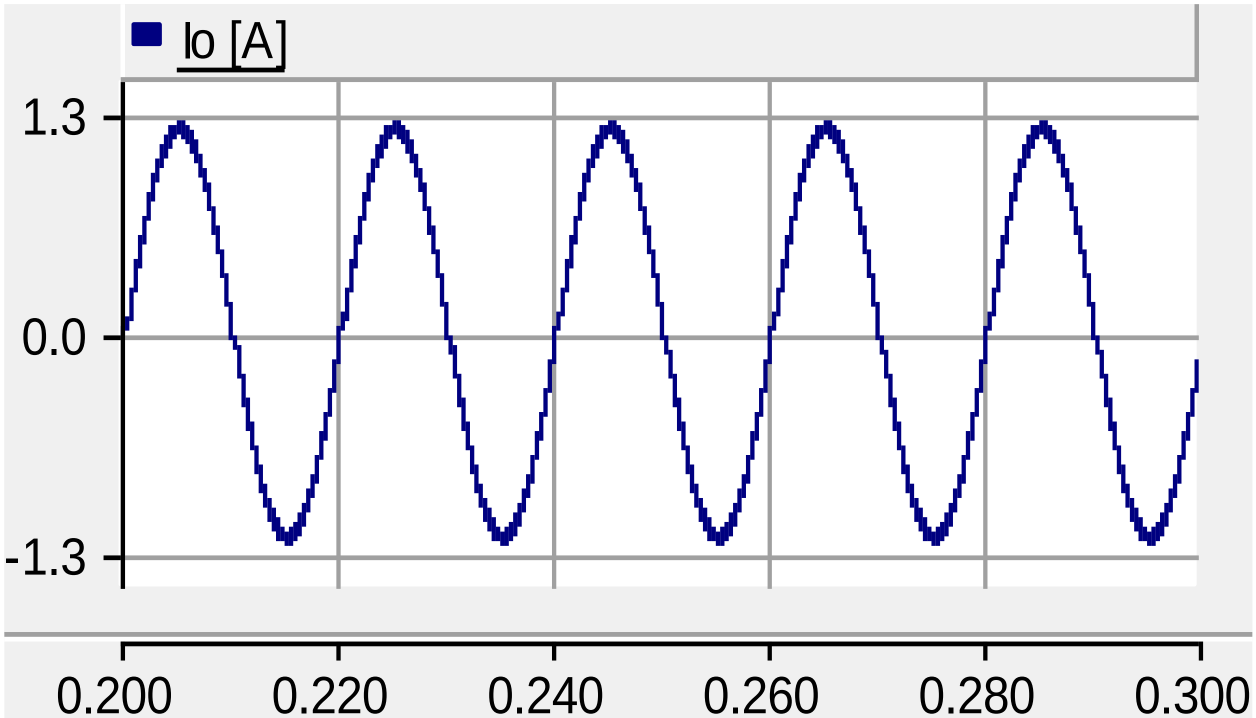

(b)

3.5.3. Boost Mode With a Frequency of 25HZ

Figure (3.17) shows the voltage waveform at the input and output side when the converter operates with a duty cycle of 0.6 and the boost ratio is 3. In Figure (3.17.a), the waveform of the input voltage is depicted, which has a peak value of 73.5V and is a pure sinusoid. Figure (3.17.b) illustrates the waveform of the output voltage, which is 223V. According to equation (3.42), the peak value of the main component of the output voltage is 220.5V with THD equal to 60.4 Considering Figure (3.17.b). As expected from the obtained waveforms, the input voltage of 73.5V increases effectively to the output voltage of 220.5V.

Figure (3.17):

Voltages *Waveforms of The Converter in The Boost Mode; (a) Input Side; (b) Output Side.*

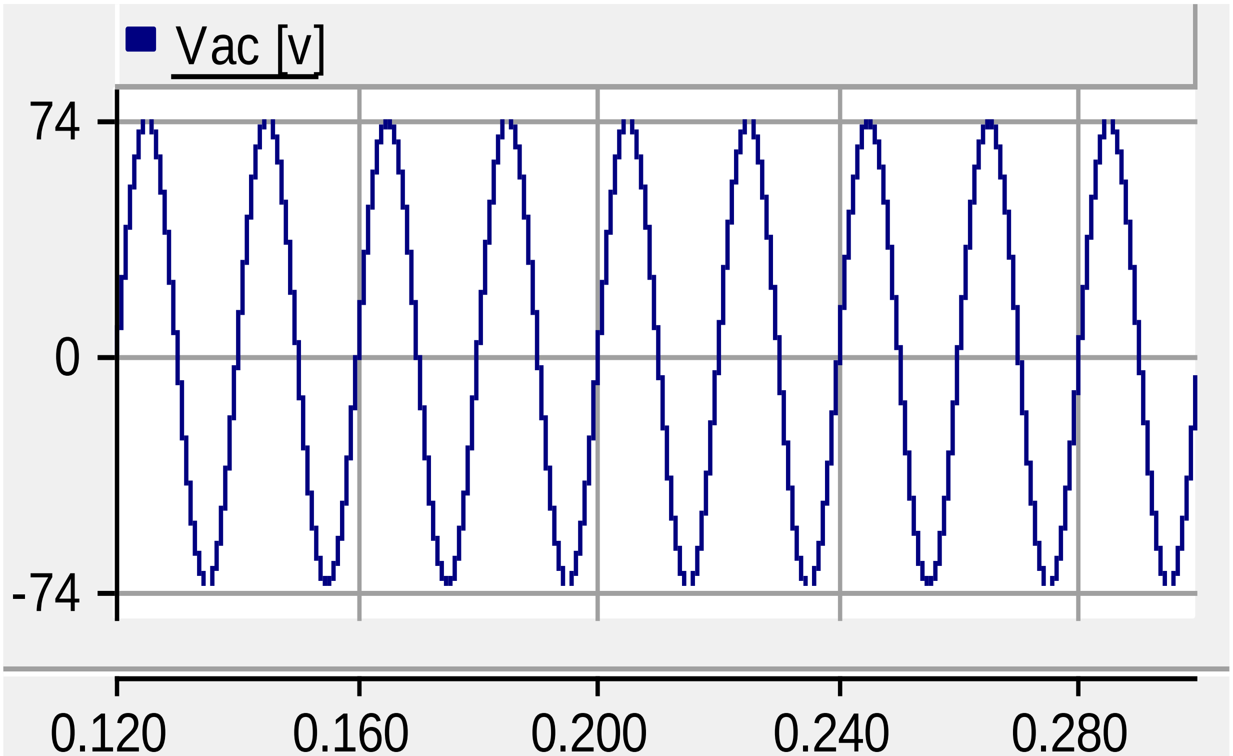

(a)

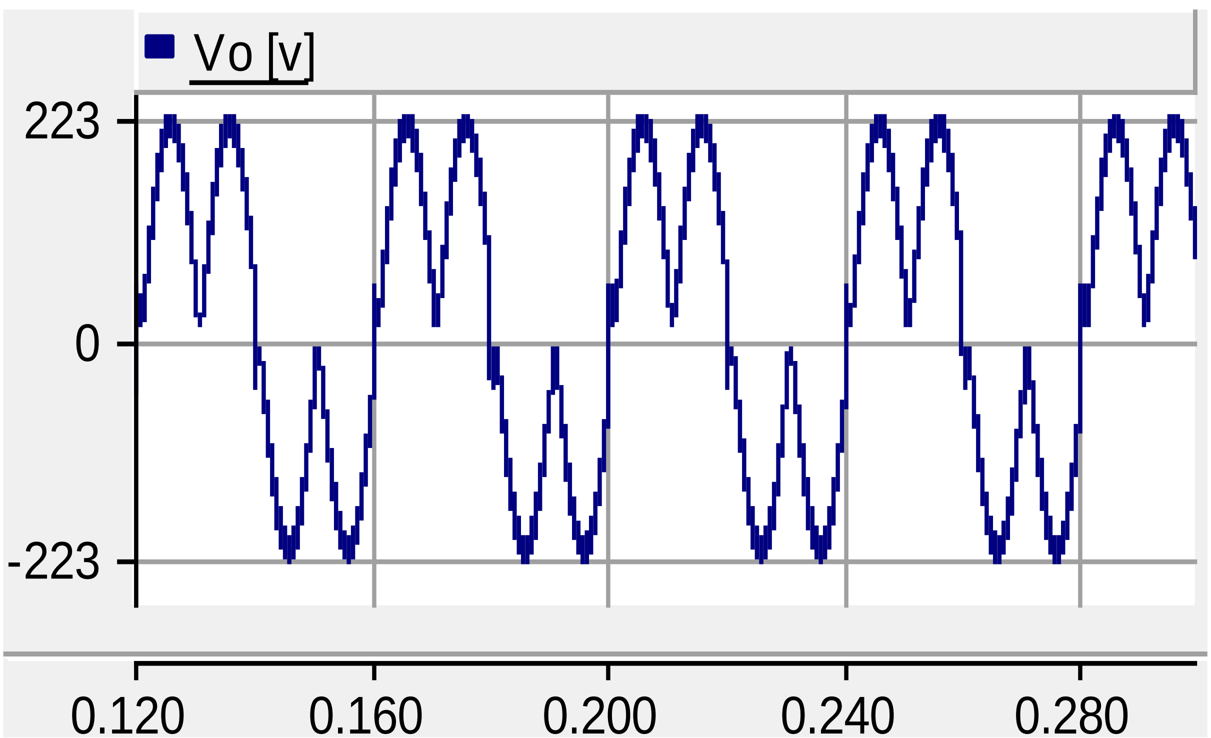

(b)

Figure (3.18): The currents waveforms at the input and output side of the converter at a frequency of 25Hz when operating with a duty cycle of 0.6. Figure (3.18.a) illustrates the waveform of the input current, with its main peak value being 13A. According to theory, assuming an ideal converter, the peak value of the input current should be 12.72A based on equation (3.88). Figure (3.18.b) depicts the waveform of the output current, with its peak value being 4.3A. According to equation (3.9), 4.2 is the theoretical peak value of the output current.

Figure (3.18):

Currents Waveforms of The Converter in The Boost Mode; (a) Input Side; (b) Output Side

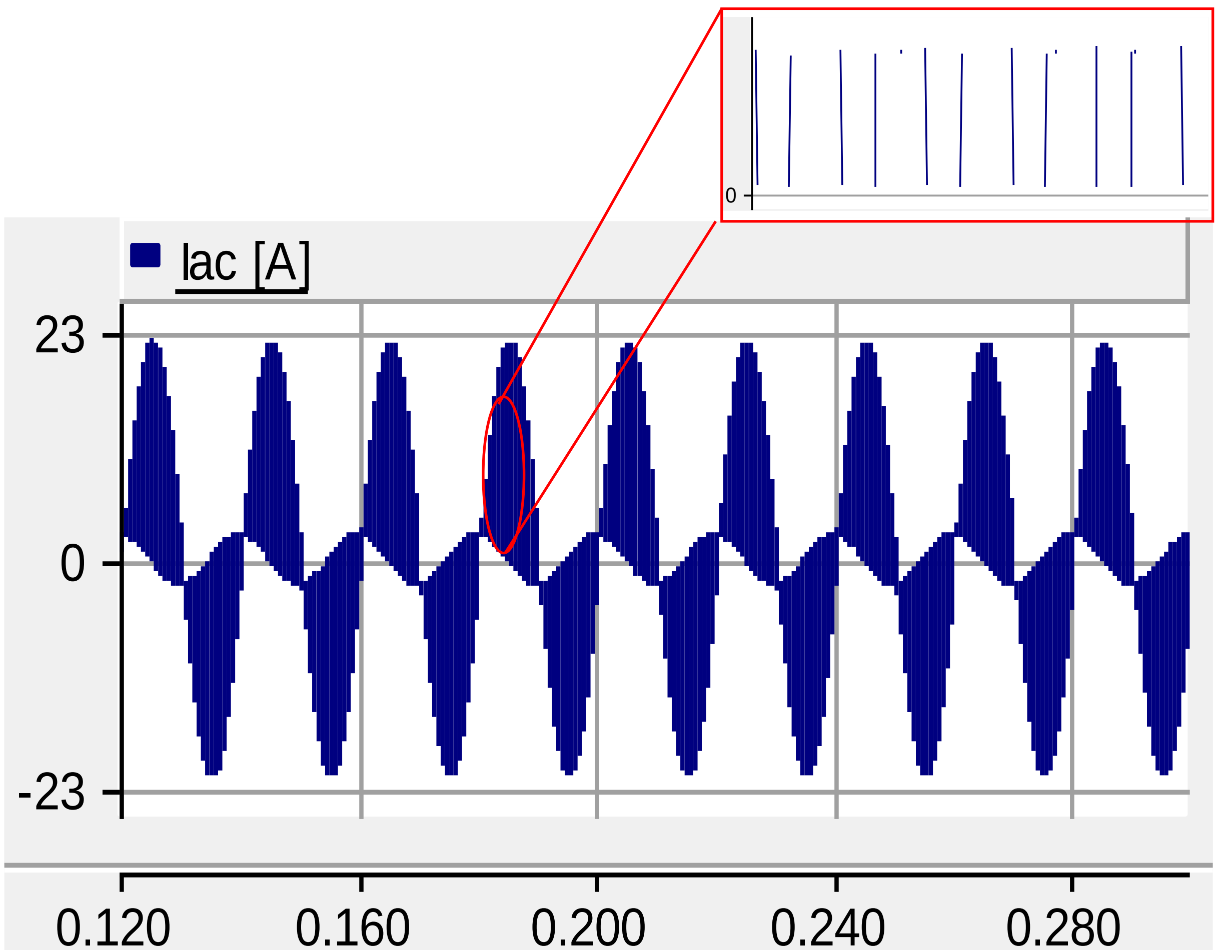

(a)

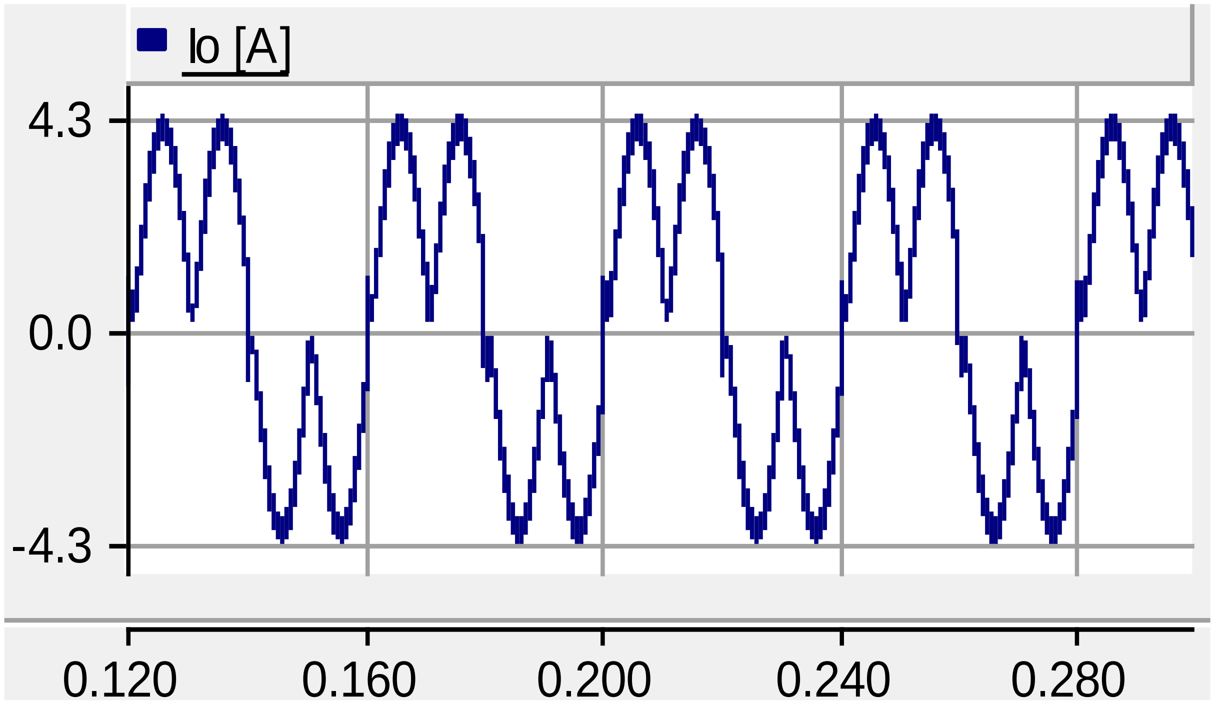

(b)

3.5.4. Buck Mode With a Frequency of 25Hz

Figure (3.19) illustrates the voltages waveforms at the input and output sides when the converter operates with a duty cycle of 0.3 at a frequency of 25Hz. Figure (3.19.a) depicts the input voltage waveform, which has a peak value of 73.5V and is a pure sinusoid. Figure (3.19.b) shows the output voltage waveform, which measures 64V. According to equation (3.42), the peak value of the main output voltage component is 63V. As expected from the obtained waveforms, the input voltage of 73.5V decreases to the output voltage of 63V with THD equal to 62.44 Considering Figure (3.19.b). Therefore, it is confirmed that with duty cycle of 0.3 and a voltage buck ratio of 0.86, the proposed converter operates in the buck mode.

Figure (3.19):

Voltages Waveforms of The Converter in The Buck Mode; (a) Input Side; (b) Output Side

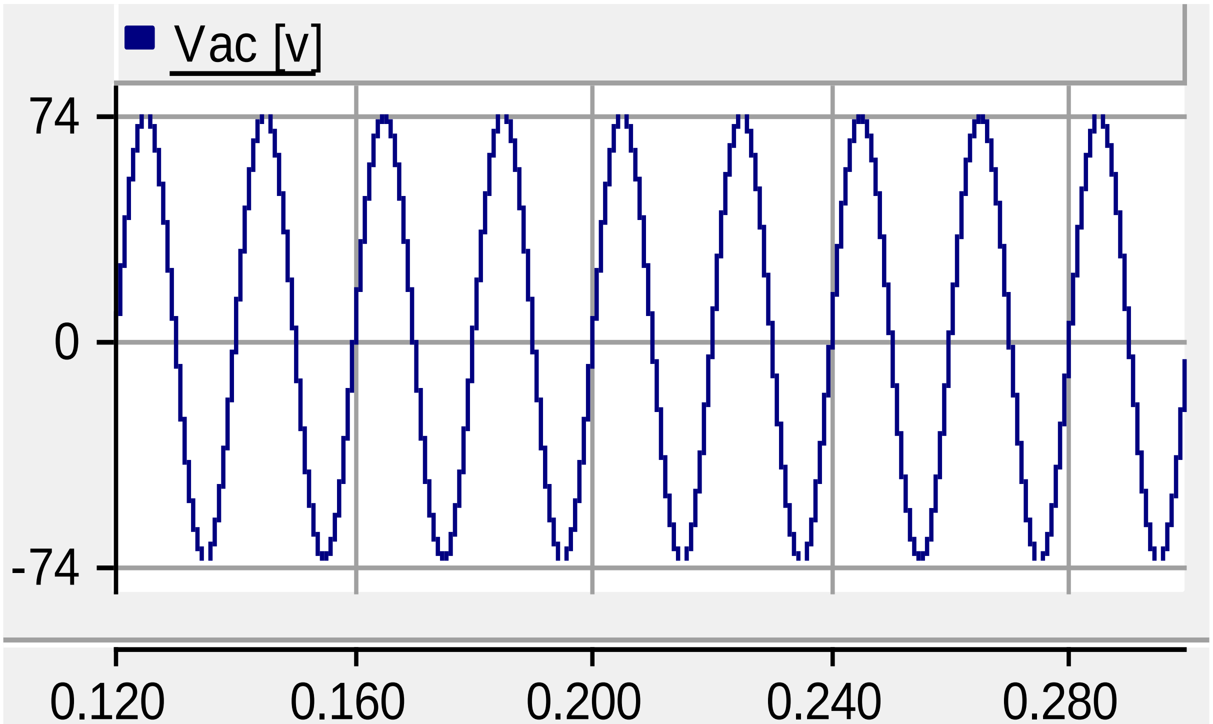

(a)

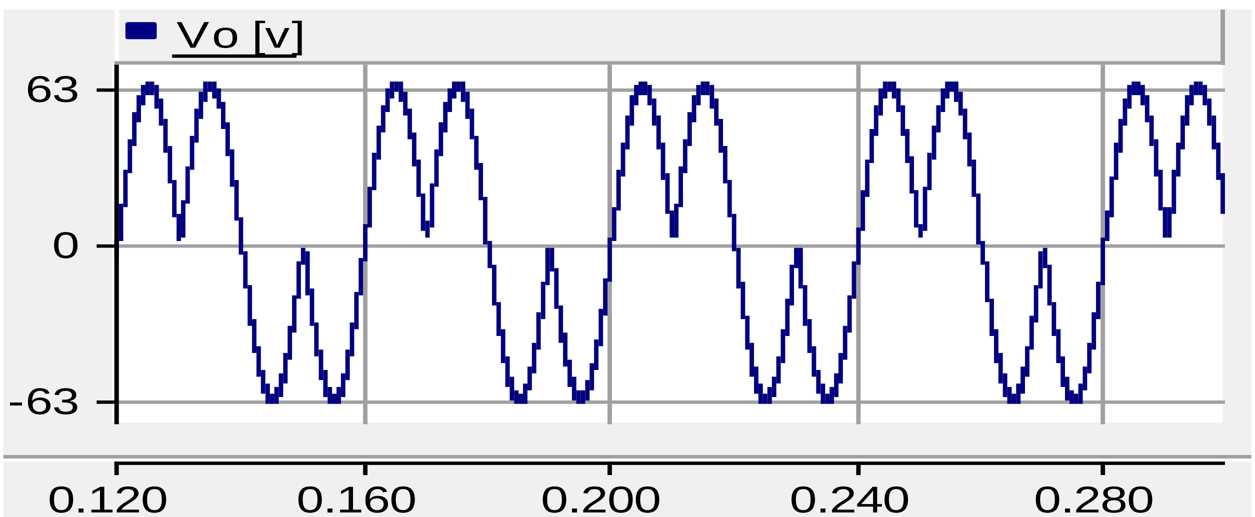

(b)

Figure (3.20): Currents waveforms at the input and output sides of the converter at a frequency of 25Hz when operating with a duty cycle of 0.3; (a) Input current waveform showing a peak main component of 1.3A. According to theory, assuming an ideal converter, the peak input current should be 1.03A as per equation (3.88). (b) Output current waveform showing a peak of 1.3A. According to equation (3.9), the theoretical peak output current should be 1.2A.

Figure (3.20):

Currents Waveforms of The Converter In The Buck mode; (a) Input Side; (b) Output Side

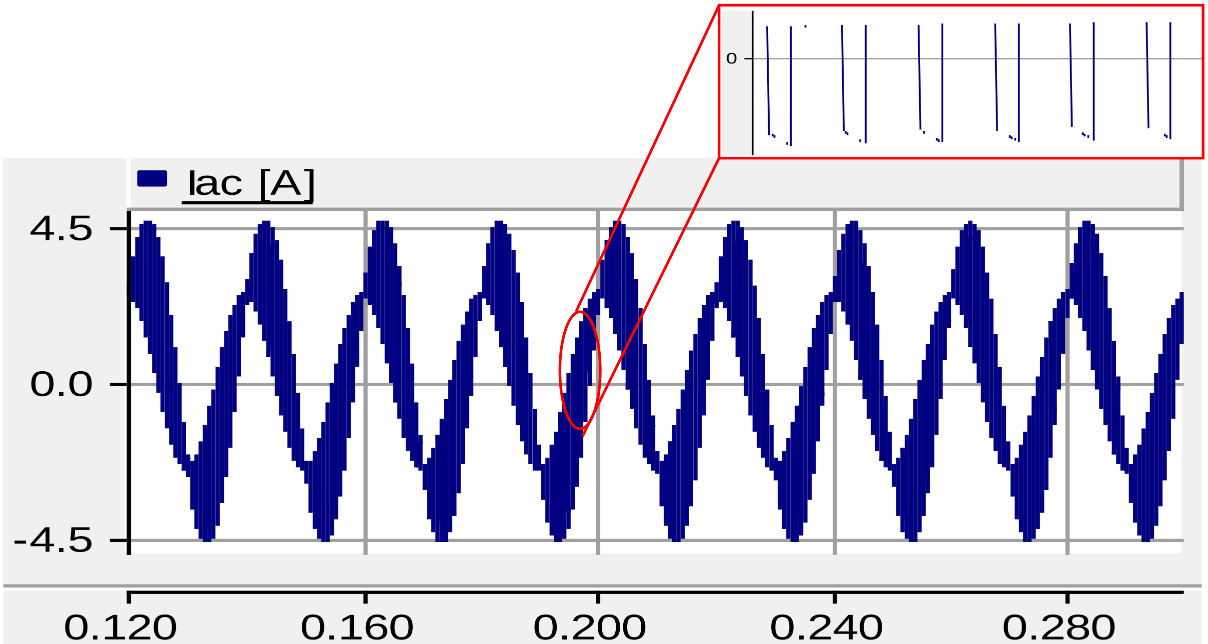

(a)

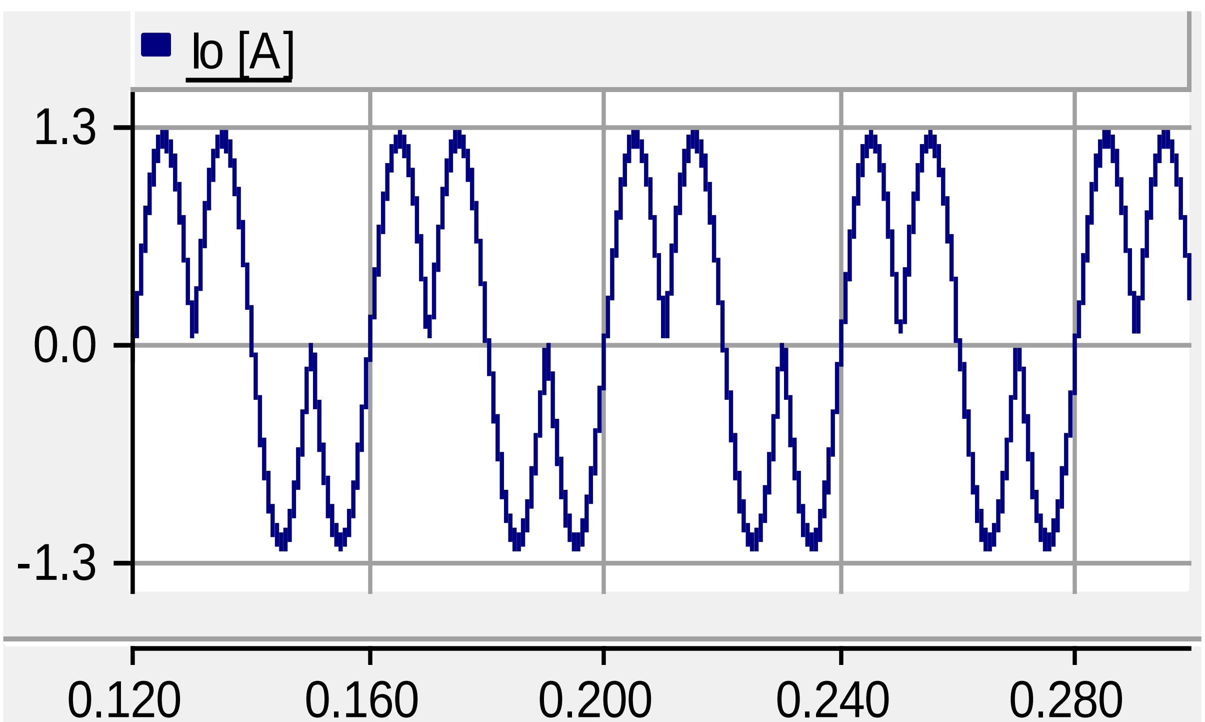

(b)

3.5.5. Boost Mode a Frequency of 100HZ

Figure (3.21) illustrates the voltage waveforms at the input and output sides at a frequency of 100Hz when the converter operates with a duty cycle of 0.6. Figure (3.21.a) depicts the input voltage waveform, with its peak value being 73.5V and exhibiting pure sinusoidal behavior. Figure (3.21.b) displays the output voltage waveform, which measures 223V. According to Equation (3.42), the peak value of the main component of the output voltage is 220.5V. As expected from the obtained waveforms, the input voltage of 73.5V increases effectively to the output voltage of 220.5V with THD equal to 58.5 Considering Figure (3.21.b). Therefore, it is confirmed that with duty cycle of 0.6 and a voltage boost ratio of 3, the proposed converter operates in boost mode.

Figure (3.21):

Voltages Waveforms of The Converter in Boost Mode; (a) Input Side; (b) Output Side

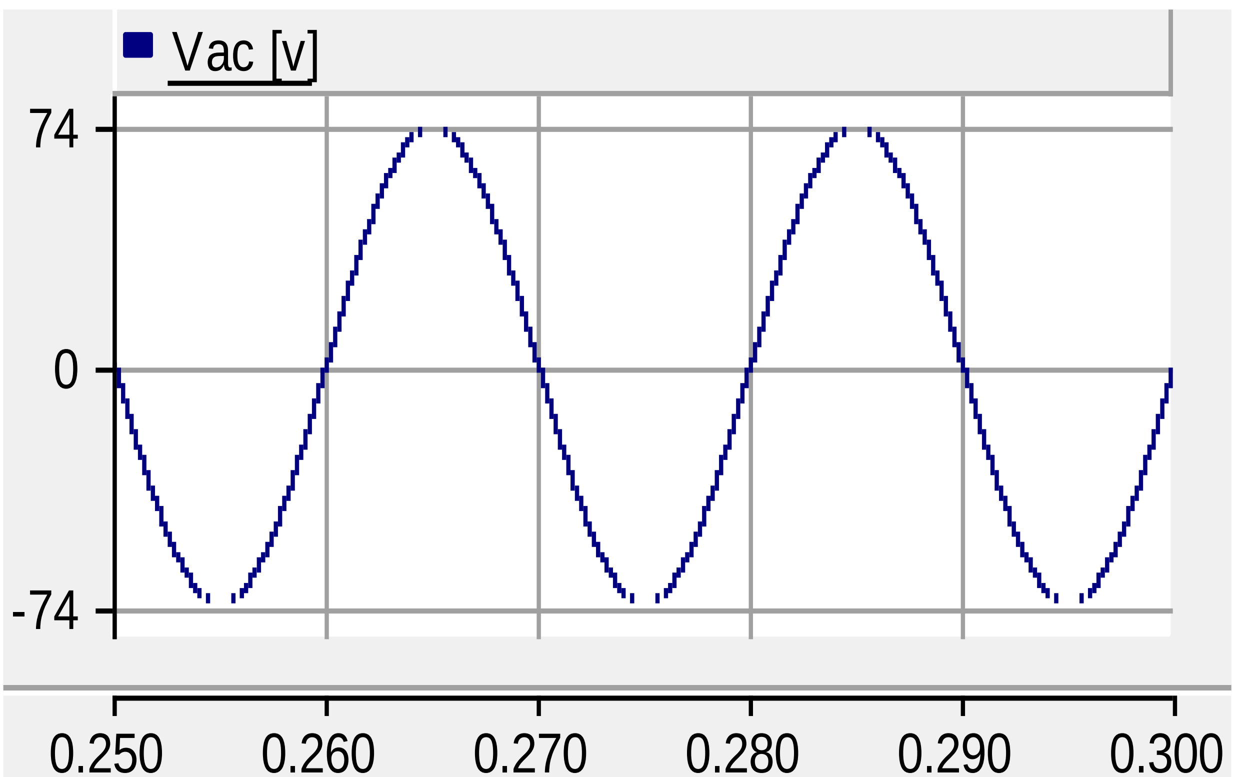

(a)

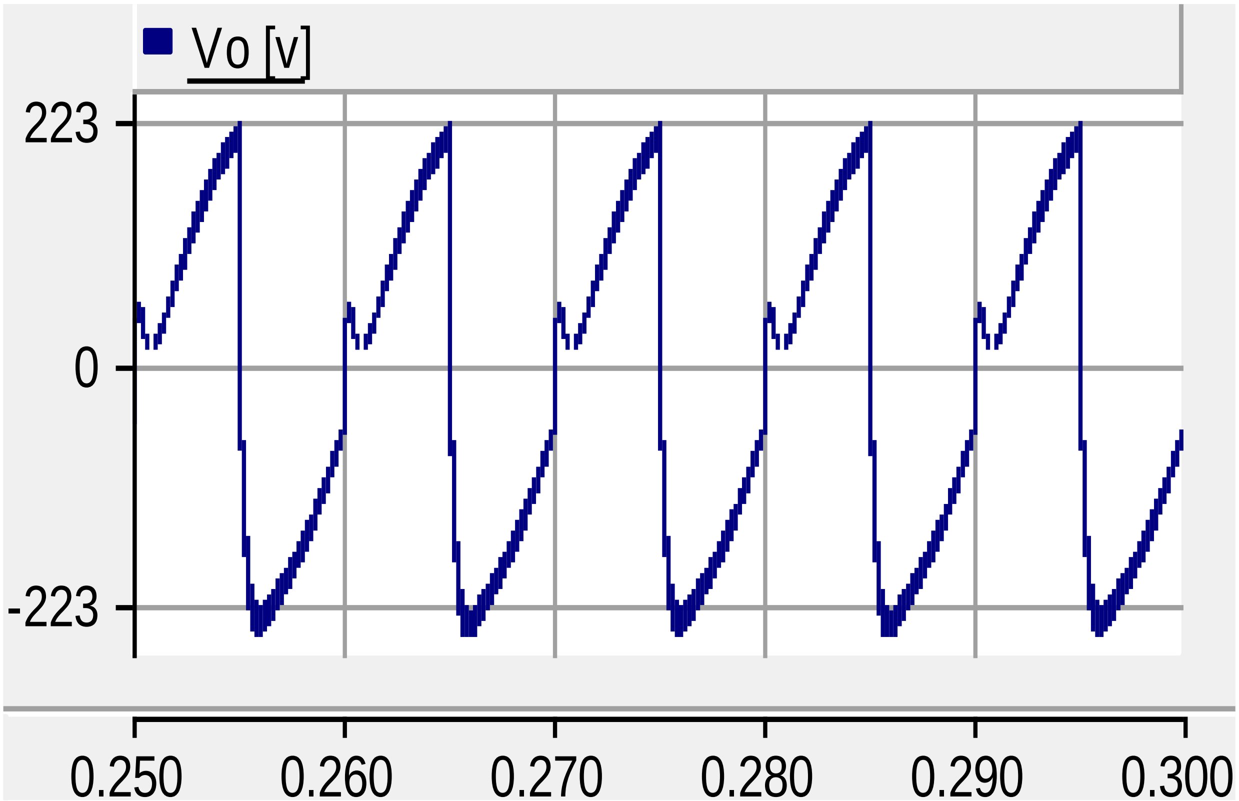

(b)

Figure (3.22) show the currents waveforms at the input and output sides of the converter at a frequency of 100Hz when operating with a duty cycle of 0.6. (a) The waveform of the input current shows a peak value of 13A, theoretically assumed to be 12.72A based on Equation (3.88) and ideal converter assumptions. (b) The waveform of the output current exhibits a peak value of 4.3A, theoretically expected to be 4.2A according to Equation (3.9).

Figure (3.22):

Currents Waveforms of The Converter In The Boost Mode; (a) Input Side; (b) Output Side

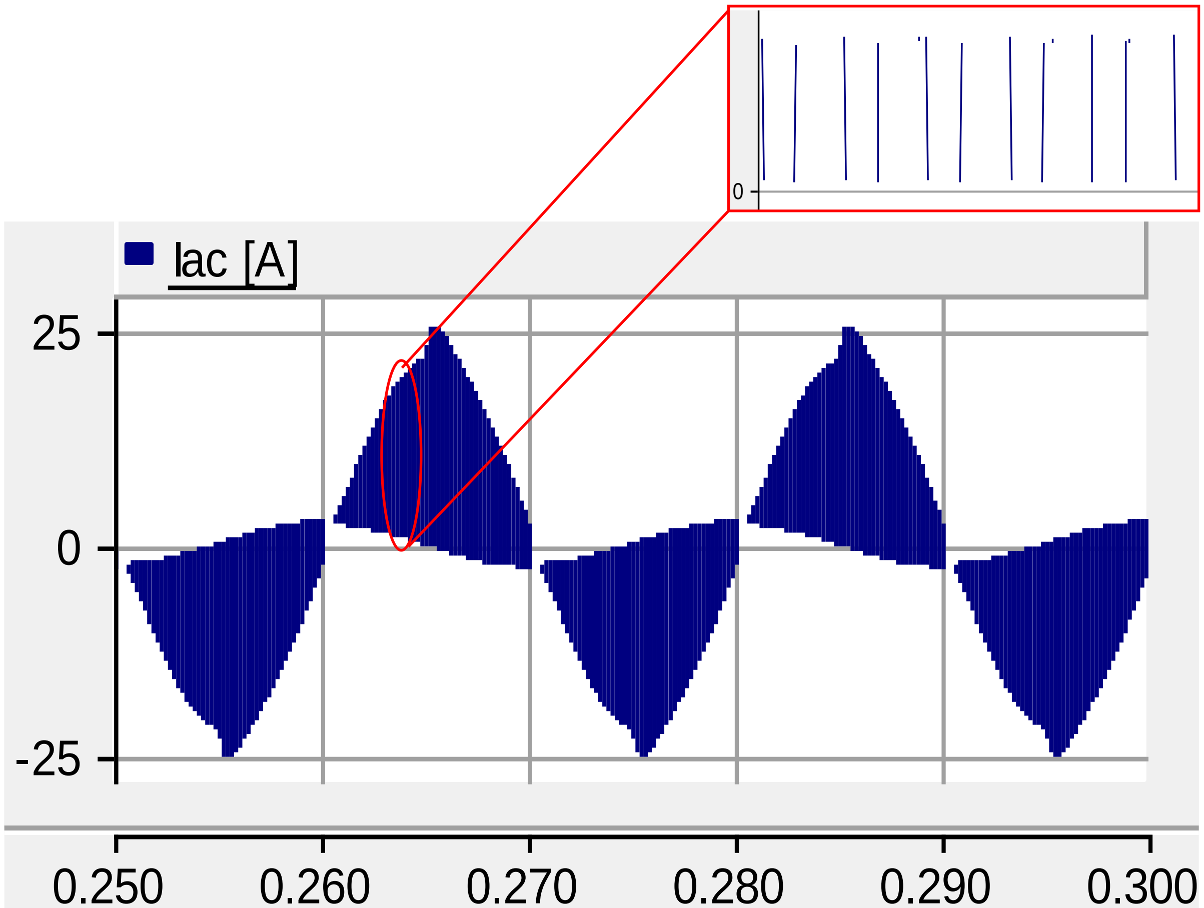

(a)

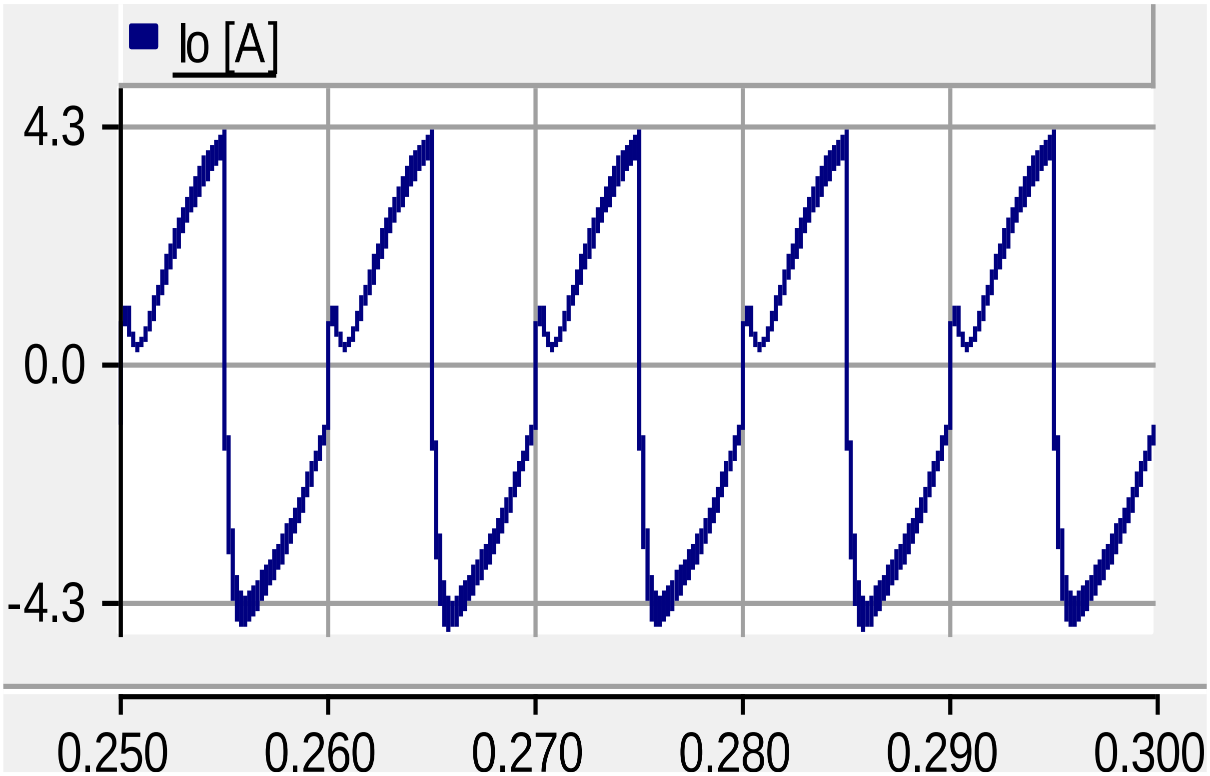

(b)

3.5.6. Buck Mode With a Frequency of 100HZ

Figure (3.23) illustrates the waveforms of the input voltage and output voltage with a frequency of 100Hz when the converter operates with a 0.3 duty cycle. Figure (3.23.a) shows the voltages waveform at the input side, with a peak value of 73.5V and a pure sinusoidal shape. Figure (3.23.b) shows the voltage waveform at the output side, which is 64V. According to equation (3.42), the peak value of the main component of the output voltage is 63V. As expected, the input voltage of 73.5V decreases to the output voltage of 63V with THD equal to 62.9 Considering Figure (3.23.b). Therefore, it confirms that with a duty cycle of 0.3 and a voltage buck ratio of 0.86, the designed converter operates in a decreasing mode.

Figure (3.23):

Voltages Waveforms at The Input and Output Sides of The Converter in Buck Mode; (a) Input Voltage; (b) Output Voltage.

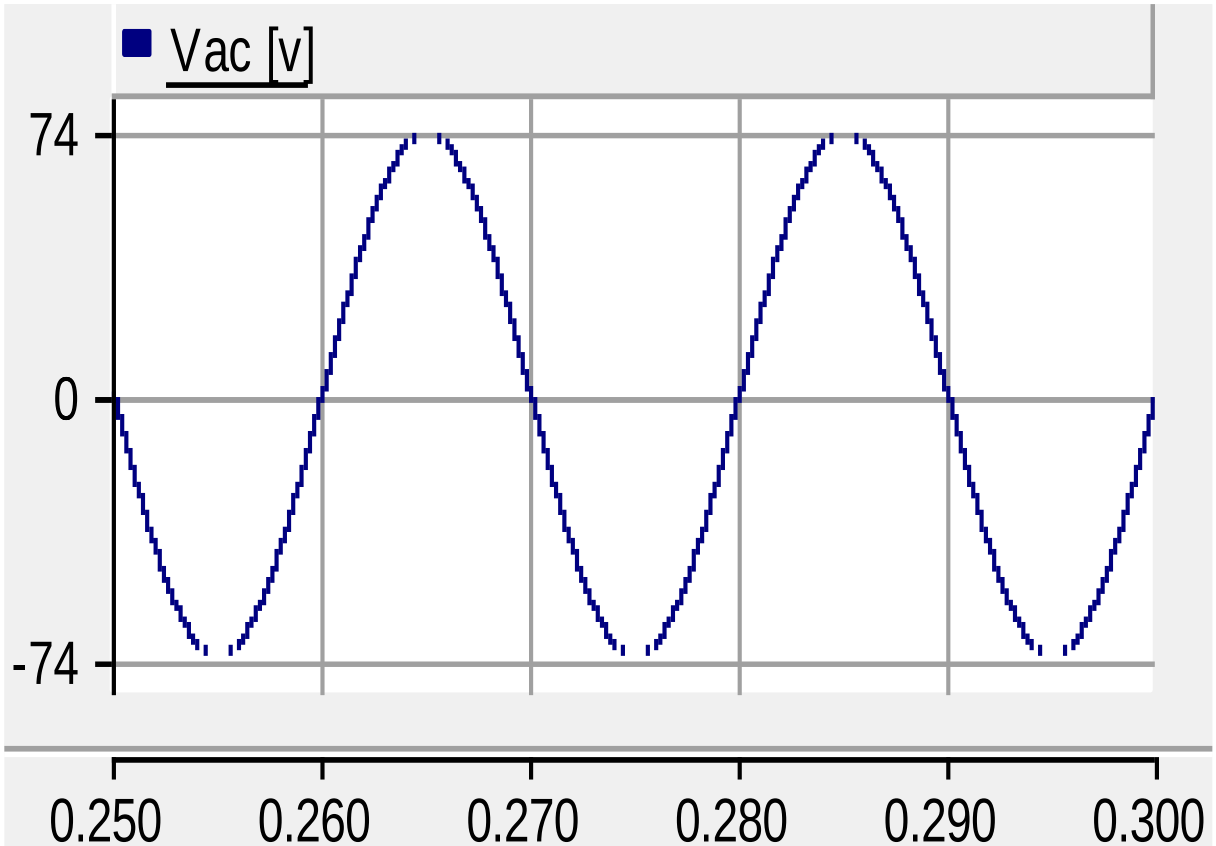

Vac [v]
74
0
-74
0.250
0.260
0.270
0.280
0.290
0.300

(a)

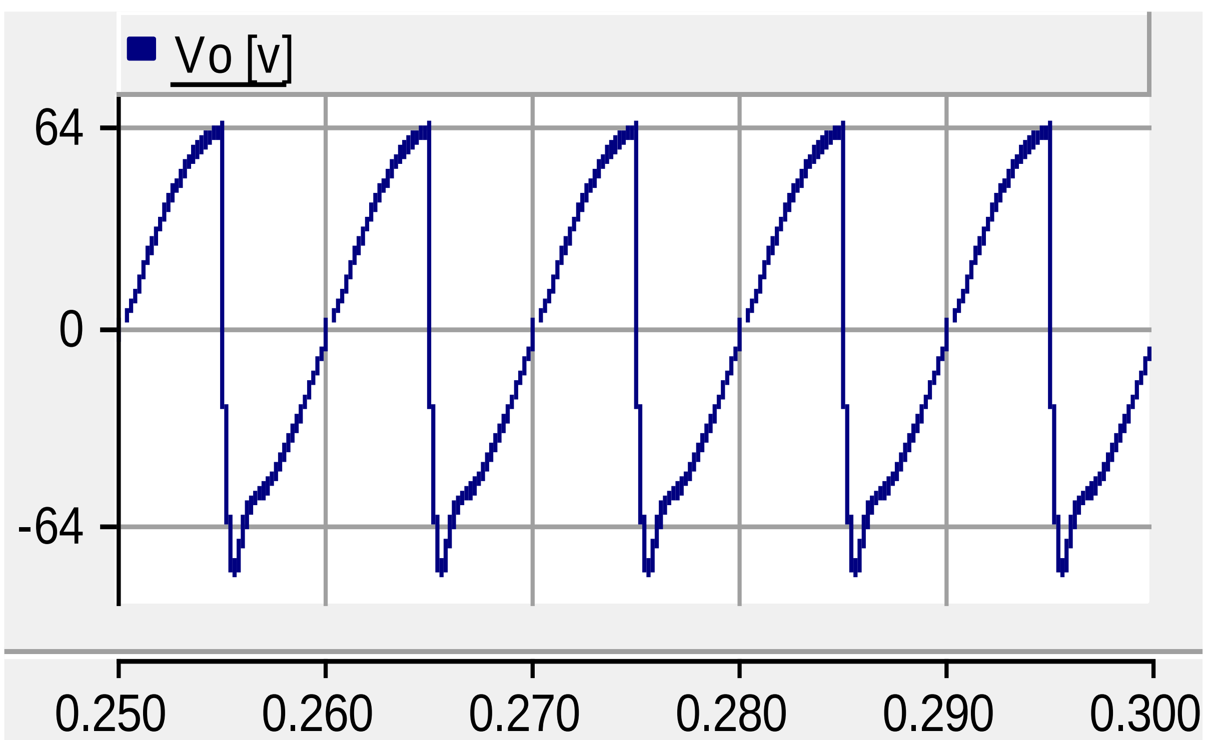

Vo [v]
64
0
-64
0.250
0.260
0.270
0.280
0.290
0.300

(b)

Figure (3.24): Current waveforms at the input and output sides at a frequency of 100Hz when the converter operates with a duty cycle of 0.3. Figure (3.24.a) shows the waveform of the input current, with its main peak value being 1.3A. The theoretical prediction, based on equation (3.88) and the ideal assumption of the converter, suggests a peak input current value of 1.03A. Figure (3.24.b) illustrates the waveform of the output current, with its peak value being 1.3A. According to equation (3.9), the theoretical peak output current value is 1.2A.

Figure (3.24):

Current Waveforms of The Converter in Buck Mode; (a) Input Side; (b) Output Side

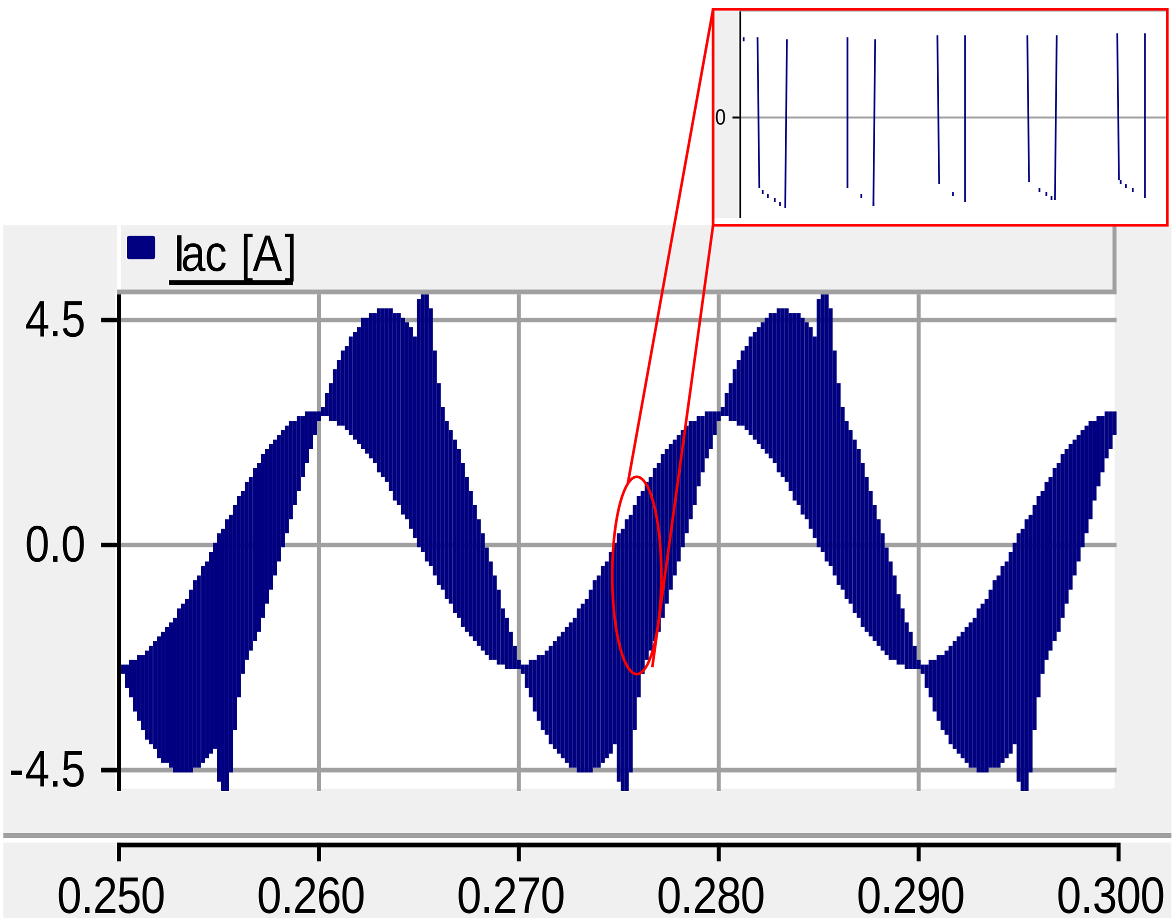

(a)

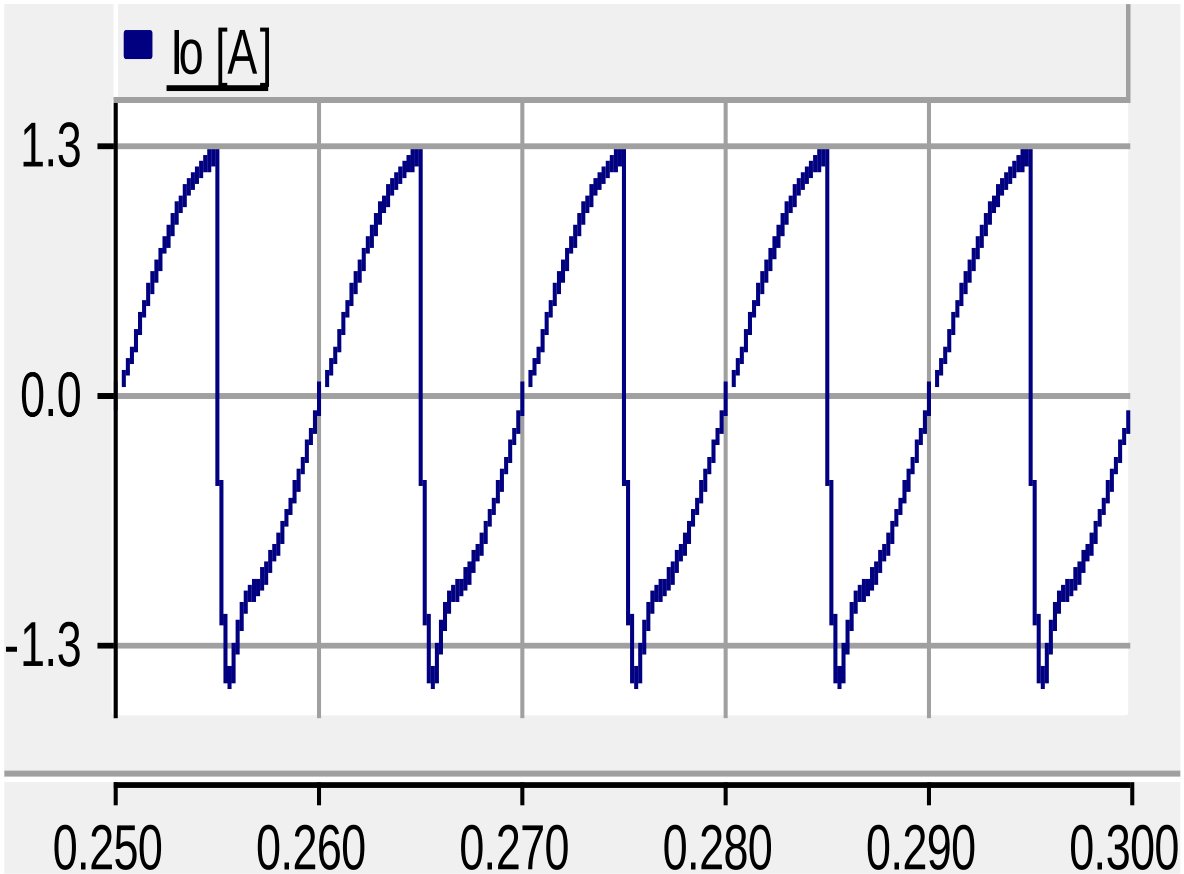

(b)

3.5.7. Summary of The Obtained Results

Table (3.2), shows the waveform quality of the output voltage of the converter in both boost and buck modes for duty cycles D = 0.3 and D = 0.6 at three different frequencies: 25Hz, 50Hz, and 100Hz. According to Table (3.2), the THD values obtained for this converter at a frequency of 50Hz fall within an acceptable range, but these values for frequencies of 25Hz and 100Hz are not within the acceptable range.

Table (3.2):

Total Harmonic Distortion (THD) of Input and Output Components of The Converter

Mode	Output Voltage	Input Current
Boost Mode (50Hz, D=0.6)	11.36%	4.1%
Buck Mode (50Hz, D=0.3)	1.48%	0.81%
Boost Mode (25Hz, D=0.6)	60.04%	18.35%
Buck Mode (25Hz, D=0.3)	62.44%	23.5%
Boost Mode (100Hz, D=0.6)	58.5%	18.8%
Buck Mode (100Hz, D=0.3)	62.49%	62.26%

CHAPTER IV

Conclusion

As it has buck-boost feature, the single-phase AC-AC shunt impedance source converter comes with a more advanced circuit design that supports perfect management of the voltage and this also offers reduction of the power losses. Its smart design includes traditional parts such as diodes, switches, capacitors and inductors which enable this converter to work with positive and negative states with the accuracy of regulation for voltage. It is interesting to note that this AC-AC converter has fewer switches than do the traditional ones. That adds to the efficiency of the converter and facilitates its operation. Finally, this system expands its performance to the input where a capacitor is added to the circuitry that not only simplify the whole system but also acts as an input filter.

Power losses are the main concerns and happen as a result of conduction and switching losses. Conduction losses, which is dependent on current flow and voltage drop, are effectively overcome in converter design. Next, switching losses, which happens when the state of a device changes, are compensated through deliberate regulation of the switching frequency.

Converter simulation results have validated its performance under different operating conditions, thus demonstrating its ability to adapt to different operating conditions. The converter with switching frequency of 100 kHz and duty ratios of 0.6 for boosting and 0.3 for bucking, indicate its capability to regulate the voltage at frequencies of 25 Hz, 50 Hz, and 100 Hz. Particularly, in boost mode the converter is fully effective by increasing input voltage level to match the target Nonetheless, particular care in component selection will be required to lower total harmonic distortion (THD) appearing in the output waveform.

The converter dominates the transparency contests with its feature of achieving a very high gain with the minimum hardware requirement. Applying an increase to one half-bridge in each operating mode improves its efficiency and functioning. Experimental validation of theoretical framework will put its reliability on a strong pedestal varying with operational conditions, processing a yield of 92.5%, 94.58% and 94.68% at the output side with frequency value ranging between double, equal to, or half of the input frequency, correspondingly.

Furthermore, the converter provides a tempered control over the DT ranging from 0 to 0.33 for bucking mode and 0.33 to 1 for boosting mode and a noticeable performance at 0.6. This remarkable fine-adjustment results in a converter which is very versatile regarding the dynamic load variations and the grid requirements, therefore it can perform better in various scenarios.

The buck-boost converter maintains a smooth operation independently, in buck and boost mode. It is highly gainful and allows for the independent regulation of output voltage, output current magnitude, and frequency. This variability makes it a good match for applications as found in adjustable speed drives and traction systems. Moreover, by resolving an issue of undershooting-shoot through risks the converter leads to the better operational stability and safety.

To sum up, the single-phase AC-AC shunt impedance source booster with buck-boost capabilities gives promising development in converter technology, offering high efficiency, exact voltage regulation, and many applications which require high mains systems. Its simplified design and its efficient action make it having great significance for flexible power systems installed at present.

Recommendations and Future work

Improvements in component optimization, control algorithms, Energy storage integration, experimental revalidation, application-specific assessments, and cost effectiveness can be further achieved through prolonged research and development efforts which will in turn lead to enhancement of performance, reliability, and economic competitiveness of the single-phase impedance converter with buck-boost capacity. An improvement can be made to increase the boosting ratio of the converter to a higher range with smallest total harmonic distortion that could be get from the output wave. Through the solutions in these domains, the converter can achieve full potential and become the significant performers in power conversion pushing technological breakthrough evolution.

References

[1] Lucanu, M., Ursaru, O., Aghion, C., & Lucanu, N. (2017). Single-phase buck direct AC-AC converter with two inductances and improved efficiency. buletinul institutului politehnic din iaşi, volumul 63 (67)(1).

[2] Mousavi, S. M. J., Babaei, E., & Alizadeh, D. (2022, February). Non-isolated single-phase trans-Z-source converter for dynamic voltage restorer application. In 2022 13th Power Electronics, Drive Systems, and Technologies Conference (PEDSTC) (pp. 368-373). IEEE.

[3] Alizadeh, D., Babaei, E., & Sabahi, M. (2022). Analysis of the non-isolated step-up network based on impedance source converter. IET Power Electronics. Advance online publication.

[4] Lucanu, M., Ursaru, O., Aghion, C., & Lucanu, N. (2014). Single Phase Direct AC-AC Step-Down Converter. IET Power Electronics, 7(12), 3101-3109.

[5] Soliero, T. B., Petry, C. A., Fagundes, J. C. dos S., & Barbi, Y. (2011). Direct AC-AC Converters Using Commercial Power Modules Applied to Voltage Restorers. IEEE Transactions on Industrial Electronics, 58(1), 278-288.

[6] Aurasopon, A., & Khamsen, W. (2013). Improvement of Input Power Factor in PWM AC Choppers by Selecting the Optimal Parameters. Przeghed Elektrotechiczny, 89(10), 210-216.

[7] Adel, F., Lashine, A. E., El-Sabbe, A. E., & Osheba, D. S. M. (2023). A single-phase direct buck-boost AC-AC converter with minimum number of components. Scientific Reports,13(1),9009.

[8] Sonar, S., Maity, T., & Minu, M. (2013). Single phase transformerless wide range AC boost voltage regulator based on Z-source network. International Journal of Electrical Power & Energy Systems,47,193-197.

[9] Wijekoon, T., Klumpner, C., Zanchetta, P., & Wheeler, P. W. (2008). Implementation of a hybrid ac–ac direct power converter with unity voltage transfer. IEEE Transactions on Power Electronics, 23(4), 1918–1926.

[10] Vargas, R., Ammann, U., & Rodriguez, J. (2009). Predictive approach to increase efficiency and reduce switching losses on matrix converters. IEEE Transactions on Power Electronics, 24(4), 894–902.

[11] Peng, F. Z., Yuan, X., Fang, X., & Qian, Z. (2003, June). Z-Source Inverter for Adjustable Speed Drives. IEEE Power Electronics Letters, 1(2), 33.

[12] Zarei, G., Babaei, E., & Banae Sharifian, M. B. (2023). Analysis, design, and implementation of switched Z-source inverter with an extra control input. IET Power Electronics. Advance online publication.

[13] Babaei, E., Babayi, M. H., SHOKATIASL, E., & Laali, S. (2015). A new topology for Z-source inverter based on switched-inductor and boost Z-source inverter.

[14] A. A. Khan, H. Cha, and H. F. Ahmed. (August 2016). "High-Efficiency Single-Phase AC–AC Converters Without Commutation Problem," IEEE Transactions on Power Electronics, vol. 31, no. 8, pp. 5655.

[15] Colak, I., & Yildirim, D. (2010, December). The control unit of a single-phase voltage regulator. In IECON 2010 - 36th Annual Conference of IEEE Industrial Electronics Society (pp. 1-5). IEEE Xplore.

[16] Liu, C., Sun, P., Lai, J.-S., Ji, Y., Wang, M., Chen, C.-L., & Cai, G. (2012). Cascaded dual-boost/buck active-front end converter for intelligent universal transfer. IEEE Transactions on Industrial Electronics, 59(12), 4671–4680.

[17] Babaei, E., Shokati Asl, E., & Laali, S. (2023). A Modified Series Z-Source Inverter Based on Switched Inductors with a High Voltage Gain and a Reduced Voltage Stress on Capacitors. Energy Engineering and Management, 10(4), 2-13.

[18] Lucanu, M., Ursaru, O., Aghion, C., & Lucanu, N. (2014). Single-Phase Direct AC-AC Boost Converter. Advances in Electrical and Computer Engineering, 14(3). Gheorghe Asachi Technical University of Iasi, Faculty of Electronics, Telecommunications and Information Technology, Bvld. Carol 1, No. 11, 700506, Iasi, Romania.

[19] Li, H. L., Hu, A. P., & Covic, G. A. (2012, February). A Direct AC–AC Converter for Inductive Power Transfer Systems. IEEE Transactions on Power Electronics, 27(2), 661.

[20] X. P. Fang, Z. M. Qian, and F. Z. Peng, "Single-Phase Z-Source PWM AC-AC Converters," IEEE Power Electronics Letters, vol. 3, no. 4, pp. 121, December 2005.

[21] Geng, X., Tang, H., Jin, N., & Lan, J. (2013). Direct Buck-type AC-AC Converters using VSC Metod. Przegląd Elektrotechniczny.

[22] Adel, F., Lashine, A. E., El-Sabbe, A. E., & Osheba, D. S. M. (2023). A single-phase direct buck-boost AC–AC converter with minimum number of components. Scientific Reports, 13, 9009.

[23] Babaei, E., Mousavi, S. M. J., Alami, M. A., & Alizadeh, D. (2022). A Review on Single-Phase AC-AC Z-Source Converters. AUT Journal of Electrical Engineering, 54(1), 137-162.

[24] Mousavi, S. M. A., Babaei, E., & Alizadeh, D. (February 2022). Non-Isolated Single-Phase Trans-Z-Source Converter for Dynamic Voltage Restorer Application. In 2022 13th Power Electronics, Drive Systems, and Technologies Conference (PEDSTC).

[25] Fang, X., Qian, Z. M., & Peng, F. (January 2006). Single-phase Z-source PWM AC-AC converters. IEEE Power Electronics Letters, 3(4), 121-124.

[26] Subhani, N., Kannan, R., Mahmud, A., & Blaabjerg, F. (20 January 2021). Z-source inverter topologies with switched Z-impedance networks.

[27] Mathew, D., Ashok, A. P., & Mathew, B. (March 2015). Modified Single Stage AC-AC Converter. International Journal of Power Electronics and Drive System (IJPEDS), 6(1), 1-9. ISSN: 2088-8694.

[28] RayMingPCB. (2023, December 29). How to Design an AC to DC Converter Circuit

[29] Rahman, K., Meraj, M., Bhaskar Ranjana, M. S., & Iqbal, A. (2019). Single Phase ZAC-Source AC-AC Converter with High Buck and Boost Voltage Conversion Capability. IEEE Transactions on Industrial Electronics, PP(99), 1-1.

[30] Martinez, J., Cano-Andrade, S., Padilla-Medina, J. A., & Perez-Pinal, F. J. (2020). Design and Implementation of an Embedded Control System for the Interconnection of a DC Microgrid to the AC Main Network. Electric Power Components and Systems, 48(5), 1-16.

[31] Editorial Team. (2015, June 6). Analysis of Four DC-DC Converters in Equilibrium

[32] Aguiar, E. L. de, Cardoso, R., Stein, C. M. de O., & Carati, E. G. (2016). Distributed Renewable Power Sources in Weak Grids — Analysis and Control. In W. Cao & Y. Hu (Eds.), Renewable Energy - Utilisation and System Integration (Chapter 9).

[33] Esmaeili, S., Azimi, E., Hafezi, H., Mahmoudi, A., Jamil, M., & Khan, A. A. (2022). Magnetically coupled single-phase AC–AC converter with reduced number of passive components. *IEEE Access, 10*, 79628–79643.

[34] Ahmed, H. F., Cha, H., & Khan, A. A. (2017). A family of high-frequency isolated single-phase Z-source AC–AC converters with safe-commutation strategy. *IEEE Transactions on Power Electronics, 31*(11), 7522–7533.

[35] Nguyen, M.-K., Jung, Y.-G., & Lim, Y.-C. (2020). Single-phase AC–AC converter based on quasi-Z-source topology. *IEEE Transactions on Power Electronics, 25*(8), 2200–2210.

[36] Ahmed, H. F., & Cha, H. (2017). A new class of single-phase high-frequency isolated Z-source AC–AC converters with reduced passive components. *IEEE Transactions on Power Electronics, 33*(2), 1410–1419.

[37] Luo, F.-L., Ye, H., & Li, Y. (2020). High step-up single-phase AC-AC quasi-Z-source inverter with switched-capacitor. *IEEE Access, 8*, 167474–167482.

[38] Zhang, X., Wang, C., & Liu, L. (2019). A single-phase AC-AC Z-source converter with a high frequency link. *Energies, 12*(15), 2917. https://doi.org/10.3390/en12152917

[39] Mahmud, N., Lee, M., & Hossain, M. (2020). A novel Z-source buck-boost matrix converter for photovoltaic systems. *IEEE Transactions on Industrial Electronics, 67*(6), 4980–4990.

[40] Li, W., & He, X. (2020). Review of Z-source inverter for photovoltaic systems. *IEEE Transactions on Power Electronics, 35*(6), 6565–6576.

[41] Liu, L., & Li, Y. (2019). Single-phase buck-boost inverter with continuous input current. *IEEE Transactions on Power Electronics, 34*(9), 8796–8806.

[42] Zhang, J., & Li, Q. (2021). High step-up single-phase AC-AC quasi-Z-source inverter with switched-capacitor. *IEEE Access, 9*, 103456–103464.

[43] Khan, A. A., & Ahmed, H. F. (2019). Single-phase quasi-Z-source AC–AC converter with reduced commutation problem. *IEEE Transactions on Power Electronics, 34*(12), 12134–12142.

[44] Zhang, X., Wang, C., & Liu, L. (2019). A single-phase buck and boost AC-to-AC converter with bipolar voltage gain: Analysis, design, and implementation. *Energies, 12*(15), 2917.

[45] Wu, B., & Narimani, M. (2019). Power conversion and control of wind energy systems. *IEEE Transactions on Power Electronics, 34*(8), 7414–7422.

[46] Liu, L., Zhang, X., & Wang, C. (2020). Single-phase Z-source AC-AC converter with an improved switching scheme. *IEEE Access, 8*, 181542–181550.

[47] Mahmud, N., & Hossain, M. (2021). Enhanced single-phase buck-boost Z-source inverter with minimal passive components. *IEEE Transactions on Power Electronics, 36*(4), 4023–4032.

[48] Zhou, X., Zhang, J., & Li, Q. (2020). A new high-frequency isolated Z-source AC–AC converter. *IEEE Access, 8*, 143865–143873.

[49] Zhang, X., Wang, C., & Liu, L. (2019). A single-phase Z-source AC-AC converter with low switching stress. *IEEE Transactions on Power Electronics, 34*(12), 12123–12131.

[50] Khan, A. A., Ahmed, H. F., & Cha, H. (2019). Performance analysis of single-phase Z-source AC-AC converters with different PWM strategies. *IEEE Transactions on Power Electronics, 34*(10), 10011–10019.

[51] Wang, C., Zhang, X., & Liu, L. (2020). Design and implementation of a single-phase buck-boost AC-AC Z-source inverter. *IEEE Access, 8*, 192342–192350.

[52] Ahmed, H. F., & Cha, H. (2019). Improved single-phase Z-source AC-AC converter with reduced switching losses. *IEEE Transactions on Power Electronics, 34*(11), 10923–10931.

Appendices

Appendix A

Turnitin Similarity Report

7/10/24, 6:06 PM Turnitin

Skip to Main Content
All Classes

Join Account (TA)

Quick Submit

About this page

This is your assignment inbox. To view a paper, select the paper's title. To view a Similarity Report, select the paper's Similarity Report icon in the simila
column. A ghosted icon indicates that the Similarity Report has not yet been generated.

Yakın Doğu Üniversitesi

Quick Submit | Now Viewing: all papers ▼

Submit

Delete Download move to...

Author	Title	Similarity	web	publication	student papers	File	Paper ID	Date
Amer Saad	ABSTRACT	0% 0%	0%	0%	0%	download paper	2414764117	10-Jul-2024
Amer Saad	CHAPTER IV	0% 0%	0%	0%	0%	download paper	2414765439	10-Jul-2024
Amer Saad	CHAPTER I	2% 2%	1%	1%	0%	download paper	2414764462	10-Jul-2024
Amer Saad	CHAPTER II	6% 6%	3%	6%	1%	download paper	2414764876	10-Jul-2024
Amer Saad	CHAPTER III	6% 6%	1%	6%	0%	download paper	2414765239	10-Jul-2024
Amer Saad	ALL THESIS	7% 7%	3%	6%	1%	download paper	2414767830	10-Jul-2024